博士論文番号：1081202

Analysis and Modification of *Bacillus subtilis* genome-reduced strain MGB874 for the high production of industrial enzymes

産業用酵素高生産に向けた

枯草菌ゲノム縮小株 MGB874 株の解析と改良

Kenji Manabe
Nara Institute of Science and Technology
Graduate School of Biological Science
Laboratory of Microbial Molecular Genetics
Prof. Hisaji Maki

眞鍋　憲二
奈良先端科学技術大学院大学
バイオサイエンス研究科　原核生物分子遺伝学講座
（真木 寿治　教授）

平成２４年２月１２日提出

List of Contents

Introduction

1. Background of this research area

In recent years, with the progression of genetic engineering technology, a variety of useful substances, including enzymes, have been produced on industrial scales using microorganisms. Improvement of production level is a major topic of interest in such industrial-scale production of useful substances. To achieve these improvements, several attempts have been made to generate hyper-producing microbial cells for useful substances through mutation breeding, or genetic engineering. The experimental genome reduction strategy (Feher et al., 2007), a relatively new field in synthetic genomics, has been used extensively in recent years with several model microorganisms, especially *Escherichia coli* (Hashimoto et al., 2005; Posfai et al., 2006) and *Bacillus subtilis* (Ara et al., 2007; Morimoto et al., 2008; Westers et al., 2003), to investigate the genome architecture or to improve their characteristics.

B. subtilis, a gram-positive sporiferous *Bacillus*, is an attractive organism for industrial uses for a variety of reasons, including its high growth rate, ability to secrete proteins into the extracellular medium, and GRAS (generally regarded as safe) status (Schallmey et al., 2004; Simonen and Palva, 1993). *B. subtilis* is also one of the best-characterized model microorganisms by biochemical, genetic, and molecular biological studies. Furthermore, the complete genomic sequence of the *B. subtilis* strain 168 has been determined (Barbe et al., 2009; Kunst et al., 1997). Among the 4106 genes identified on the 4.2 Mb genome, only 271 genes were shown to be indispensable for growth of *B. subtilis* in rich medium (Kobayashi et al., 2003).

B. subtilis has numerous genes activated only under specific conditions or in response to environmental stresses. Therefore, under controlled conditions, such as industrial production systems, many of the genes are expected to be unnecessary and could be wasteful in terms of

energy consumption. For the effective production of enzymes, it may be beneficial to delete such unnecessary and wasteful genome regions. As an example of a strain with a genome-reduced, *B. subtilis* Δ6 strain with 7.7% genome reduction (0.53 Mb) was reported by Westers et al. (Westers et al., 2003). However, phenotypic characterization of the Δ6 cells revealed no unique properties, including secretion of α-amylase AmyQ protein, relative to the wild-type 168 cells.

2. Genome-reduced strain MGB874

Recently, we constructed a multiple-deletion mutant, MGB874, by sequential deletion of all prophage and prophage-like sequences, *pks* and *pps* operons, and the 11 non-essential gene clusters (Ara et al., 2007; Morimoto et al., 2008)(Figure 1). MGB874 had deletion of 874 kb (20.7%) of the sequence encoding 865 genes from the original *B. subtilis* 168 genome. Notably, strain MGB874 showed enhanced production of exogenous extracellular alkaline cellulase Egl-237 (Hakamada et al., 2000) and a subtilisin-like alkaline protease M-protease (Kobayashi et al., 1995), which were expressed from a multi-copy plasmid, in modified 2xL-Mal medium, a model medium for industrial protein production (Figure 2).

Enzyme production in the wild-type 168 cells was arrested after the transition state, while the production level continued to increase in strain MGB874 throughout the culture period. Transcriptome analyses revealed that earlier development of genetic competence, delayed entry sporulation, and maintenance of metabolic activity in MGB874 cells in comparison to the wild-type 168 cells (Morimoto et al., 2008). However, it is not clear how these changes contributed to the increased level of protein production, and whether these phenomena in MGB874 were due to a global synergistic effect of large-scale genome reduction or mainly due to the deletion of several functional genes.

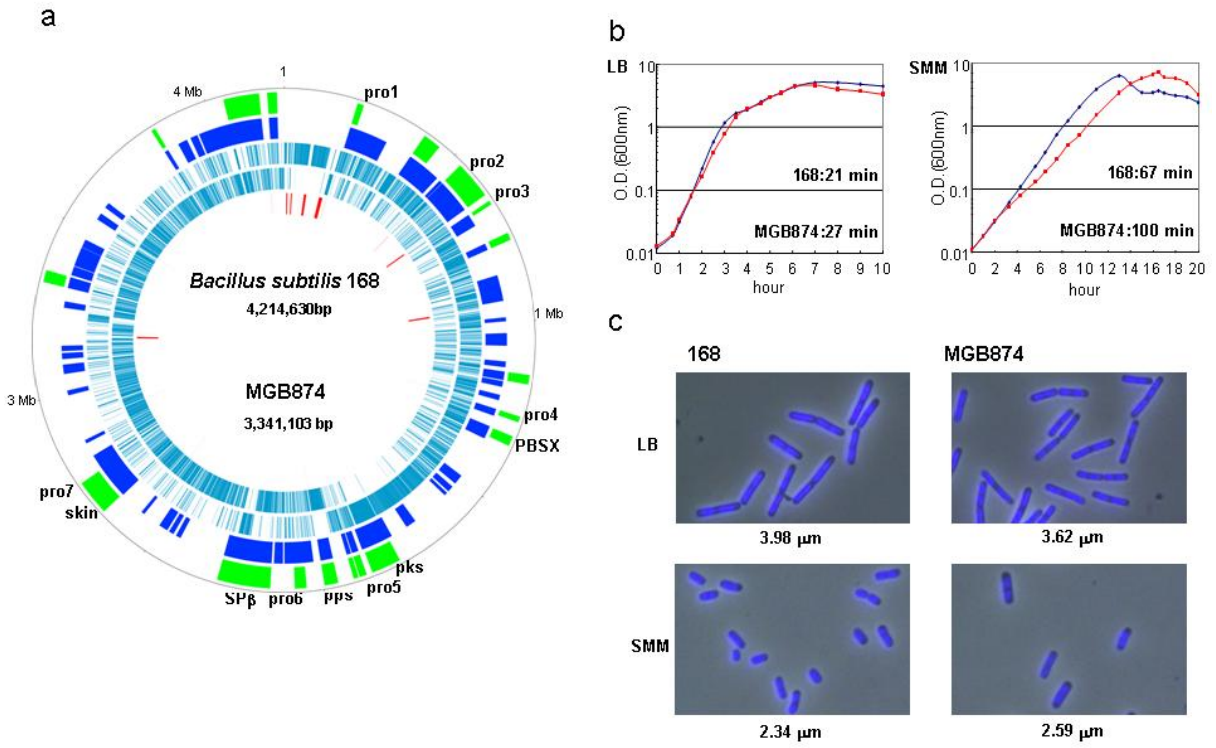

Figure 1. Design and basal phenotypic analysis of MGB874.

(A) Outer concentric ring: genome coordinate (bases) of the *B. subtilis* 168 genome. Ring 2 (green): positions of deleted sequences in MGB874, including prophages and prophage-like regions (SPb, PBSX, skin, pro1-7) and polyketide and plipastatin synthesis operons (*pks*, *pps*). Ring 3 (dark blue): regions of single deletion. Rings 4 and 5 (light blue): protein coding regions in clockwise (Ring 4) and counterclockwise (Ring 5) orientations. Ring 6 (red): rRNA and tRNA genes. (B) Growth profiles of MGB874 (red squares) and wild-type 168 (blue diamonds) cells in LB and SMM medium. The doubling time of growth is specified. (C) Cell morphology, chromosome distribution, and mean values of cell lengths of wild-type 168 and MGB874 cells. MGB874 and 168 cells were cultured at 378C in LB or SMM medium, and images were obtained during the exponential growth phase after staining with 4,6-diamindino-2-phenylindole (DAPI). The average cell length is indicated (200 cells analyzed). This figure was cited from reference (Morimoto et al., 2008).

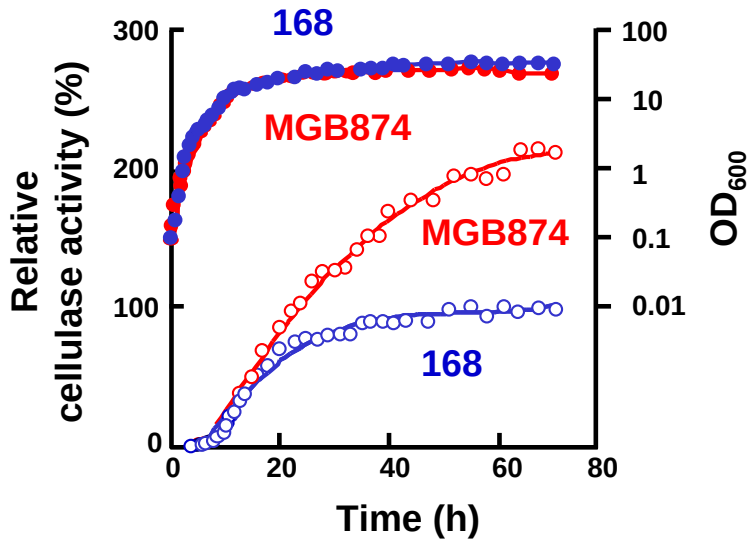

Figure 2. Cultivation of strains 168 and MGB874 for cellulase production.

The strains 168 (Blue) and MGB874 (Red) harboring pHYS237, expression vectors for alkaline cellulase Egl-237, cultured in 2L-Mal medium (2.0% Tryptone peptone, 1.0% Yeast extract, 1.0% NaCl, 7.5% maltose hydrate, 7.5ppm MnSO4). Relative cellulase activities in the growth medium (closed circles) and the growth profiles (open circles) of wild-type 168 are presented.

3. Purposes of this research

Here, we attempted to elucidate the mechanism underlying the improved enzyme production and further enhance enzyme production in strain MGB874 through genetic approaches and modified cultivated condition.

we divided my research into three sections:

Chapter 1: Elucidation of the mechanism underlying enhanced enzyme production in strain MGB874. This study was performed to clarify the reasons for the improved level of enzyme production in *B. subtilis* strain MGB874, which would provide insight into further improvement. We focused on determining which gene deletions contributed to the enhanced enzyme production. Here, we report that the absence of the gene cluster, *rocDEF* operon and *rocR*, which constitute the arginine degradation pathway (Calogero et al., 1994; Gardan et al.,

1995), increases the cell mass through increases in the internal glutamate pool and contributes to the enhanced enzyme production level in MGB874.

Chapter 2: Investigation of the suitability of strain MGB874 for the production of α-amylase. In addition, we investigated the suitability of strain MGB874 for the production of novel alkaline α-amylase. In this Chapter, we found that the optimization of external pH is an important prerequisite for the efficient production of AmyK38 in *B. subtilis*. Under controlled pH conditions, the genome-reduced strain MGB874 was demonstrated to be a beneficial host for the production of AmyK38.

Chapter 3: Improved enzyme production in strain MGB874 via modification of glutamate metabolism and growth conditions. From the results of Chapter 1, we predicted that deletion of the RocG gene, a bi-functional protein that acts as a glutamate dehydrogenase and an indirect repressor of glutamate synthesis, would improve glutamate metabolism, leading to further increased enzyme production. However, deletion of *rocG* dramatically decreased production of the alkaline cellulase Egl-237 in strain MGB874 (strain 874ΔrocG). Here, we investigated the mechanisms underlying decreased enzyme production in strain 874ΔrocG and attempted to boost production of Egl-237 by overcoming the rate-limiting factors we identified.

Materials and Methods

1. Bacterial strains, plasmids, and growth media

The bacterial strains and plasmids used in this study are listed in Table 1. *E. coli* HB101 (Takara Bio, Inc.) was used as the host for plasmid preparation and was routinely cultured in Luria-Bertani (LB) medium (1% [w/v] Bacto tryptone [Difco], 0.5% [w/v] Bacto yeast extract [Difco], and 1% [w/v] NaCl). For preparation of *B. subtilis* competent cells, Spizizen minimal medium (Anagnostopoulos and Spizizen, 1961) was used as the basal medium. LB medium containing 1.5% (w/v) agar and supplemented with 100 μg ml^{-1} ampicillin, 10 μg ml^{-1} chloramphenicol (Cm), 20 μg ml^{-1} neomycin (Nm), 100 μg ml^{-1} spectinomycin (Sp), or 0.3 μg ml^{-1} erythromycin (Em) was used as the selective medium. The protoplast transformation method (Chang and Cohen, 1979) was used for the introduction of plasmids into *B. subtilis*, and the transformants were selected on DM3 medium (Chang and Cohen, 1979) containing 50 μg ml^{-1} tetracycline (Tet). For enzyme production, 2xL-Mal medium (2% [w/v] Bacto tryptone [Difco], 1% [w/v] Bacto yeast extract [Difco], 1% [w/v] NaCl, 7.5% [w/v] maltose monohydrate, 7.5 μg ml^{-1} manganese sulfate 4-5 hydrate, and 15 μg ml^{-1} Tet) was used. As necessary, IPTG was added to a final concentration of 1 mM, and various concentrations of Na_2CO_3 were added after 12 h of cultivation.

2. Construction of *B. subtilis* mutant strains

The DNA manipulation techniques used for the construction of mutants were previously described (Liu et al., 2008). MGB625Δr1 was constructed from MGB625 as follows. A 0.9-kb Cm-resistance gene (*cat*) fragment was PCR amplified from plasmid pC194 (Horinouchi and Weisblum, 1982) using primers CmFW and CmRV. Approximately 1.0-kb upstream (UPr1) and downstream (DNr1) flanking sequences of the rl region, which included the *pdp-yxeD* region (nucleotides 4,048,987 to 4,066,589 in National Center for Biotechnology Information

(NCBI) Reference Sequence (RefSeq) NC_000964.3(Barbe et al., 2009)), were PCR amplified from genomic DNA of *B. subtilis* strain MGB625 using primer pairs r1FW and r1/CmR, and r1/CmF and r1RV, respectively. The two amplified fragments (UPr1 and DNr1) contained overlapping sequences with *cat* at the 3'- and 5'-ends, respectively. The three fragments (*cat*, UPr1, and DNr1) were then ligated together in the order UPr1-cat-DNr1 by SOE-PCR using primers r1FW2 and r1RV2, which were designed using internal sequences of the fragments to minimize the minor products of PCR ligation. The resulting 2.9-kb PCR product was then introduced into *B. subtilis* MGB625 cells by competent cell transformation (Anagnostopoulos and Spizizen, 1961), and Cm-resistant transformants were selected from LB agar plates containing Cm. Deletion of the r1 region was confirmed by PCR using primers r1FW and r1RV. A similar approach was used for the constructions of mutant strains MGB625Δr1, MGB625Δr2, MGB625Δr3, MGB625Δr4, MGB625ΔyydD-yycN, MGB625ΔrapG-phrG, MGB625ΔrocF-rocR, MGB625ΔrocF-rocD, MGB625ΔrocR, MGB625Δpdp-phrG and MGB625Δpdp-rocD using the primers listed in Table 2. The r2, r3, and r4 regions represent the *yxeC-yxnA* (nucleotides 4,066,582 to 4,109,154 in NCBI RefSeq NC_000964.3), *yxaD-fbp* (nucleotides 4,109,167 to 4,130,074 in NCBI RefSeq NC_000964.3), and *yydD-rocR* regions (nucleotides 4,130,538 to 4,147,174 in NCBI RefSeq NC_000964.3), respectively (Figure 3A).

Strain 874DEFR was constructed by transformation of strain MGB874 with chromosomal DNA from strain MGB625Δpdp-phrG. As a result of the transformation, the *rocDEF-rocR* and *cat* region was re-introduced into the Δ*pdp-rocR* region in strain MGB874. PCR was used to confirm that only the *rocDEF-rocR* region and *cat* were introduced into the resulting strain 874DEFR. In addition, strain 874DEFR(spec) was constructed by replacement of *cat* with the Sp-resistance gene (*spec*) in strain 874DEFR. The Sp-resistance gene was amplified from plasmid pDG1727(Guerout-Fleury et al., 1995)using primers Spf and Spr.

Strain 168ΔgudB was constructed from strain 168 using a slightly modified method from that used for the construction of strain MGB625Δr1. Briefly, a 0.8-kb fragment of the Nm-resistance gene (*neo*) was first amplified from plasmid pUB110 (Horton et al., 1989) using primers Nmf and Nmr. Approximately 1.0-kb upstream (UPgudB) and downstream (DNgudB) flanking sequences of the coding region of *gudB* were PCR amplified from strain 168 genomic DNA using primer pairs gudBFW and gudB/NmR, and gudB/NmF and gudBRV, respectively. The three amplified fragments (*neo*, UPgudB, and DNgudB) were ligated by SOE-PCR using primers gudBFW2 and gudBRV2, and template DNA was then removed by digestion with DpnI (Takara Bio, Inc.). The resulting 3.0-kb PCR product was introduced into *B. subtilis* strains 168, MGB874, and 874DEFR, and Nm-resistant transformants were selected on LB agar plates containing Nm and designated as strains 168ΔgudB, MGB874ΔgudB, and 874DEFRΔgudB, respectively. Successful deletion of the *gudB* region was confirmed by PCR using primers gudBFW and gudBRV. A similar approach was used for the construction of mutant strains MGB874ΔahrC, MGB874ΔargC-F, MGB874ΔahrCΔargC-F, MGB874ΔcitB, 874DEFRΔcitB, 168ΔrocG, MGB874ΔrocG, MGB874ΔrocG(cat), MGB874ΔgltAB, 874DEFRΔrocG, 874DEFRΔgltAB, 874DEFRΔrocABC, 168ΔdltB and 874ΔdltB using the primers listed in Table 2. The Em-resistance gene (*erm*) was amplified from plasmids pMUTIN4(Vagner et al., 1998), using the primer sets Emf and Emr. In the three Δ*ahrC* strains, the coding region of *ahrC* was replaced by a promoter- and terminator-less Nm-resistance gene to avoid influencing the expression of genes downstream of *ahrC*.

The insertion of the 3.1-kb *egl-237* fragment, consisting of the promoter, SD sequence, and coding region for the signal sequence, mature protein, and terminator of *egl-237* into the *amyE* locus of the *B. subtilis* chromosome was performed as follows. The 3.1-kb *egl-237* fragment was amplified from plasmid pHYS237 using primers amyE-egl237.f and

amyE-egl237.r. The front (*amyE-front*) and back sequences of *amyE* fused to *cat* (*cat-amyE-back*) were PCR amplified from plasmid pX (Kim et al., 1996) using primer pairs amyE.up-F and amyE.up-R, and amyE.down-F and amyE.down-R, respectively. The three fragments (*egl-237*, *amyE-front*, and *cat-amyE-back*) were ligated by SOE-PCR using primers amyE.up-F and amyE.down-R, and template DNA was then removed by DpnI digestion. The obtained PCR products were introduced into *B. subtilis* strains 168, MGB874, and 874DEFR(spec), and Cm-resistant transformants were selected on LB agar plates containing Cm and designated as strains 168egl-237, MGB874egl-237, and 874DEFRegl-237, respectively. Successful introduction of *egl-237* was confirmed by PCR using primers amyE.up-F and amyE.down-R.

B. subtilis strain R-726, in which the *rocG* gene was expressed under control of the IPTG-inducible Pspac promoter from pAPNC213, was constructed as follows. PCR-amplified *rocG* gene fragments containing the ribosome-binding site of *rocG* was cloned into the SalI/SacI sites of pAPNC213 (Morimoto et al., 2002). The resulting plasmid, named pAPNC213-rocG, was transformed into strain MGB874 to integrate the *rocG* gene into the *aprE* site by homologous recombination. A Sp-resistant transformant was selected and designated strain R-726.

A transcriptional *htrB-lacZ* fusion gene was generated by modification of plasmid pDL2 (Asai et al., 2000). First, plasmid pDN110 was constructed by cloning a 263-bp PCR-generated fragment (synthesized with primers YVTAPF and YVTAPR) using the procedure described by Noone et al (Noone et al., 2001). Strains R-1645, R-1646, and R-1926 were generated from strains 168, MGB874, and R-726, respectively, by introducing plasmid pDN110 and then selecting for Cm-resistant transformants.

2. Expression vectors used for evaluation of exogenous enzyme production

Primers used for the construction of *B. subtilis* mutants and plasmids are listed in Table 2. pHYS237, pHP237-K16 and pHYK38, expression vectors for alkaline cellulase Egl-237 from *Bacillus* sp. strain KSM-S237 (Hakamada et al., 2000), subtilisin-like alkaline protease (M-protease) from *Bacillus clausii* strain KSM-K16 (Kageyama et al., 2007) and alkaline α-amylase AmyK38 from *Bacillus* sp. strain KSM-K38 (Hagihara et al., 2001b), respectively, were used for evaluation of exogenous enzyme production.

pHYS237 was previously constructed by introducing a 3.1-kb DNA fragment containing the promoter, Shine-Dalgarno (SD) sequence, and region coding for the signal sequence, mature protein, and terminator of *egl-237*, which was PCR amplified from the *Bacillus* sp. strain KSM-S237 genome using primers Egl-237-F.BamHI and Egl-237-R.BamHI (Table 2), into the BamHI site of *E. coli* and *B. subtilis* shuttle vector pHY300PLK (Takara Bio, Inc.) (Shibahara, 1985).

pHP237-K16 was previously constructed as follows. A 1.3-kb DNA fragment coding for the pro and mature protein of M-protease was PCR amplified using *B. clausii* KSM-K16 genomic DNA as a template and primers S237pMpm-F and Mter-R.BglII (Table 2). In addition, a 0.6-kb DNA fragment including the promoter, SD sequence, and region coding for the signal sequence of the *egl-237* was PCR amplified using *Bacillus* sp. KSM-S237 genomic DNA as a template and primers S237p-F.BamHI and S237pMpm-R (Table 2). The 1.3-kb and 0.6-kb fragments were mixed and fused together by splicing using overlap-extension PCR (SOE-PCR) (Horton et al., 1989) with primers S237p-F.BamHI and Mter-R.BglII (Table 2) to yield a 1.8-kb DNA fragment in which the M-protease gene was ligated downstream of the promoter region of the *egl-237* gene. The 1.8-kb DNA fragment was then inserted into the BamHI-BglII sites of shuttle vector pHY300PLK.

Plasmid pHYK38 was constructed as follows. A 1.5-kb DNA fragment coding for the mature form of AmyK38 was PCR amplified using genomic DNA extracted from *Bacillus sp.*

KSM-K38 strain as template and primers K38matu-F2 (ALAA) and K38matu-R (XbaI) (Table 2). In addition, a 0.6-kb DNA fragment including the promoter, Shine-Dalgarno (SD) sequence, and coding region for the signal sequence of the alkaline cellulase Egl-237 was PCR amplified using *Bacillus* sp. KSM-S237 genome as template and primers S237ppp-F2 (BamHI) and S237ppp-R2 (ALAA) (Table 2). The amplified 1.5-kb and 0.6-kb fragments were fused together by SOE-PCR with primers S237ppp-F2 (BamHI) and SP64K38-R (XbaI) (Table 2) to generated a 2.1-kb DNA fragment that contained the AmyK38 gene downstream of the promoter, SD sequence, and coding region of the *egl-237* signal sequence. The 2.1-kb DNA fragment was inserted into the BamHI-XbaI cleavage site of the shuttle vector pHY300PLK (Takara Bio, Inc.) (Shibahara, 1985).

3. Culture methods for assessment of heterologous enzyme production

For shake-flask fermentation, transformants were pre-cultured in LB medium with 15 μg ml^{-1} Tet with shaking at 120 rpm at 30°C for 15 h, and 600 μl of the pre-culture was inoculated into 30 ml of 2xL medium with 7.5% (w/v) maltose monohydrate in a 500-ml Sakaguchi flask.

For jar fermentation, *B. subtilis* harboring expression vector stored in 10% glycerol at –80°C were inoculated onto LB agar medium with 15 μg ml^{-1} Tet. After incubation at 37°C for 12 h, cells were collected and inoculated into pre-culture medium at an optical density at 600 nm (OD_{600}) of 0.02. For batch fermentation, cells were pre-cultured in 200 ml of 2xL medium with 7.5% (w/v) maltose monohydrate with shaking at 210 rpm at 30°C to an OD_{600} of 0.3 to 0.5, then inoculated into a 30-L jar fermentor (working volume, 18 liters). The 30-L jar fermentor was operated at an aeration rate of 0.4 vvm and an agitation rate of 300 rpm. For pH-stat fermentation, cells were pre-cultured in 30 ml of 2xL medium with 12.5% (w/v) maltose monohydrate with shaking at 120 rpm at 30°C to an OD_{600} of 0.3 to 0.5, then

inoculated into a 2-L jar fermentor (working volume, 0.8 liters). The 2-L jar fermentor was operated at an aeration rate of 0.5 vvm and an agitation rate of 800 rpm. The pH was kept at 7.2 via automatic addition of 1M NaOH or 10% (w/v) aqueous NH_3. Fermentation without pH adjustments was used as a control.

As appropriate to specific assays, cultured cells were removed by centrifugation at 9,000 x *g* and the supernatants were stored at –30°C. For RNA extraction, cells were separated by centrifugation, washed with 10 mM Tris-HCl (pH 7.5), frozen with liquid nitrogen, and stored at –80°C.

4. Viable cell counts

The detection of viable bacteria was performed by cultivation and enumeration of colony forming units (CFU). A dilution series of bacterial cell suspensions were plated on LB agar plates. After overnight incubation at 37 °C, colonies formed on the agar plates were enumerated.

5. Assay of enzyme activity

For the determination of cellulase activity, 50 μl aliquots of 0.4 mM *p*-nitrophenyl-β-D-cellotrioside (Seikagaku Kogyo) were mixed with 50 μl sample solution appropriately diluted with 130 mM phosphate buffer (pH 7.4) (Wako Pure Chemical Industries). The amount of *p*-nitrophenol released during reaction at 30 °C was then determined quantitatively based on the change in absorbance at 420 nm (A_{420}). The amount of enzyme required for the release of 1 μmol *p*-nitrophenol per min was defined as 1 U. Specific productivity (U g^{-1} h^{-1}) was calculated by dividing the cellulase production rate (U l^{-1} h^{-1}) by cell dry weight (CDW, g l^{-1}). CDW was determined by centrifuging cell suspensions in pre-weighed tubes for 20 min at 9,000 x *g*, washing the sample with 1% (w/v) NaCl, and then

drying cells at 85 °C to a constant weight.

For the determination of protease activity, 100 μl of 75 mM borate-KCl buffer (pH 10.5) containing 7.5 mM succinyl-L-alanyl-L-alanyl-L-alanine *p*-nitroanilide (STANA; Peptide Institute, Inc.) was mixed with 50 μl culture supernatant appropriately diluted with a 2 mM calcium chloride solution, and the amount of *p*-nitroaniline released during reaction at 30 °C was determined quantitatively based on the change in A_{420}. The amount of enzyme required for the release of 1 μmol *p*-nitroaniline per min was defined as 1 U.

Amylase activity in culture supernatants was measured using a Liquitec Amy EPS kit (Roche Diagnostic), which uses 4,6-ethylidene-4-nitrophenyl-α-D-maltoheptaoside as a substrate (Lorentz, 1998). Specifically, 100 μl of R1-R2 mixture (R1 [coupling enzyme]: R2 [amylase substrate]= 5 : 1 [vol] was mixed with 50 μl sample solution appropriately diluted with 125 mM glycine-NaOH buffer (pH 10.0), and the amount of *p*-nitrophenol released during incubation at 30 °C was quantitatively determined by the change in absorbance at 405 nm (A_{405}). The amount of enzyme required for the release of 1 μmol *p*-nitrophenol per minute was defined as 1 unit (U).

β-galactosidase assay was performed according to the method described by Hyyryläinen et al. (Hyyrylainen et al., 2001). Briefly, cells were collected from 50 μl samples by centrifugation at 12,000 x *g* for 2 min at 4 °C and then washed once in 0.5 ml ice-cold 25 mM Tris-HCl (pH 7.4). After centrifugation at 12,000 x *g* for 2 min at 4 °C, the pellet was first re-suspended in 0.64 ml Z buffer (60 mM Na_2HPO_4-H_2O, 40 mM NaH_2PO_4-H_2O, 10 mM KCl, and 1 mM $MgSO_4$-$7H_2O$) supplemented with 2 mM dithiothreitol (DTT) and then mixed with 0.16 ml lysozyme solution (2.5 mg/ml). After a 10-min incubation at 37 °C, the sample was mixed with 8 μl of 10% (v/v) Triton-X 100 and then stored at -30 °C until assayed. The assay was initiated by the addition of 0.2 ml *o*-nitrophenyl-β-D-galactoside (ONPG; 4 mg dissolved in Z buffer) to the pre-warmed sample, followed by incubation of the mixture at 30 °C. The

reaction was terminated once the mixture turned yellow by adding 0.4 ml of 1 M Na_2CO_3, and the total incubation time was recorded. β-galactosidase-specific activities are reported in units (U) calculated using the following formula: 1000 x A_{420}/reaction time (min) x OD_{600} of culture.

6. Measurement of extracellular amino acid concentrations

The collected culture supernatants were first diluted 21-fold and suspended in 2% (w/v) trichloroacetic acid. After the precipitate was removed by filtration through a 0.2-μm cellulose acetate filter (DISMIC-13CP; Advantec), the filtrates were subjected to determination of amino acid concentrations using an L-8900 Amino Acid Analyzer (Hitachi).

7. Measurement of intracellular amino acid concentration

Metabolites were extracted from cells according to the methods described by Soga (Soga et al., 2003) and Bolten (Bolten et al., 2007). Briefly, culture medium corresponding to 10 OD_{600} (*e.g.*, 10 ml of a culture with OD_{600} = 1.0) was passed through a 0.4-μm HTTP filter (Millipore). Cells retained on the filter were washed twice with 1% (w/v) NaCl and then immersed in 2 ml methanol containing 150 μM α-amino butyrate as an internal standard. After incubation for 30 min on ice, 1 ml chloroform and 380 μl Milli-Q water were added to the cell suspension, and 1 ml of the resulting methanol-water layer was centrifugally filtered through a Microcon YM-3 filter (Millipore). After drying the filtrate under reduced pressure at room temperature, amino acids were quantified using an HP6890 Series Gas Chromatography (GC) system (Hewlett Packard) by GC detection-flame ionization (EZ:faast; Phenomenex) or an L-8900 Amino Acid Analyzer (Hitachi). The intracellular amino acid levels were calculated by determining the amount of amino acids per cell dry weight (CDW).

8. Measurement of ammonia concentration

The concentration of ammonia in culture supernatants was determined by enzymatic analysis according to the F-Kit UV method (Boehringer GmbH)

9. Purification of AmyK38

For the purification of AmyK38 protein, *B. subtilis* strain 168 harboring pHYK38 was cultivated in 2xL-Mal medium at 30 °C for 72 h. The purification procedure was performed essentially as described by Hagihara et al. (Hagihara et al., 2001b). Briefly, the centrifuged supernatant of the culture broth was loaded onto a Biogel P-6 DG desalting column (Bio-Rad Laboratories) equilibrated with 10 mM Tris-HCl buffer (pH 7.0). The eluate was collected as a single fraction and subjected to further purification by chromatography using DEAE-Toyopearl 650M column (Tosoh, Tokyo, Japan) and the identical protocol. Purified protein was quantified by a modified method of Lowry et al. (Lowry et al., 1951) using the DC Protein Assay kit (Bio-Rad) and bovine serum albumin as the standard. The specific activity of purified AmyK38 towards 4,6-ethylidene-4-nitrophenyl-α-D-maltoheptaoside, as measured using a Liquitec Amy EPS kit (Roche Diagnostic) was 22,800 U mg of protein^{-1}.

10. Antibodies

Rabbit polyclonal antibodies against purified AmyK38 protein were prepared by Operon Biotechnology Co. (Tokyo, Japan).

11. Western blotting

Culture samples were harvested, and cells were then separated from the culture medium by centrifugation. Supernatants were diluted 40-fold with 10 mM Tris-HCl (pH 7.0) containing Complete Mini, Protease Inhibitor Cocktail Mixture (Roche Applied Science). Cells were

washed twice with 2xL-Mal fresh medium, and re-suspended to an OD_{600} of 3.0 in 10 mM Tris-HCl (pH 7.0) containing the cocktail mixture. After adding 3x SDS-PAGE Loading Buffer (BioVision), the samples were incubated at 95 °C for 1 min. For Western blotting analysis, the samples were subjected to sodium dodecyl sulfate polyacrylamide gel electrophoresis (SDS-PAGE) using 10% polyacrylamide gels (Ready Gels; Bio-Rad Laboratories) and 1x Tris-glycine-SDS running buffer (Bio-Rad Laboratories). The separated proteins were transferred to a PVDF membrane using a semi-dry transfer apparatus (Bio-Rad Laboratories) and then probed with primary antibodies against AmyK38 (1:2500) and visualized with a Western Breeze Colorimetric kit (Invitrogen) according to the manufacturer's instructions. MagicMark XP Western Protein Standard (Invitrogen) was used as a protein standard.

12. Preparation of culture supernatants for assessment of AmyK38 stability

B. subtilis cells harboring pHYK38 were grown for 48 h in 30 ml 2xL-Mal medium, and cells were then removed by centrifugation at 9,000 x *g* for 30 min at 4 °C. The obtained supernatants were filtered through a 0.22-μm pore-size MF microfilter (Millipore) to ensure complete removal of cellular material. The cell-free supernatants were incubated at 30 °C, and samples were removed at various intervals for the determination of α-amylase activity and Western blotting analysis.

13. DNA sequencing

DNA sequencing was performed using the dideoxy chain termination method with the BigDye Terminator v3.1 Cycle Sequencing kit and an ABI 3100 Sequencer (Applied Biosystems). If necessary, the target regions were amplified using specific primers and the PCR products were used as templates for sequencing. Primers for sequencing were designed

according to the manufacturer's instructions.

14. Quantitative real-time PCR

Total RNA was extracted from *B. subtilis* cells as described previously (Igo and Losick, 1986) and reverse transcribed to cDNA using an AffinityScript QPCR cDNA Synthesis kit (Stratagene). As negative controls, all RNA samples were subjected to the identical reaction conditions without reverse transcriptase. Quantitative real-time PCR amplification, detection, and analysis were performed with the Mx3000 Real-time PCR system (Stratagene) and Brilliant II Fast SYBR Green QPCR Master Mix (Stratagene). The primer sequences used in the real-time PCR were designed using Primer 3 (version 0.4.0) (Rozen and Skaletsky, 2000) and are listed in Table 3 in the supplemental material. The source code of Primer 3 is available at http://frodo.wi.mit.edu/primer3/.

Real-time PCR was performed in 25-μl reaction mixtures consisting of 1xSYBR Green Master Mix, 0.4 μM each forward and reverse primer, 3.2 μM reference dye, and 10 μl template. The PCR conditions were 95 °C for 2 min, followed by 40 cycles of 95 °C for 5 s and 60 °C for 20 s. All of the amplified products were confirmed by dissociation curve analysis. To estimate the quantity of initial template in the sample, serial real-time PCR was performed by amplifying inserted target DNA in pUC118 (Takara Bio, Inc.) with specific primers. For each gene, a standard curve was generated as the log of the quantity of initial template DNA plotted against the threshold cycle (Ct) values for the standard wells. The generated standard curves were used to convert the Ct values of each amplified gene in the cDNA preparations to copy numbers of cDNA molecules. The estimated copy number was normalized to the value of *gyrA* (Morimoto et al., 2008; Pietiainen et al., 2005) *or 16S rRNA* (Chan and Lim, 2003), which is constantly expressed in *B. subtilis* under different growth conditions and phases.

15. Estimation of plasmid copy number

According to the method reported by Skulj *et al.* (Skulj et al., 2008), total DNA samples were prepared as follows. Cells were cultivated in 2xL-MaL medium for 24 h, and the cultures were heated at 95 °C for 15 min, allowed to cool, and then frozen at –20 °C. After thawing, the samples were diluted 100-fold with Milli-Q water, and real-time PCR was then performed by a method similar to that described above. Plasmid copy number was estimated using the primer set for amplifying the Egl-237 gene (*egl-237*) and was normalized relative to the *sigA* gene, which is present as a single copy in the chromosome.

16. High-resolution transcriptome analysis

Total RNA was extracted from *B. subtilis* cells as described previously (Igo and Losick, 1986). Synthesis of cDNA, terminal labeling, and oligonucleotide chip hybridization were performed as described in the Affymetrix instruction manual. Transcriptional signals were analyzed and visualized along genome coordinates using the program IMC Array Edition (In Silico Biology**,** Japan**)**. The signal intensities of each experiment were adjusted to confer a signal average of 500 and normalized by MA plot analysis for comparison of strains MGB874 and 874ΔrocG. (Hirai et al., 2005; Quackenbush, 2002). The average signal intensities of probes in each coding sequence were calculated after removal of the lowest and highest intensities.

Table 1. Bacterial strains and plasmids used or constructed in this study

Strain or plasmid	Relevant properties[†]	Source or reference
Strain		
Bacillus subtilis		
168	*trpC2*	(Kunst et al., 1997)
MGB625	*trpC2* Δprophage1-6 ΔPBSX ΔSPβ Δ*pks* Δskin Δ*pps* Δ(*ydeK-ydhU*) Δ(*yisB-yitD*) Δ(*yunA-yurT*) Δ(*cgeE-yodU*) Δ(*ypqP-ypmQ*) Δ(*yeeK-yesX*)	(Morimoto et al., 2008)
MGB723	MGB625 Δ(*pdp-rocR*)	(Morimoto et al., 2008)
MGB874	MGB723 Δ(*ycxB-sipU*) Δ(*yrkS-yraK*) Δ(*sboA-ywhH*) Δ(*yybP-yyaJ*) Δ(*yncM-yndN*)	(Morimoto et al., 2008)
MGB625 Δr1	MGB625 Δ(*pdp-yxeD*)::*cat*	This study
MGB625 Δr2	MGB625 Δ(*yxeC-yxnA*)::*cat*	This study
MGB625 Δr3	MGB625 Δ(*yxaD-fbp*)::*cat*	This study
MGB625 Δr4	MGB625 Δ(*yydD-rocR*)::*cat*	This study
MGB625 ΔyydD-yycN	MGB625 Δ(*yydD-yycN*)::*cat*	This study
MGB625 ΔrapG-phrG	MGB625 Δ(*rapG-phrG*)::*cat*	This study
MGB625 ΔrocF-rocR	MGB625 Δ(*rocF-rocR*)::*cat*	This study
MGB625 ΔrocF-rocD	MGB625 Δ(*rocF-rocD*)::*cat*	This study
MGB625Δpdp-rocD	MGB625 Δ(*pdp-rocD*)::*cat*	This study
MGB625 ΔrocR	MGB625 Δ*rocR*::*cat*	This study
MGB625 Δpdp-phrG	MGB625 Δ(*pdp-phrG)*::*cat*	This study
874DEFR	MGB874 *cat-rocDEF-rocR* was inserted at the Δ(*pdp-rocR*) locus	This study
874DEFR(spec)	MGB874 *spec-rocDEF-rocR* was inserted at the Δ(*pdp-rocR*) locus	This study
874RocR	MGB874 *cat -rocR* was inserted at the Δ(*pdp-rocR*) locus	This study
168 ΔgudB	*trpC2* Δ*gudB*::*neo*	This study
MGB874ΔgudB	MGB874 Δ*gudB*::*neo*	This study
874DEFRΔgudB	874DEFRcat Δ*gudB*::*neo*	This study
MGB874ΔahrC	MGB874 Δ*ahrC*::*neo* (promorterless, terminatorless)	This study
MGB874ΔargC-F	MGB874 Δ*argCJBD-carAB-argF*::*spec*	This study
MGB874ΔahrCΔargC-F	874ΔahrC Δ*argCJBD-carAB-argF*::*spec*	This study
MGB874ΔcitB	MGB874 Δ*citB*::*spec*	This study
874DEFRΔcitB	874DEFR Δ*citB*::*spec*	This study
MGB874ΔrocG	MGB874 Δ*rocG*::*spec*	This study
MGB874ΔrocG(cat)	MGB874 Δ*rocG*::*cat*	This study
MGB874ΔgltAB	MGB874 Δ*gltAB*::*erm*	This study
874DEFRΔrocG	874DEFR Δ*rocG*::*spec*	This study
874DEFRΔgltAB	874DEFR Δ*gltAB*::*erm*	This study
168egl-237	*trpC2* Δ*amyE*::*egl-237 cat*	This study
MGB874egl-237	MGB874 Δ*amyE*::*egl-237 cat*	This study
874DEFRegl-237	874DEFR(spec) Δ*amyE*::*egl-237 cat*	This study
874DEFRΔrocABC	874Δ DEFRΔ*rocABC*::*spec*	This study
R-726	MGB874 Δ*aprE*::P_{spac}-*rocG spec* (pAPNC213-rocG)	This study
R-1645	168 Δ*amyE*::P_{htrB}-*lacZ cat* (pDN110)	This study
R-1646	MGB874 Δ*amyE*::P_{htrB}-*lacZ cat* (pDN110)	This study
R-1926	MGB874 Δ*aprE*::P_{spac}-*rocG spec* Δ*amyE*::P_{htrB}-*lacZ cat* (pDN110)	This study

168ΔdltB	*trpC2* Δ*dltB*::*neo*	This study
874ΔdltB	MGB874 Δ*dltB*::*neo*	This study
874DEFRΔrocABC	874Δ DEFRΔ*rocABC*::*spec*	This study
HB101	*supE44 Δ(mcrC-mrr) recA13 ara-14 proA2 lacY1 galK2 rpsL20 xyl-5 mtl-1 leuB6 thi-1*	Takara Bio
Plasmid		
pHY300PLK	Shuttle vector for *E. coli* and *B. subtilis*	Takara Bio
pHYS237	pHY300PLK carrying the gene for alkaline endo-1,4-β-glucanase (Egl-237) from *Bacillus* sp. strain KSM-S237, containing *amp* and *tet*	(Morimoto et al., 2008)
pHP237-K16	pHY300PLK carrying the gene for M-protease from *Bacillus clausii* KSM-K16 fused to the promoter, SD and leader peptide sequences of *egl-237*, containing *amp* and *tet*	(Morimoto et al., 2008)
pHYK38	pHY300PLK carrying the gene for AmyK38 from *Bacillus* sp. strain KSM-K38 fused to the promoter, SD, and leader peptide sequences of *egl-237*, containing *amp* and *tet*	This study
pX	The integration vector containing the Px promoter used for integration into the *amyE* locus by double crossover using *cat*	(Kim et al., 1996)
pAPNC213	The integration vector containing P_{spac} promoter into the *aprE* locus by double crossover using *spec*	(Morimoto et al., 2002)
pAPNC213-rocG	pAPNC213 containing the SD sequence and coding region of *rocG* (-25 to 1275, 1325 bp)	This study
pDL2	Integration vector for introduction of single-copy transcriptional fusions to *lacZ* by double crossover at the *amyE* locus (*cat*)	(Asai et al., 2000)
pDN2	pDL2 containing the *htrA* control region	This study

†Antibiotic resistance genes are shown as follows: *cat*, chloramphenicol; *spec*, spectinomycin; *neo*, neomycin; *erm*, erythromycin; *amp*, ampicillin; *tet*, tetracycline . SD, Shine-Dalgarno.

Table 2 Primers used for the construction of mutants and plasmids.

Primer	Sequence (5'-3')[a]	Purpose in this study[b]
CmFW	CAACTAAAGCACCCATTAG	Cloning of *cat*
CmRV	CTTCAACTAACGGGGCAG	
Spf	ATCGATTTTCGTTCGTG	Cloning of *spec*
Spr	CATATGCAAGGGTTTATTG	
Nmf	GGGAATGAGTTTATAAAATAAAAA	Cloning of *neo*
Nmr	CCTTTATTCCGTTAATGCGC	
Nmf2	AAGGGAATGAGAATAGTGAATGGA	Cloning of *neo* (promorterless, terminatorless)
Nmr2	TCAAAATGGTATGCGTTTTG	
Emf	GATACACCAATCAGTGC	Cloning of *erm*
Emr	CAAGAGTTTGTAGAAACGC	
r1FW	GCGATTTTTGCAGCCCTTCTTTTTATA	Construction of MGB625Δr1
r1/CmR	CTGCCCCGTTAGTTGAAGTAAAAAATAAAGCACATCCCATGCT	
r1/CmF	CTAATGGGTGCTTTAGTTGATATAAAAGGCTCAACACAATGCGA	
r1RV	TGCTGACTGTGTCTTCTACGTT	
r1FW2	TCAGTTAAGTTATTTGCGGAAACTG	
r1RV2	GGTATGACAACAGTCGGAGCGATTT	
r2FW	TAAGGAATTCACCCACAAGGAG	Construction of MGB625Δr2
r2/CmR	CTGCCCCGTTAGTTGAAGGGAAAAAGGCTCAACACTCGCATTG	
r2/CmF	CTAATGGGTGCTTTAGTTGCTCTGACCATAAGAAAAACCCATGC	
r2RV	TAATAGCTGGCTGGCGAATCC	
r2FW2	AACCCTTATCAATATTACAGCCCTC	
r2RV2	GTGACGATGGTGCTGAGAACGACTG	
r3FW	CGCCATAAAAACAAAGCTCAAACTGAAA	Construction of MGB625Δr3
r3/CmR	CTGCCCCGTTAGTTGAAGCGATTAACAGCTGAAAAACCCATGG	
r3/CmF	CTAATGGGTGCTTTAGTTGGTGGGGTTCAGGGATGGTGATATGC	
r3RV	GATTAATGAACTTCAACATGAAATATTAAGAGTTA	
r3FW2	ATCGTCATTACCGGCGCTTCAAGCG	
r3RV2	ATGATGAGTTTCAATCTTATAGCGC	
r4FW	GCTTGGTATTTATGGACAGG	Construction of MGB625Δr4
r4/CmR	CTGCCCCGTTAGTTGAAGCTAGGGAGTTCTTATAGAACTTCCT	
r4/CmF	CTAATGGGTGCTTTAGTTGGATCAGAAAAACAGTGCCTCTGCCG	
r4RV	CGGGAACCCGTTAGGCCT	
r4FW2	CCTCTTCGGAAAACGCGCCATGACG	
r4RV2	CTCTGTCACACAAGGCGTCATCTCG	
yydDFW	TCATCAAAGAGAAGGAAACG	Construction of MGB625ΔyydD-yycN
yydD/CmR	CTAATGGGTGCTTTAGTTGCCAAATAATATTAAACTAGG	
yycN/CmF	CTGCCCCGTTAGTTGAAGGTGTACGTGAGATAAGACCG	
yycNRV	TAAATGGCATATAAAATGTC	
yydDFW2	CTGCCGAAACATCCTGGCAG	
yycNRV2	CGTCTTGGTAATAAGATAAG	
rapGFW	ATAGACATGCCGCTTTCCTT	Construction of MGB625ΔrapG-phrG
rapG/CmR	CTAATGGGTGCTTTAGTTGGTGAAACTCCTTTCTCTAGT	
phrG/CmF	CTGCCCCGTTAGTTGAAGATGAAAAACCCCCGCGGGAT	
phrGRV	ACGGTTGAAGATCTCGGTGA	
rapGFW2	GTTTTAGGATAACGTCCTGC	
phrGRV2	TGAATTCCGTTTTGGCGGGA	
pdpFW	TCCAGCGTAAAGATTGTCACC	Construction of MGB625Δpdp-rocD
pdp/CmR	CTAATGGGTGCTTTAGTTGGCTGATTCATACGTTAATTACAG	

rocR/CmF	CTGCCCCGTTAGTTGAAGTTGTTGGCTCCGTAATGAGAC	
rocRRV	GATTTTCCGTTCTTGAAGGGC	
pdpFW2	CATTTTCAGTTAAGTTATTTGCGG	
rocRRV2	TTGGGTCTTCATTCATCGTGG	
rocFFW	ACACGGCAAGCAGTCAAAAC	Construction of MGB625ΔrocF-rocR, MGB625ΔrocF-rocD or MGB625ΔrocR
rocF/CmR	CTAATGGGTGCTTTAGTTGTAAGAAAACCCCCGCACCCG	
rocR/CmF	CTGCCCCGTTAGTTGAAGTCCGGAGCAGGAAGCCTGAT	
rocRRV	GGGCGATCCCAGTAGATTCA	
rocFFW2	CCATGTCAGGCAATTTTACA	
rocRRV2	GGCCATTAACCCTGGGAACA	
rocD/CmF	CTGCCCCGTTAGTTGAAGATTTGAATTCCCCCTTGTTT	Construction of MGB625ΔrocF-rocD
rocDRV	GCTTCGCCTGAAGGCTGAGA	
rocDRV2	AAACAGGCCGGGCTGGTCGA	
rocR FW	ACATATCCGGAACAATGCCG	Construction of MGB625ΔrocR
rocR/CmR	CTAATGGGTGCTTTAGTTGTGTATGAACCTCCCTCAATT	
rocR FW2	TTCATCCGCAATAAACAAGA	
pdpFW	TCCAGCGTAAAGATTGTCACC	Construction of MGB625Δpdp-phrG
pdp/CmR	CTAATGGGTGCTTTAGTTGGCTGATTCATACGTTAATTACAG	
phrG2/CmF	CTGCCCCGTTAGTTGAAGTGAAGTCTAGGAAGAACGAGC	
phrG2RV	TTGGAATGCCAATGGATTTAGG	
pdpFW2	CATTTTCAGTTAAGTTATTTGCGG	
phrG2RV2	GTTGTCCGCAAGTCATCTTTG	
pdp/SpR	CACGAACGAAAATCGATGCTGATTCATACGTTAATTACAG	Construction of 874DEFR(spec)
phrG2/SpF	CAATAAACCCTTGCATATGTGAAGTCTAGGAAGAACGAGC	
rocABCFW	ATGATAAATAAGCCCGCAGC	Construction of 874DEFRΔrocABC
rocABC/SpR	CAATAAACCCTTGCATATGAAAAAGCTCTCCGGGAGGCC	
rocABC/SpF	CACGAACGAAAATCGATATGTAGTCCCCCTCGTGTTA	
rocABCRV	ATGGATGAGTACAGCCGGCT	
rocABCFW2	ACATACCGTAAAAACCAATC	
rocABCRV2	GAGGATCGCAAGGACGGGAA	
gudB FW	TGTTTCCCGCAGCAATAACA	Construction of Δ*gudB* strains
gudB/NmR	GCGCATTAACGGAATAAAGGGCTTCGCGTTTTAGAGGCTG	
gudB/NmF	TTTTTATTTTATAAACTCATTCCCCTCACATGCTCCCTTTCAGAG	
gudB RV	GCGGCATATCTGATCAGCAA	
gudB FW2	AAATGGACGCCCTGTTTCTT	
gudB RV2	CTCACATTGTGACTCTTTGC	
ahrC FW	GTTCAGGCGTTCCGGAT	Construction of 874ΔahrC
ahrC/Nm2R	CAAAACGCATACCATTTTGAAATTATTTGCCGGACTCC	
ahrC/Nm2F	TCCATTCACTATTCTCATTCCCTTGTAAGCACCTCTATTTCC	
ahrC RV	GTGGCAAATCGTATTAGA	
ahrC FW2	AGCAAATAGTAGGAGTTC	
ahrC RV2	AAAGAACGATTAGATGTATT	
argC FW	GATATGTTTTCGCTCGTA	Construction of 874ΔargC-F and 874ΔahrCΔargC-F
argC/SpR	CACGAACGAAAATCGATAACAAGTTCACCCTCTTG	
argF/SpF	CAATAAACCCTTGCATATGTCAAAAAACTGCTGAGCC	
argF RV	CTGCTTTTTCCGCCCCC	
argC FW2	AATCATCAGGCGCATGA	
argF RV2	CAACATGCTCAGAAGCT	
citB FW	AAAGAAGAGCCATCTTCT	Construction of Δ*citB* strains
citB/SpR	CACGAACGAAAATCGATTCTCCAAAATCCCCCTT	
citB/SpF	CAATAAACCCTTGCATATGTGCTTCGTGAAAAAATGAA	

citB RV	CCGCTGTCCTGAAGTAT	
citB FW2	AATGTTTTTGTCATTAAAATAA	
citB RV2	AAGTGGCTTGGAACATAT	
rocGFW	ACCTGTAAATGAGACAAAC	Construction of 874ΔrocG and 874DEFRΔrocG
rocG/SpR	CAATAAACCCTTGCATATGTTTGAGAAGCCTCCGCA	
rocG/SpF	CACGAACGAAAATCGATCTTTTTCACCTCATTGTTT	
rocGRV	ACGATCGGTTTTAACTGG	
rocGFW2	CGGAATGTAATTCAGAAC	
rocGRV2	CATCTTCGACTTTTTTTGC	
rocG/CmR	CTGCCCCGTTAGTTGAAGTTTGAGAAGCCTCCGCA	Construction of 874ΔrocG(cat)
rocG/CmF	CTAATGGGTGCTTTAGTTGCTTTTTCACCTCATTGTTT	
gltAB FW	TTTCCACGCGCTCTCACCTG	Construction of Δ*gltAB* strains
gltAB/EmR	CATGATACTGGGTTCTGACG	
gltAB/EmF	GCACTGATTGGTGTATCAAATCAGTGCAGCATATGGG	
gltAB RV	GCGTTTCTACAAACTCTTGGCATCATGTTCAAATTCAGG	
gltAB RV2	GGGAAATTCAAAAGCGGTTC	
gltAB FW2	CATTCGCGGAAGGCGCAAGC	
amyE.up-F	TGTTTGCAAAACGATTCAAAACCTCTTTAC	Construction of Δ*amyE*::*egl-237* strains
amyE.up-R	GATCAGACCAGTTTTTAATTTGTGTGTTTC	
amyE.down-F	GGATCCTCTAGAGTCGACCT	
amyE.down-R	AATGGGGAAGAGAACCGCTTAAG	
amyE-egl237.f	AATTAAAAACTGGTCTGATCAACAGGCTTATATTTAGAGGAAATTTCTTTTTAAATTG	
amyE-egl237.r	AGGTCGACTCTAGAGGATCCTCCAGTTATGCAAGAAAAAG	
dltB FW	TGCCTTCAATCAGGCGG	Construction of Δ*dltB* mutants
dltB/NmR	TTTTTATTTTATAAACTCATTCCCATGTTGTATGCTTGAAATC	
dltB RV	TCGTTGAATAATACAGATC	
dltB/NmF	GCGCATTAACGGAATAAAGGATTCTCGCTATTGTGATC	
dltB FW2	TTGAAGAGCTGAAGAAGT	
dltB RV2	TCACTTTCCACGTCTGA	
Egl-237-F.BamHI	TTGCggatccAACAGGCTTATATTTAG	Construction of pHYS237
Egl-237-R.BamHI	AACAACTCTggatccAGTTATGCAAG	
S237pMpm-R	TTTCCCCAACGGTTTCTTCATATTACCTCCTAAATATTTTTAAAGT	Construction of pHP237-K16
Mter-R.BglII	GGGagatctTCAGCGATCTATTTCTCTTTTTC	
S237p-F.BamHI	CCCggatccAACAGGCTTATATTTA	
S237pMpm-F	ACTTTAAAAATATTTAGGAGGTAATATGAAGAAACCGTTGGGGAAA	
S237ppp-F2(BamHI)	CCCGGATCCAACAGGCTTATATTTA	Construction of pHYK38
S237ppp- R2 (ALAA)	TTCAATCCATCTGCTGCAAGAGCTGCCGG	
K38matu-F2 (ALAA)	GCTCTTGCAGCAGATGGATTGAACGGTACG	
K38matu-R (XbaI)	TTGGTCTAGACCCCAAGCTTCAAAGTCGTA	
RocG.F.SalI	AAAAgtcgacTTACATTACAGCCGGCCAAAAAAAC	Cloning of *rocG*
RocG.R.SacI	AAAAgagctcTCATTAGACCCATCCGCGGAAACGC	
YVTAPF	TACACggatccAACGGTTATTCATTTATCGTTACATATTC	Cloning of *htrB* control region
YVTAPR	GTGTAgaattcGGCTCTTCACATCCTTTCAAC	

[a]Overlapping sequences for SOE-PCR are underlined and restriction enzyme recognition sites are indicated in lowercase.
[b]*cat*, chloramphenicol; *spec*, spectinomycin; *neo*, neomycin; *erm*, erythromycin;

Table 3. Primers used in real-time PCR analysis

Target gene	Forward primers (5'-3')	Reverse primers (5'-3')
gyrA	GGGACTGGAACGTGAAAAGA	CGTTGATCCACTCACCCTTT
rocA	TTGCTGCATCCTCTATCGTG	TTTCCGACATGGAAATCCTC
rocD	GAAGGGCGTAGCTGACAATC	ATGCAAGAGATCGGGAACAC
rocG	AACGGGACAGCTTTGGTATG	TTTCTGATGCCCGTCATGTA
argC	TATTCATCCAGCGGAGAAGG	TCCCATGGATGCTTTTCTTC
gltA	GGGCGTCGTAAAAGTGATGT	CTCCAACTTCAAAGGCTTGC
citB	GACGTATTCACCCGCTTGTT	GTGACTGAATCGCCGAATTT
sigA	CGGATTCCCGTTCATATGGT	GTCTTAGTTTCCGCAACGCT
egl-237	AACGGGTATTGGGTACAAGC	CTCCCTGCAAAGTCACTTTC
16Sr RNA	TCCGCAATGGACGAAAGTCT	ACGATCCGAAAACCTTCATCA
amyK38	CATCCGATGCATGCAGTTAC	GGTTCACGTACACGGATACA
htrA	GCAGCAAACGCAATCTGTTA	CTGATTTGGAGGACGGCTAA
htrB	ACCGGACAATTGATGTGGAT	CACCTTTGCCCAATTGATCT
nrgA	TTTTGCGCTTTACTCGTGTG	ACCCCGGAGGAAATATGAAC

Chapter 1: Elucidation of the mechanism underlying enhanced enzyme production in strain MGB874.

Background

Bacillus subtilis genome-reduced strain MGB874, which was derived from strain 168 and has a total genomic deletion of 874 kb (20.7%), exhibits enhanced production of recombinant enzymes. However, it is not clear how the genomic reduction resulted in the elevated enzyme production. Here, we attempted to elucidate the mechanism underlying the improved enzyme production

Results

1. Determination of gene deletions contributing to enhanced enzyme production.

Previously, we constructed a multiple-deletion mutant, strain MGB874, by stepwise introduction of 23 large-scale deletions of genomic regions, and found that exogenous enzyme production increased in proportion to the genomic deletion size (Morimoto et al., 2008). In addition, we detected a significant increase in the enzyme production level of strain MGB723, which was generated from strain MGB625 by deletion of the *pdp-rocR* region (nucleotides 4,049,059 to 4,147,133 in NCBI RefSeq NC_000964.3) (Figure 3A). Here, we attempted to determine which genes deleted in this region were involved in the enhanced production of enzymes by strain MGB874.

First, the *pdp-rocR* region was divided into four regions, r1, r2, r3, and r4 (Figure 3A), and each region was individually deleted from strain MGB625. The resulting mutant strains were transformed with pHYS237 to evaluate production of the cellulase Egl-237 (Hakamada et al., 2000). As cellulase activity was not detected in the culture broth of strains 168 and MGB874

harboring pHY300PLK (empty vector) in the assay conditions used in this study, the indirect effects of endogenous endoglucanase production could be excluded. As shown in Figure 3C, deletion of the r4 region from MGB625 resulted in enhanced Egl-237 production, which was similar to that of strain MGB874. The r4 region contained 16 genes, including the *rapG-phrG* operon, encoding one of the Rap-Phr extracellular peptide signaling systems (Ogura et al., 2003), and the *rocF-rocR* region, which includes the *rocDEF* operon and *rocR* gene that are involved in the arginine degradation pathway (Calogero et al., 1994; Gardan et al., 1995) (Figure 3B).

To determine which deleted genes in the r4 region contributed to the enhanced Egl-237 production, we performed targeted deletions of genes within the r4 region and found that deletion of the *rocF-rocR* region was associated with an increase in Egl-237 production (Figure 3C). Furthermore, we determined that deletion of the monocistronic *rocR* gene markedly increased Egl-237 production, whereas deletion of the *rocDEF* operon only slightly increased cellulase activity in the culture broth (Figure 3C).

We next evaluated Egl-237 production in strain 874DEFR, which was constructed by reintroducing *rocDEF* and *rocR* into MGB874, and found that cellulase activity in the growth medium was considerably lower than that detected for MGB874, and was nearly equivalent to that of wild-type strain 168 (Figure 3D). Conversely, Egl-237 production by strain 168ΔrocDEF-rocR, in which the *rocDEF-rocR* region was deleted, was approximately 1.2-fold higher than that by parental strain 168, although Egl-237 production by strain MGB874 was approximately 1.6-fold higher than that by the strain 874DEFR (Figure 3D). These data suggest that one of the 22 other regions missing from the 874DEFR genome or the extensive genome reduction itself enhanced the positive effect of the deletion of *rocDEF-rocR* on Egl-237 production in genome-reduced strain MGB874.

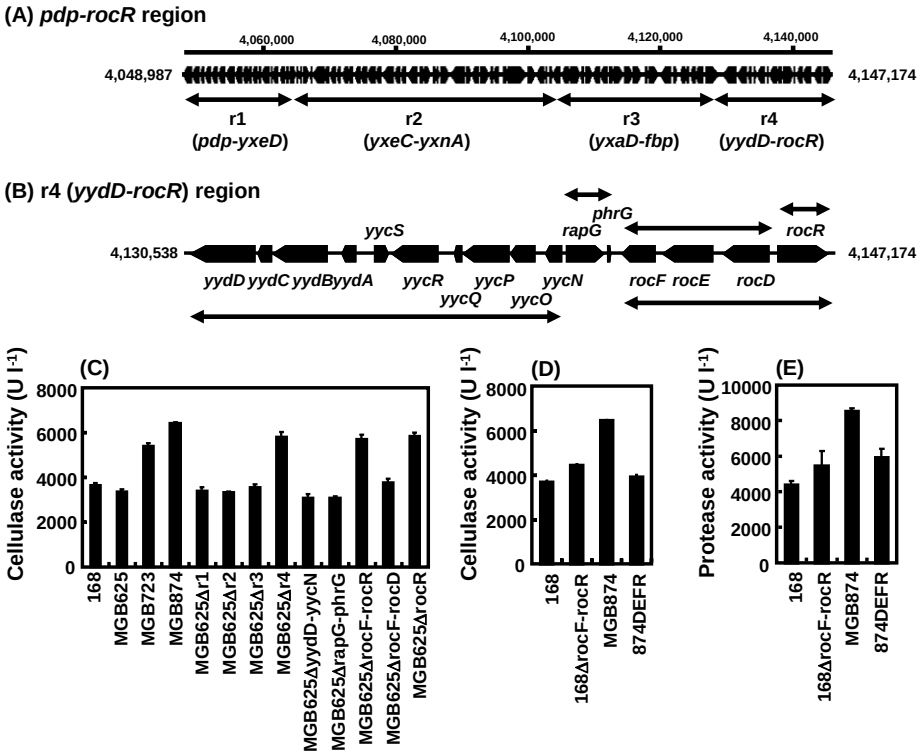

Figure 3. Determination of the deletion contributing to enhanced enzyme production in genome-reduced strains of *B. subtilis.*

(A) The *pdp-rocR* region deleted from MGB625 to construct MGB723. The newly deleted regions (r1, r2, r3, and r4) from MGB625 are indicated as arrows. (B) Clusters of genes contained in the r4 region. Arrows indicate the regions deleted from MGB625. (C) and (D) Cellulase activities cultured at 30 °C for 75 h in the growth media of *B. subtilis* derivative strains harboring pHYS237 for Egl-237 production. (E) Protease activities cultured at 30 °C for 75 h in the growth media of *B. subtilis* derivative strains harboring pHP237-K16 for M-protease production. The results presented are the means of three individual experiments. Error bars represent standard deviations (n = 3).

To verify whether deletion of the *rocDEF-rocR* region influenced the production of other enzymes, the levels of the alkaline protease, M-protease, were evaluated. As indicated in Figure 3E, the production of M-protease was also improved by deletion of the *rocDEF-rocR* region.

2. Changes in cell yield and specific enzyme productivity caused by *rocDEF-rocR* deletion.

To obtain insight into the enhancement of exogenous enzyme production by strain MGB874, we conducted time course analyses of cell yield and Egl-237 production. Cell yield was determined by the measurement of OD_{600} in the culture medium, which was correlated to cell dry weight (CDW). As we reported previously (Morimoto et al., 2008), the level of Egl-237 production in strain MGB874 was higher than that in strain 168, whereas here, the rates and yields of cell growth were comparable (Figures 4A and 4B). Thus, specific productivity (U g^{-1} h^{-1}), which was calculated by dividing the cellulase production rate (U l^{-1} h^{-1}) by CDW (g l^{-1}), was higher for strain MGB874 than for strain 168 (Figure 4C). In contrast, the cell yield at stationary phase and level of Egl-237 production in strain 874DEFR were lower than those in parental strain MGB874 (Figures 4A and 4B). However, the specific productivity (U g^{-1} h^{-1}) of strain 874DEFR was nearly equal to that of strain MGB874 and was higher than that of strain 168 (Figure 4C). The viable cell counts in stationary phase (40 h) were proportional to the cell yields for strains 168, MGB874, and 874DEFR (2.48 x 10^9, 2.23 x 10^9, and 2.32 x 10^9 CFU ml^{-1} OD_{600}^{-1}, respectively). Collectively, the specific productivities of the genome-reduced strains (MGB874 and 874DEFR) were higher than that for wild-type strain 168, although strain 874DEFR had a lower cell yield than strains 168 and MGB874. These results indicated that the *rocDEF-rocR* deletion increased the cell yield of strain MGB874, allowing the cell yield level of strain 168 to be reached, and that the deletion of other gene(s) or the genomic reduction itself was responsible for the higher specific productivity in strain MGB874. Therefore, the *rocDEF-rocR* deletion compensated for the decrease of cell yield that resulted from a prior deletion(s). Supporting these findings, the cell yield of strain MGB625 was lower than that of strain 168, and deletion of the *rocDEF-rocR* region in strain MGB625 increased the cell yield with the maintenance of high specific

enzyme productivity that was almost equal to that of strain MGB874 (Figure 5). Interestingly, deletion of the *rocDEF-rocR* region in strain 168 also increased the cell yield while maintaining the specific enzyme productivity (Figure 5).

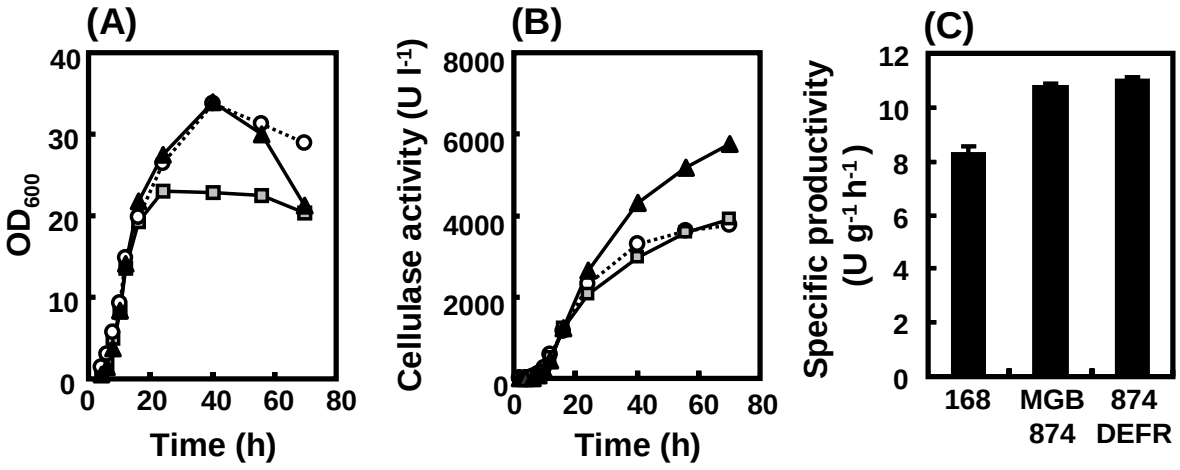

Figure 4. Growth characteristics of strains 168, MGB874, and 874DEFR producing cellulase Egl-237. Strains 168 (white circles), MGB874 (black triangles), and 874DEFR (gray squares) harboring pHYS237 were cultured for time course experiments. (A) Growth profiles. (B) Cellulase activities in the growth medium. (C) Specific productivities (U g^{-1} h^{-1}) calculated after 40 h of culture. Specific productivity (U g^{-1} h^{-1}) was calculated by dividing the cellulase production rate (U l^{-1} h^{-1}) by cell dry weight (CDW, g l^{-1}). The results presented are the means of three individual experiments. Error bars represent standard deviations (n = 3).

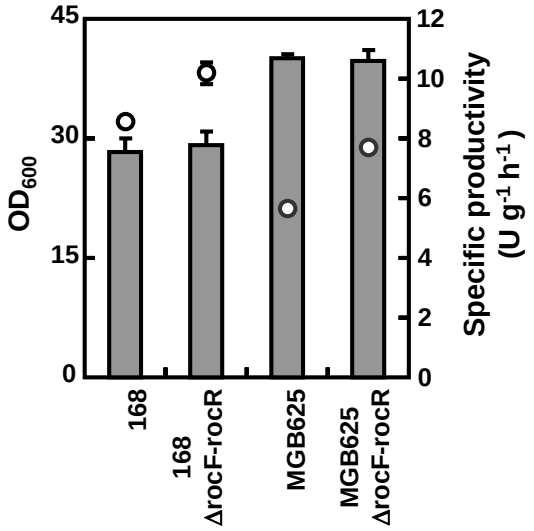

Figure 5. Contribution of *rocDEF-rocR* deletion to cell yields and specific productivities in strains 168 and MGB625. Strains 168, 168ΔrocF-rocR, MGB625, and MGB625ΔrocF-rocR were transformed with pHYS237 and then cultured in 2xL-Mal medium with shaking at 30 °C. The cell yield (open circles) and specific productivities (gray bars) were measured after 48 h of culture. The results presented are the means of three individual experiments. Error bars represent standard deviations (n = 3).

3. Molecular basis of enhanced Egl-237 production.

To determine whether the high specific productivities of Egl-237 in strains MGB874 and 874DEFR resulted from elevated mRNA levels, we determined the transcriptional levels of the Egl-237 gene (*egl-237*) and found that the levels of *egl-237* transcripts were higher for strains MGB874 and 874DEFR cells than for strain 168 cells during stationary phase (Figure 6A). Additionally, the *egl-237* transcript level from plasmid pHYS237 in strain MGB874 was slightly higher than that in strain 874DEFR (Figure 6A).

We also examined the pHYS237 plasmid copy number and promoter activity of *egl-237*. To estimate the promoter activity, we inserted a single copy of *egl-237* in the chromosomal *amyE* locus of strains 168, MGB874, and 874DEFR, and designated the resulting mutant strains as 168egl-237, MGB874egl-237, and 874DEFRegl-237, respectively. As indicated in Figure 6B and 6C, the plasmid copy numbers and transcript levels, respectively, from a single copy of

egl-237 in the genome-reduced strains were significantly higher than those in the wild-type strain during stationary phase. In addition, pHYS237 copy number and *egl-237* promoter activity in strain MGB874 were slightly higher than those in strain 874DEFR (Figures 6B and 6C).

The plasmid copy numbers in strains 168, MGB874, and 874DEFR harboring multi-copy plasmid pHYS237 were determined to be 5.0 x 10, 1.6 x 10^2 and 1.3 x 10^2 copies per cell, respectively, and the transcript levels from a single copy of *egl-237* in strains 168egl-237, MGB874egl-237, and 874DEFRegl-237 relative to that of *gyrA* were found to be 2.8, 1.5 x 10, and 8.4, respectively (Figure 6B and 6C). Thus, the estimated relative transcript levels of *egl-237*, which were calculated by multiplying the plasmid copy number by the transcript levels from a single copy of *egl-237*, were 1.4 x 10^2, 2.4 x 10^3, and 1.1 x 10^3 for strains 168, MGB874, and 874DEFR harboring pHYS237, respectively. However, the actual values were only 1.1 x 10^2, 3.5 x 10^2, and 2.6 x 10^2, respectively (Figure 6A; 24 h), which were lower than expected, suggesting that the transcript levels of *egl-237* in the genome-reduced strains might be saturated. Evaluation of the growth and enzyme characteristics of strains 168egl-237, MGB874egl-237, and 874DEFRegl-237 showed that higher specific enzyme productivities were also observed for a single copy of the *egl-237* gene in the genome-reduced strains, although the absolute cellulase production levels were decreased to approximately one-tenth of those in strains harboring pHYS237 (Figure 7).

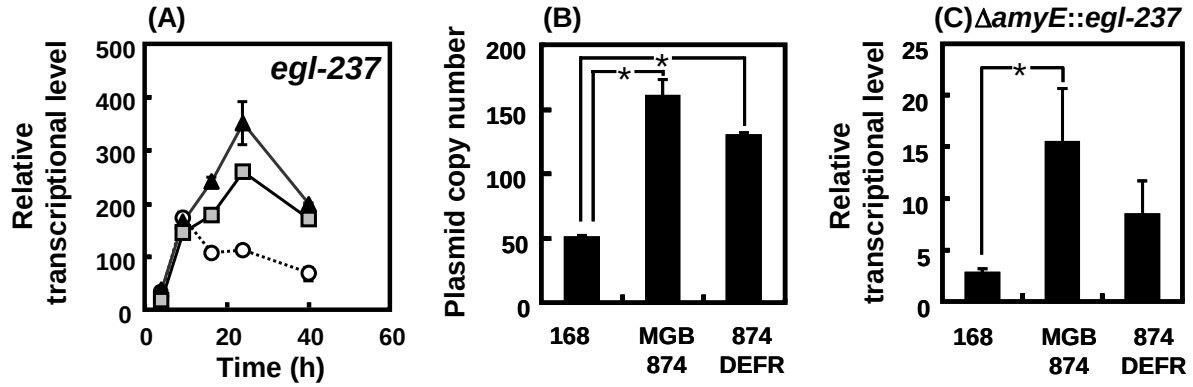

Figure 6. Transcriptional levels of cellulase Egl-237 and plasmid copy numbers of pHYS237. (A) Time course of transcription of *egl-237*. Strains 168 (white circles), MGB874 (black triangles), and 874DEFR (gray squares) harboring pHYS237. B) Plasmid copy numbers of pHYS237. The plasmid copy numbers were measured after 24 h of cultivation. (C) The transcriptional level of a single copy of *egl-237* integrated in the *amyE* locus of the *B. subtilis* chromosome. Strains were transformed with pHY300PLK (empty vector) and then cultured for 24 h. The results are the means of three individual experiments. Error bars represent standard deviations (n = 3). Asterisk (*) indicates a significant increase between two samples (t test; $P < 0.05$).

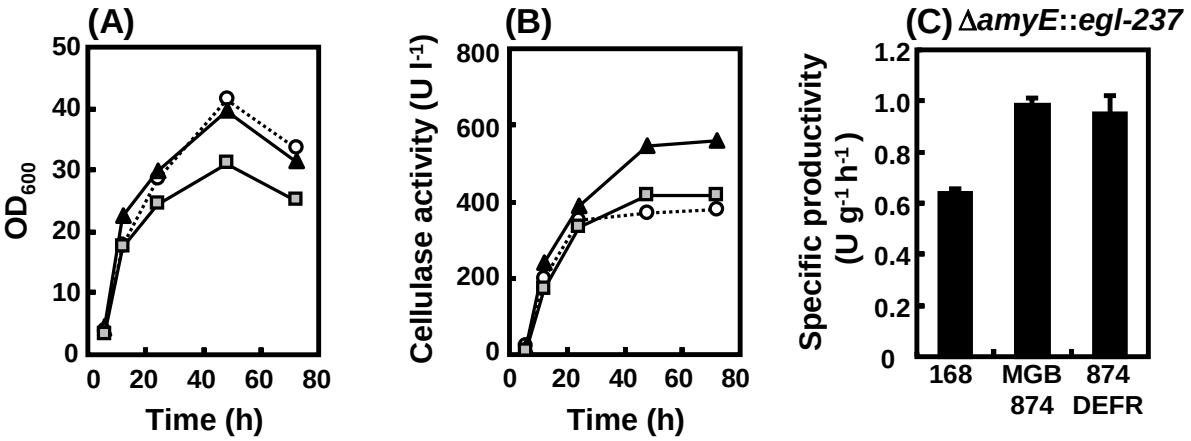

Figure 7. Growth and enzyme characteristics of single-copy mutants. Strains 168egl-237 (white circles), MGB874egl-237 (black triangles), and 874DEFRegl-237 (gray squares) were transformed with pHY300PLK and then cultured for time course experiments. (A) Growth profiles. (B) Cellulase activities in the growth medium. (C) Specific productivities (U g^{-1} h^{-1}) for strains 168egl-237, MGB874egl-237, and 874DEFRegl-237 calculated after 48 h of culture. The results presented are the means of three individual experiments. Error bars represent standard deviations (n = 3).

4. Metabolic changes caused by *rocDEF-rocR* deletion in strain MGB874.

RocR is a positive regulator for genes related to the arginine degradation pathway involving RocG (a major catabolic glutamate dehydrogenase) (Ali et al., 2003; Belitsky and Sonenshein, 1998, 1999; Calogero et al., 1994; Gardan et al., 1995, 1997), which also serves as a regulatory protein that inhibits GltC (Commichau et al., 2007a), a transcriptional regulator specific to the *gltAB* operon that encodes large and small subunits of glutamate synthase (GOGAT) (Bohannon and Sonenshein, 1989; Picossi et al., 2007) (Figure 8).

To investigate the influence of deletion of the *rocDEF-rocR* region on carbon and nitrogen metabolism, we measured extracellular and intracellular amino acid levels (Figure 9). Among the amino acids analyzed in the culture broth, a significant difference between the strains was only detected for arginine (Figure 9A). In the culture broth of strains 168 and 874DEFR, both arginine and glutamate were depleted before cells entered the stationary phase (Figure 9A). In contrast, in the culture medium of strain MGB874, the arginine level decreased gradually throughout the culture period due to the inactivation of arginine degradation pathway. Glutamine was below the limit of detection in the culture broths of strains 168 MGB874 and 874DEFR.

Additionally, to investigate the influence of deletion of the *rocDEF-rocR* region on intracellular amino acid levels, cells were harvested from each culture at 16 h (Figure 9A-a) and 40 h (Figure 9A-b), and were subjected to amino acid analyses (Figure 9B). At the two examined time points, the intracellular glutamate level in strain MGB874 cells was significantly larger compared to that in strains 168 and 874DEFR cells ($P < 0.05$). However, the intracellular glutamine level in strain MGB874 cells was marginally larger than in strain 168 cells at 16 h ($P < 0.1$) and was significantly smaller than in the other two strains at 40 h ($P < 0.05$). The intracellular arginine levels were below the limit of detection.

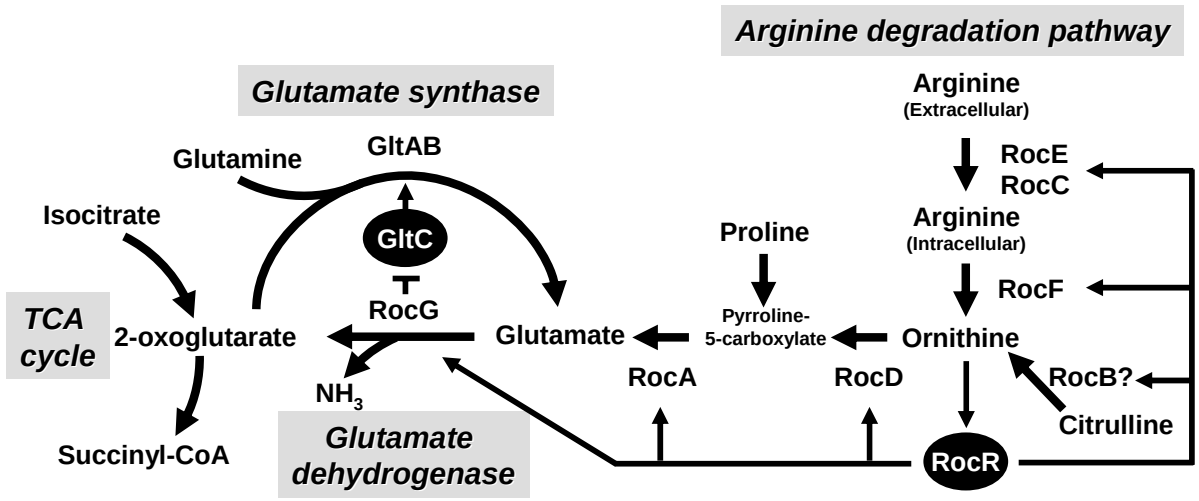

Figure 8. Major reactions and regulatory controls involved in the arginine utilization pathway. The enzymes and transporters shown in this figure are indicated by the names of the corresponding genes as follows: ArtPQM, high-affinity arginine transporter; RocE and RocC, putative arginine permeases; RocF, arginase; RocB, putative citrullinase; RocD, ornithine aminotransferase; RocA, Δ1-pyrroline-5-carboxylate dehydrogenases; RocG, glutamate dehydrogenase; and GltAB, glutamate synthase. RocR is a positive regulator of the genes involved in the arginine degradation pathway and is activated in the presence of ornithine. GltC is a positive regulator of *gltAB* and is inhibited by the glutamate dehydrogenase RocG..

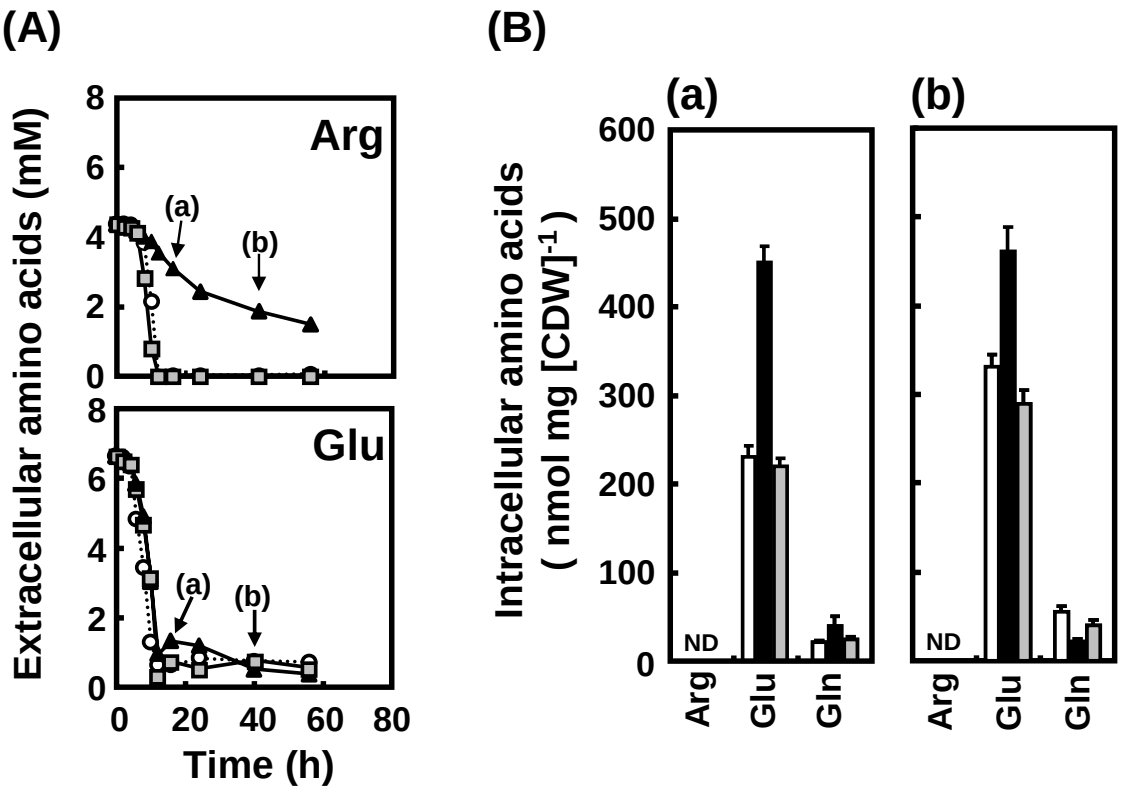

Figure 9. Extracellular and intracellular amino acid concentrations in strains 168, MGB874, and 874DEFR. Strains 168, MGB874, and 874DEFR harboring pHYS237 were cultured for time course experiments. (A) Concentrations of amino acids in the growth media. Concentrations of L-arginine (Arg), L-glutamate (Glu), and glutamine (Gln) in growth media of strains 168 (white circles), MGB874 (black triangles), and 874DEFR (gray squares) were measured by HPLC. Gln was undetectable in the culture media. Arrows indicate the times of cell collection for determination of intracellular amino acid levels. (B) Intracellular amino acid levels of strains 168 (white), MGB874 (black) for 16 h (a) and 40 h (b). Intracellular amino acids were extracted with methanol and measured by GC. The data are presented in nmol per mg of CDW. The mean CDW was 0.300 mg ml^{-1} OD_{600}^{-1} and did not vary by more than 10% between strains 168, MGB874, and 874DEFR. The results presented are the means of three individual experiments. Error bars represent standard deviations ($n = 3$). Asterisk (*) indicates a significant increase between two samples (t test; $P < 0.05$). ND: not detected.

5. Expression levels of genes related to arginine and glutamate metabolism.

To understand the influence of the deletion of the *rocDEF-rocR* region on metabolism in greater detail, changes in the expression levels of genes related to arginine and glutamate

metabolism were monitored (Figure 10). RNA samples prepared from the cultures of strains 168, MGB874, and 874DEFR at different stages of growth were subjected to qRT-PCR analysis using the specific primer sets shown in Table 3. The metabolic changes in MGB874 cells are illustrated in Figure 11, with reference to these results and the data of tiling array analyses reported previously (Barbe et al., 2009).

(i) Arginine metabolism. In strain MGB874 cells, deletion of the *rocDEF-rocR* region would cause impairment of the arginine degradation pathway, and the arginine remaining in the culture medium would likely lead to repression of the arginine synthetic pathway by activation of transcriptional factor AhrC. Indeed, we found that expression levels of *rocA* and *rocD* of the *rocABC* and *rocDEF* operons, respectively, which are related to the arginine degradation pathway, and *argC* of the *argCJBD-carAB-argF* operon, which is related to the arginine synthetic pathway, were markedly low in strain MGB874 cells throughout the culture period (Figure 10). In contrast, in strains 168 and 874DEFR cells, *rocA* and *rocD* were expressed transiently during the arginine consuming phase, and *argC* was expressed after depletion of arginine in the culture broth (Figures 9A and 10). As arginine synthetic enzymes convert glutamate to arginine-related compounds (Figure 11), their repression in strain MGB874 cells would contribute to maintenance of intracellular glutamate levels (Figure 9B).

(ii) Aconitase. The expression of *citB* was reported to be repressed by arginine catabolism (Blencke et al., 2006), in which 2-oxoglutarate generated from arginine competitively repressed the reaction of citrate synthase (CitZ), leading to the repression of *citB* by CcpC in the absence of the effector citrate (Cruz Ramos et al., 2000; Sonenshein, 2007) (Figure 11). Consistent with this previous observation (Blencke et al., 2006), the transcriptional level of *citB* in MGB874 cells was found to be 2-fold higher than that in 874DEFR cells at 24 h (Figure 10). Unexpectedly, however, after 24 h of culture, the expression level of *citB* in 874DEFR was higher than that in 168 cells (Figure 10), despite complete restoration of the

arginine degradation pathway in strain 874DEFR. Although the mechanism is unclear, the deletion of the *rocDEF-rocR* region appears to have partly contributed to the high level of *citB* expression in MGB874. It is possible that the activation of aconitase *citB* might contribute to not only the generation of reducing power through the TCA cycle, but also to improvement of metabolic flux from carbon sources to glutamate synthesis (Figure 11).

(iii) Glutamate dehydrogenase. The major glutamate dehydrogenase RocG was strongly repressed in strain MGB874 cells, as expected by deletion of the *rocR* gene (Figure 10). In contrast, a second cryptic glutamate dehydrogenase gene, *gudB*, was constitutively expressed in strain 168, MGB874, and 874DEFR cells (Figure 10). Previously, Belitsky *et al*. (Belitsky and Sonenshein, 1998) reported that the GudB protein in laboratory *Bacillus subtilis* strains contains an insertion of 3 aa (9 bp) with respect to the common ancestral GluDH sequence, and that the enzyme activity of GudB is extremely low or undetectable. In agreement with this observation, sequence analysis of the *gudB* alleles in strains 168, MGB874, and 874DEFR revealed the presence of the 9-bp insertion mutation, and deletion of the *gudB* gene minimally influenced the cell yield and production levels of Egl-237 compared to the parental strains. These results suggested that GudB in strains 168, MGB874, and 874DEFR was inactive, although its expression was constitutively high. Therefore, the deletion of *rocR* resulted in decreased expression of the major catabolic glutamate dehydrogenase RocG and likely contributed directly to the increased intracellular glutamate levels in strain MGB874 cells (Figure 11).

(iv) Glutamine synthetase-Glutamate synthase (GS-GOGAT) pathway. In MGB874 cells, the first gene of the glutamate synthase (GOGAT) operon, *gltAB*, was abundantly expressed (Figure 10), likely due to the repression of *rocG* expression (Figures 8 and 11). The activation of *gltA* may have significantly contributed to the increase in intracellular glutamate levels observed during the stationary phase (Figure 9B). The transcriptional levels of the

glutamine synthetase (GS) gene *glnA* were also higher for strain MGB874 than those for strains 168 and 874DEFR at 24 and 40 h (Figure 10). Upon activation of the glutamate synthetic pathway (GltAB), conversion of glutamine to glutamate would be expected to decrease the intracellular glutamine level (Figure 9B-b), and *glnA* expression would be de-repressed by inactivation of transcriptional factor GlnR in the absence of glutamine (Fisher, 1999; Fisher and Wray, 2006). Collectively, the decreased expression of *rocG* in strain MGB874 resulted in activation of the genes encoding the GS-GOGAT pathway during the stationary phase (Figure 11).

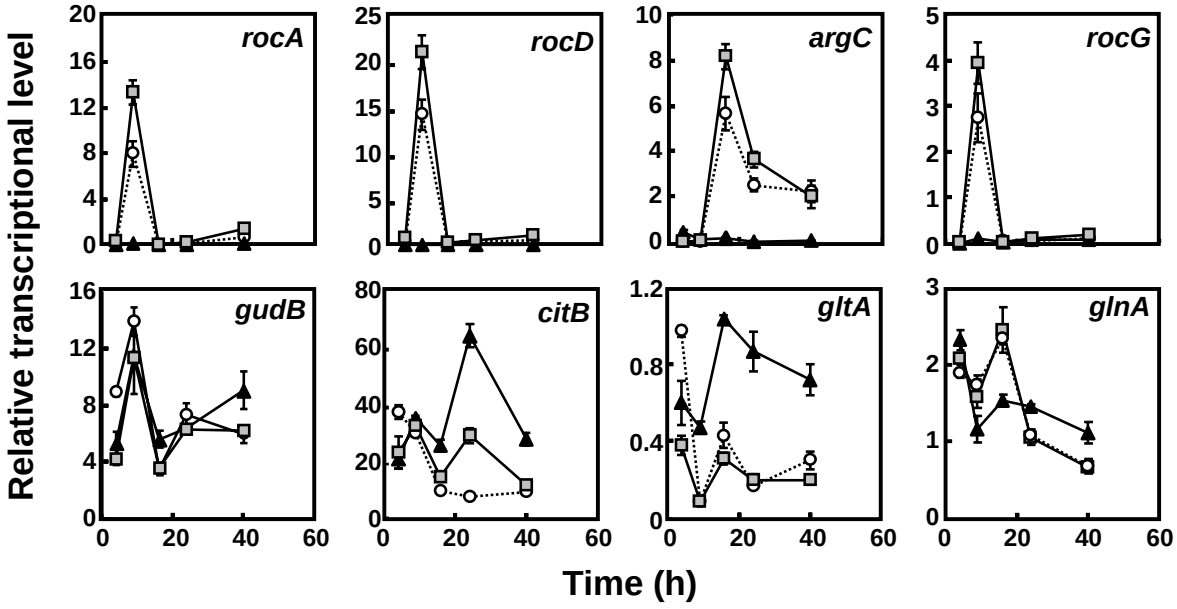

Figure 10. Time course of transcription during growth of *B. subtilis*. Strains 168 (white circles), MGB874 (black triangles), and 874DEFR (gray squares) harboring pHYS237 were cultured for time course experiments. Transcript levels were determined by quantitative RT-PCR using specific primers for *gyrA*, *rocA*, *rocD*, *argC*, *citB, rocG*, *gudB, gltA*, and *glnA* (Table 3). Among these genes, *rocA*, *rocD*, *argC*, and *gltA* are the first genes of the operons *rocABC*, *rocDEF*, *argCJBD-carAB-argF*, and *gltAB*, respectively. The transcriptional levels are expressed relative to that of *gyrA*. The results presented are the means of three individual experiments. Error bars represent standard deviations (n = 3).

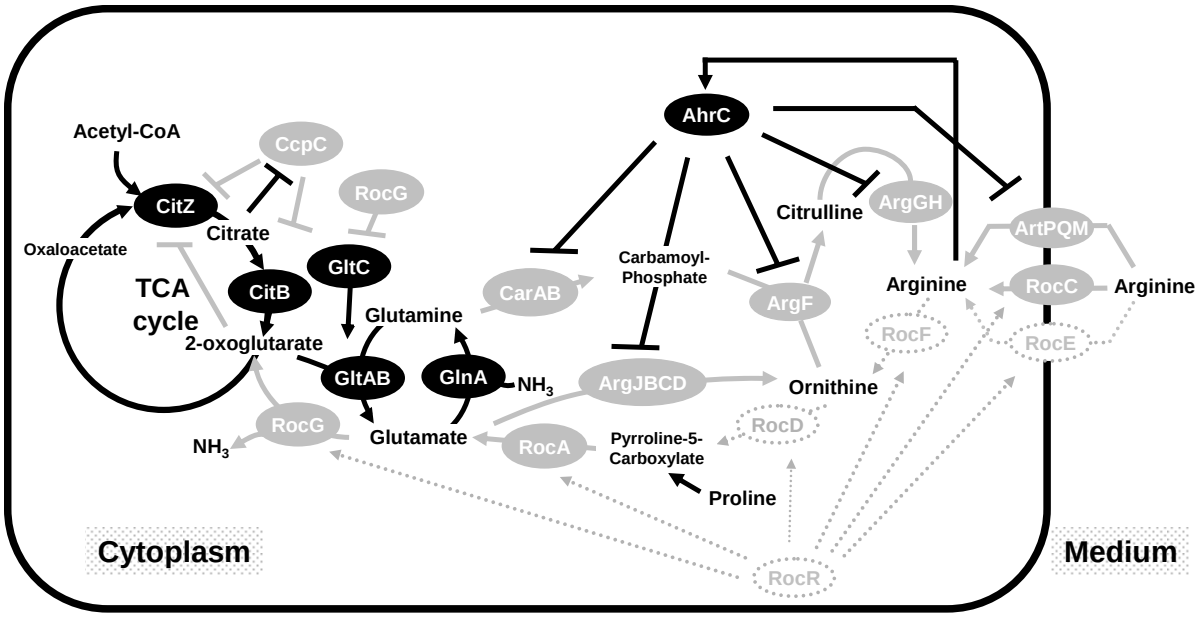

Figure 11. Illustration of the proposed intersection between nitrogen and carbon metabolism in MGB874 during the stationary phase. Proteins are shown as circles and their names are indicated. Open gray circles indicate the corresponding proteins of genes that were deleted in strain MGB874. Closed black and gray circles indicate proteins whose expression or function are activated and repressed, respectively, in MGB874, in comparison to wild-type strain 168. The tiling array data reported previously (Morimoto et al., 2008) were used as a reference. Deletion of the *rocDEF-rocR* region resulted in not only the inactivation of the arginine degradation pathway, but also the repression of the genes related to the arginine synthetic pathway and high-affinity arginine transporter ArtPQM (Makarova et al., 2001). In addition, reduced expression of *rocG* due to the absence of transcriptional activator RocR resulted in the activation of the genes encoding aconitase (CitB) and glutamate synthase (GltAB).

6. Contribution of deletion of genes related to arginine and glutamate metabolism in strain MGB874 to cell yield and specific productivity.

In MGB874 cells, the deletion of *rocR* induced considerable changes in metabolism and resulted in an increase in_intracellular glutamate levels, which may have contributed to the improvement of cell yield. We further examined the contribution of each metabolic gene related to glutamate metabolism on cell yield and specific protein productivity by constructing several deletion mutants.

(i) Arginine metabolism. The deletion of *ahrC*, encoding the repressor of the *argCJBD-carAB-argF* operon, increased the expression level of *argC* in strain MGB874 to a level comparable to that in strain 874DEFR (Figure 12A-b) and decreased cell yield and specific productivity (Figure 12A-a). However, the additional deletion of the *argCJBD-carAB-argF* operon in the *ahrC* mutant of MGB874 recovered the reduced cell yield and specific productivity (Figure 12A-a). Therefore, inhibition of the conversion of glutamate to arginine is essential for the improved cell yield in strain MGB874.

(ii) Aconitase. The deletion of *citB* caused severe growth inhibition in the genome-reduced strains MGB874 and 874DEFR; thus, the direct contribution of *citB* expression to Egl-237 production could not be investigated (Figure 12B). Growth inhibition following *citB* inactivation also occurred in wild-type strain 168, suggesting that *citB* is an essential gene for cell growth in *Bacillus subtilis* under the cultivation conditions used in this study.

(iii) Glutamate dehydrogenase. The deletion of *rocG* resulted in increases in cell yield in both strains MGB874 and 874DEFR (Figure 12C). However, specific productivities were significantly decreased in these *rocG* mutants. We found that this phenomenon was due to the impairment of Egl-237 secretion caused by a drastic decrease of external pH in the growth media of the *rocG* mutants, and that the high specific productivities in these strains could be maintained by controlling the external pH (Please refer to Chapter 3 in this thesis)

Belitsky *et al*. (Belitsky et al., 2004) reported that even in the absence of the activator RocR, *rocG* is expressed due to readthrough transcription from the upstream *yweA* promoter. Therefore, *rocG* is likely expressed at low levels in strain MGB874. The low-level expression of *rocG* is expected to play a crucial role in the control of cell yield, as the deletion of *rocG* increased the cell yield of strain MGB874 (Figure 12C). In addition, the deletion of *rocG* in strain 874DEFR significantly increased the cell yield to a level similar to that of strain MGB874ΔrocG. Based on these results, the decreased expression of *rocG* by deletion of the *rocR* gene appears to be the main underlying factor for improving the cell yield of strain MGB874.

(iv) Glutamine synthetase-Glutamate synthase (GS-GOGAT) pathway. The deletion of *gltAB* decreased the cell yields of strains MGB874 and 874DEFR, but did not markedly affect specific productivities (Figure 12C). As mentioned above, the expression of the *gltAB* operon is indirectly inhibited by RocG (Commichau et al., 2007a). Therefore, the activation of *gltAB* due to the decreased expression of *rocG* would contribute to the improvement of cell yield of strain MGB874.

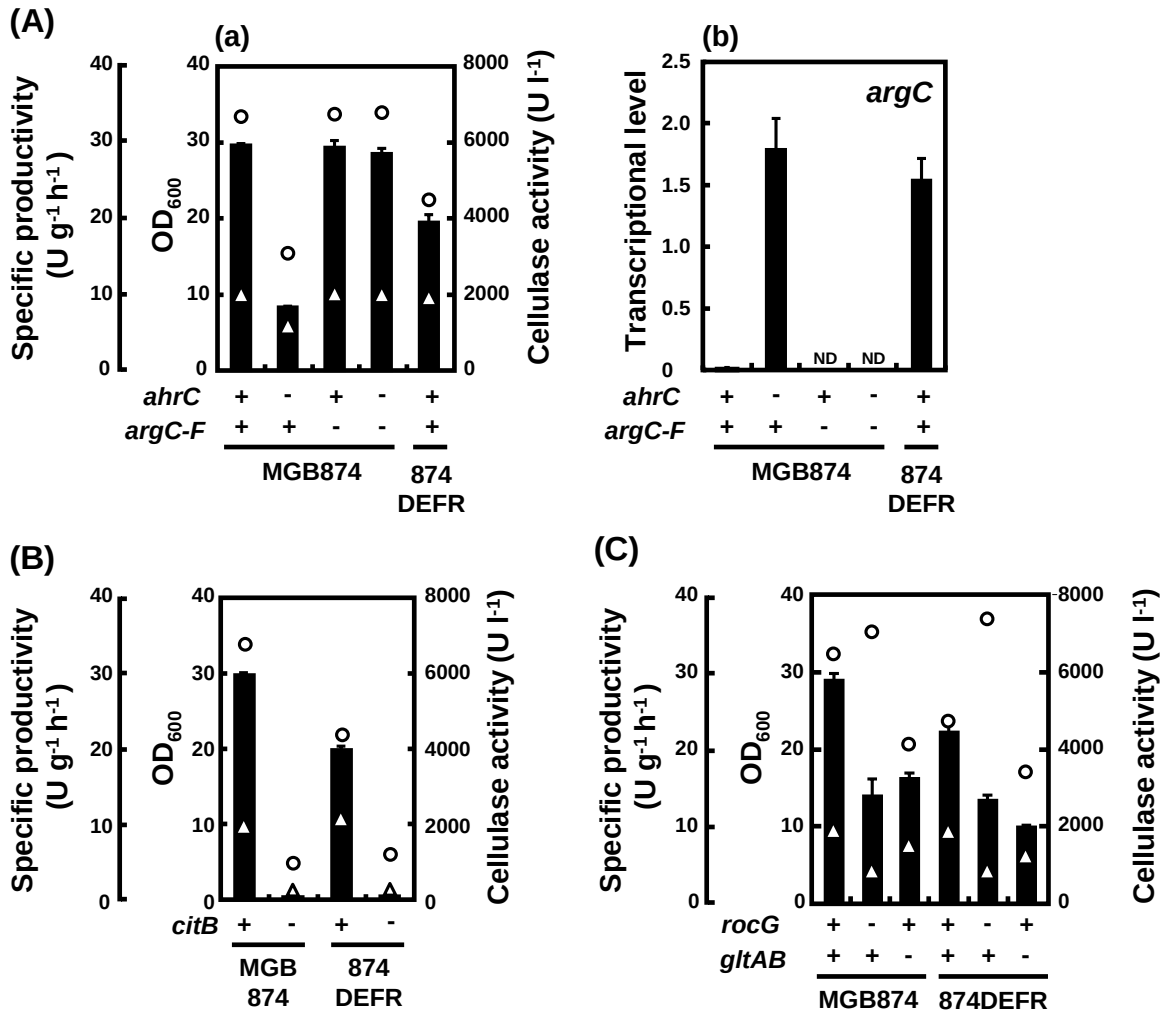

Figure 12. Contribution of the *argCJBD-carAB-argF* operon, *citB* gene, *rocG* gene, and *gltAB* operon to cell yield, Egl-237 production, and specific productivity. Strains MGB874 and 874DEFR harboring pHYS237 were cultured. The cell yield (open circles, 48 h), specific productivities (open triangles, 48 h), and cellulase activities (black bars, 72 h) in the growth media in the presence (+) or absence (–) of the corresponding genes were measured. (A) (a) Contribution of the *argCJBD-carAB-argF* operon. (b) Transcript levels of *argC*, the first gene of the *argCJBD-carAB-argF* operon, were determined by quantitative RT-PCR and are expressed relative to that of *gyrA*. (B) Contribution of the *citB* gene. (C) Contribution of the *rocG* gene and *gltAB* operon. The results presented are the means of three individual experiments. Error bars represent standard deviations (n = 3).

7. Effects of glutamate feeding on cell yield and Egl-237 production.

From the metabolic and transcriptomic analyses, the maintenance of intracellular glutamate level resulting from deletion of the *rocDEF-rocR* region was strongly suggested to improve cell yield and enhance Egl-237 production in strain MGB874. Therefore, we evaluated the effects of glutamate feeding on cell yields, Egl-237 production, and specific productivities in strains 168, MGB874, and 874DEFR. The feeding of sodium glutamate at a final concentration of 20 mM after depletion of glutamate in the culture broth led to increases in cell yield and Egl-237 production of all strains (Figure 13). However, glutamate feeding had little effect on the specific productivities (U g^{-1} h^{-1}) and intracellular glutamate levels of the three strains, indicating that intracellular glutamate concentrations are not directly proportional to cell yield. We also measured the extracellular pH under glutamate-feeding conditions and observed that the pH of growth media was not significantly influenced by glutamate feeding

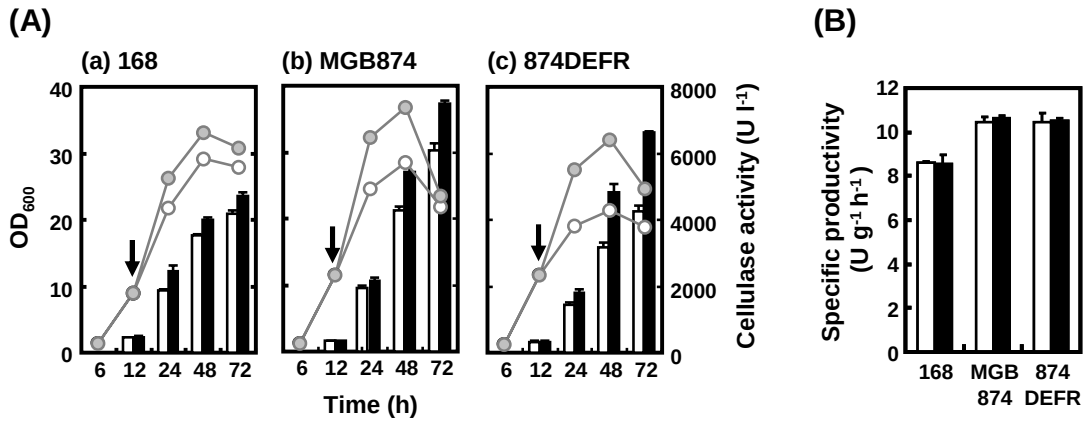

Figure 13. Effects of glutamate feeding on cell yield, Egl-237 production, and specific productivity in *B. subtilis* strains 168, MGB874, and 874DEFR. Strains 168 (a), MGB874 (b), and 874DEFR (c) harboring pHYS237 were cultured. (A) Cell yields and cellulase activities in the growth medium. Circles indicate cell yield (OD_{600}) and bars indicate cellulase activities. Arrows indicate when sodium chloride (open gray circles and white bars) or sodium L-glutamate (closed gray circles and black bars) was added to a final concentration of 20 mM. (B) Specific productivities for strains 168, MGB874, and 874DEFR in medium supplemented with sodium chloride (white bars) or sodium L-glutamate (black bars). Specific productivities (U g^{-1} h^{-1}) were calculated after 48 h of culture. The results presented are the means of three individual experiments.

Discussion

To our knowledge, *B. subtilis* strain MGB874 is the first reported genome-reduced strain to serve as an efficient host for the production of recombinant proteins. Here, we demonstrated that the combined effects of improved cell yield and increased specific productivity enhance recombinant enzyme production in MGB874 cells. Genetic analyses revealed that deletion of the *rocDEF-rocR* region in strain MGB874 was responsible for the improved cell yield and maintained the high specific productivity of genome-reduced strain MGB625 (Figure 4).

The high specific productivity in the genome-reduced strains is likely attributable to the high transcriptional levels of *egl-237* from multi-copy plasmid pHYS237 compared to the wild-type strain, which likely due to increases in the plasmid copy number and promoter

activity of *egl-237* (Figure 6). These results imply at least two independent effects of genome reduction on specific productivity. Plasmid pHYS237 was derived from plasmid pUB110 (McKenzie et al., 1986), whose copy number in *B. subtilis* decreases in stationary phase compared with that in exponential phase (Nyberg et al., 1985). In addition, the *egl-237* promoter contains the consensus sequence of a sigma A-type vegetative promoter (Hakamada et al., 2000). Previously, we reported that the activation of sporulation-specific sigma factors was delayed in MGB874 cells, suggesting that the transition state is extended in strain MGB874 compared to wild-type strain 168 (Morimoto et al., 2008). Therefore, although further experiments are needed, the increased plasmid copy number and promoter activity of *egl-237* may be attributable to the prolonged maintenance of the vegetative state in MGB874 cells.

Deletion of the *rocDEF-rocR* region in strain MGB874 not only inactivated the arginine degradation pathway, but also caused other considerable metabolic changes, including repression of the arginine synthetic pathway (*argCJBD-carAB-argF* operon) and glutamate dehydrogenase (*rocG*), and activation of aconitase (*citB*) and the GS-GOGAT pathway (*glnA* and *gltAB*) (Figures 10 and 11). The drastic changes in nitrogen metabolism increased the intracellular glutamate level and may have contributed to the improved cell yield in strain MGB874. Glutamate is an important carbon source of 2-oxoglutarate and is the main nitrogen source for the synthesis of nearly all N-containing compounds (Belitsky, 2002). Additionally, glutamate serves as a counterbalance anion to the internal pool of K^+ and is an essential cellular osmolyte (Csonka and Hanson, 1991). Yan *et al*. (Yan et al., 1996) reported that glutamate deficits result in a suboptimal K^+ pool and growth defects in *Salmonella typhimurium*. However, we found that while the intracellular glutamate levels were not affected upon glutamate feeding, cell yields of the genome-reduced strains were increased, suggesting that intracellular glutamate levels as an anion pool are not proportional to

increases in cell yield. Therefore, an increased supply of glutamate by enhanced glutamate metabolism is expected to improve the cell yield of strain MGB874. Glutamate is considered unnecessary as a carbon source in growth medium containing sufficient maltose. Thus, we favor the hypothesis that enhanced metabolism of glutamate leads to increased flux to the increased synthesis of other amino acids via transamination (Belitsky, 2002), resulting in enhanced cellular protein synthesis and corresponding increases of cell yield. Additionally, it is also possible that the increased glutamate supply modulates the stringent response, which is a stress response to amino-acid starvation conditions and represses the proliferation of cells until nutrient conditions improve (Eymann et al., 2002). Jung *et al*. (Jung et al., 2004) reported that the addition of glutamate to culture medium enhanced recombinant *Thermus* maltogenic amylase (ThMA) production and increased the growth rate of *E. coli* by overcoming the stringent response. Therefore, enhanced glutamate metabolism might relax the stringent response, leading to the improvement of cell yield of strain MGB874.

Glutamate feeding significantly improved the cell yield of strain 874DEFR, indicating that a sufficient glutamate supply from the culture medium could preclude the positive effects of *rocDEF-rocR* deletion on cell yield and enzyme production. However, in practical terms, the deletion of *rocDEF-rocR* is a cost-effective strategy for improving enzyme production, because high enzyme yields were obtained using the relatively simple 2xL-Mal growth medium without supplementation.

For further enhancement of recombinant enzyme production in strain MGB874, it is necessary to improve three factors: transcript levels of the target gene, specific productivity, and cell yields. Firstly, the increased plasmid copy numbers and promoter activities did not reflect on the actual transcript levels of *egl-237* in the genome-reduced strains (Figure 4). Overcoming this saturation of transcript levels may be important for further improvement of enzyme production. Secondly, the increased transcriptional level caused by deletion of the

rocDEF-rocR region was not reflected in the specific productivity of strain MGB874, which was nearly equal to that of strain 874DEFR (Figures 4 and 6A). Therefore, it is also important to overcome this rate-limiting factor, which might occur in the post-transcriptional phase and may be associated with secretion processes. Finally, although the deletion of *rocDEF-rocR* actually compensates for the decrease of cell yield in the genome-reduced strains, which was the result of the 17 regions missing from the MGB625 genome, it would be useful to identify the nature of this defect in the future work. Additionally, as the cell yields of strains 874DEFRΔrocG and MGB874ΔrocG were similar, other restriction factors for increasing the cell yield might exist in a considerably high cell yield in the *rocG* mutant.

In conclusion, we revealed that two factors contribute to the high enzyme production in genome-reduced strain MGB874: increased specific productivity and improved cell yield. The combined effect of the improvement of cell yield by deletion of the *rocDEF-rocR* region and the increase in specific productivity by the deletion of other genomic regions enhances enzyme production in strain MGB874. We also found that the effect of *rocDEF-rocR* deletion on enzyme production is more pronounced in MGB874 cells than in wild-type 168 cells. As full enzyme overproduction in strain MGB874 could not be achieved by single deletion of the *rocDEF-rocR* region, a multiple-deletion strategy may be necessary for the improved production of beneficial substances in *B. subtilis*. Future research to improve cell yield and increase specific productivity is expected to lead to further enhancement of Egl-237 production in strain MGB874 (Please refer to Chapter 3 in this thesis).

Chapter 2: Investigation of the suitability of strain MGB874 for the production of α-amylase

Background

Here, we investigated the suitability of strain MGB874 for the production of novel alkaline α-amylase. α-Amylase (α-1,4-glucan-4-glucanohydrolase, EC3.2.1) is an important enzyme in the food and detergent industries. We previously isolated a novel α-amylase, AmyK38 (55,097 Da), from alkaliphilic *Bacillus* sp. strain KSM-K38 (Hagihara et al., 2001b). AmyK38 has several unique properties, including high activity at alkaline pH and strong resistance to chemical oxidants. In addition, although α-amylases are generally metalloenzymes that contain at least one activating and stabilizing Ca^{2+} ion (Vallee et al., 1959), AmyK38 does not associate with Ca^{2+} ions; rather, its enzyme activity depends on the existence of Na^{+} ions and is not inhibited by chelating reagents. Due to these characteristics, AmyK38 would likely be an advantageous component of laundry and dishwashing detergents, which are alkaline solutions and typically contain bleach and chelating agents. However, improvement of production levels of AmyK38 is a necessary prerequisite for its commercial use, since strain KSM-K38 produces AmyK38 at markedly low levels (30 mg l^{-1}) (Hagihara et al., 2001b).

In *B. subtilis*, the overproduction of α-amylases from *Bacillus licheniformis* (AmyL) and *Bacillus amyloliquefaciens* (AmyQ) provokes a CssRS dependent secretion stress response (Darmon et al., 2002; Hyyrylainen et al., 2001), which represents a significant bottleneck for high-level enzyme production (Figure 14). The misfolded or aggregated forms of these α-amylases at the membrane-cell wall interface is thought to be detected by the membrane sensor protein CssS (Hyyrylainen et al., 2001), which then activates the response regulator

CssR through phosphorylation. Consequently, activated CssR leads to increased transcription of *htrA* and *htrB*, which encode the putative membrane-bound proteases HtrA and HtrB, respectively (Darmon et al., 2002).

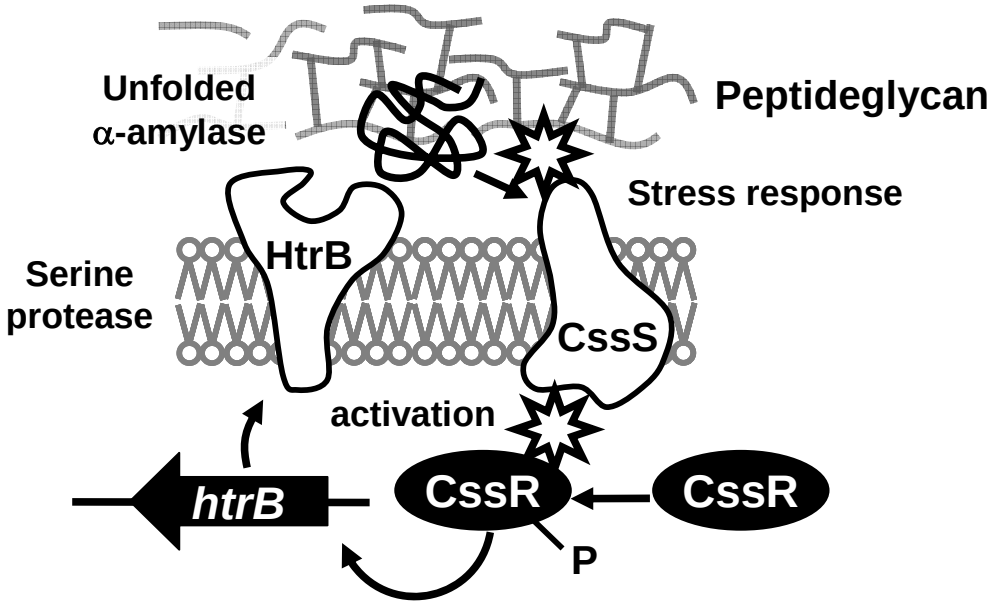

Figure 14. Secretion stress response in *Bacillus subtilis*. In *B. subtilis*, the overproduction of α-amylases provokes a CssRS dependent secretion stress response. The misfolded or aggregated forms of these α-amylases at the membrane-cell wall interface is thought to be detected by the membrane sensor protein CssS, which then activates the response regulator CssR through phosphorylation. Consequently, activated CssR leads to increased transcription of *htrA* and *htrB*, which encode the putative membrane-bound proteases HtrA and HtrB, respectively.

Previous studies have shown that inactivation of the *dlt* operon, which is involved in the D-alanylation of wall teichoic acids, leads to the stabilization and increased production of AmyQ in *B. subtilis*, likely due to increased negative charge density in the cell wall (Hyyrylainen et al., 2000). Furthermore, inactivation of the *dlt* operon led to a strongly reduced secretion stress response by the overproduction of AmyQ as compared to the wild-type strain (Hyyrylainen et al., 2007). Thus, impaired D-alanylation appears to be an

effective modification to lower secretion stress responses and enhance α-amylase production in *B. subtilis*.

Hagihara et al. (Hagihara et al., 2001a) reported that the amino acid sequence of AmyK38 exhibits moderate overall identity with AmyL (62.8%) and AmyQ (59.5%). However, it is not clear whether the overproduction of AmyK38 provokes a secretion stress response in *B. subtilis*. Here, we investigated the production and secretion stress levels of AmyK38 in genome-reduced strain MGB874.

Results and Discussion

1. Genome reduction significantly decreased production of AmyK38.

We first evaluated the production levels of exogenous AmyK38 in wild-type strain 168 and a series of multiple-deletion mutants using plasmid pHYK38 directing the overexpression of the AmyK38 protein. After 72 h cultivation in 2xL-Mal medium, the amylase activity in the culture broth of each strain was measured (Figure 15). As amylase activity was barely detected in the culture supernatant of *B. subtilis* harboring pHY300PLK (empty vector), the indirect effects of endogenous amylase production were considered to be negligible under the assay conditions used in this study. In contrast to our previous report (Morimoto et al., 2008), we found that the production of AmyK38 gradually decreased in the order of strains 168, MGB625, MGB723, and MGB874, and was markedly impaired due to the genomic deletion process from strains MGB625 to MGB723 (Figure 15). As no significant differences in cell yields (OD at 600 nm) or cell viabilities were detected, the decrease in AmyK38 produced was not caused by impaired cell growth. Based on the measured amylase activity (Figure 15) it was estimated that the amount of AmyK38 produced in strains 168, MGB625, MGB723 and MGB874 after 72 h of culture was 1.68×10^2, 1.15×10^2, 30.0, and 4.57 mg l^{-1}, respectively.

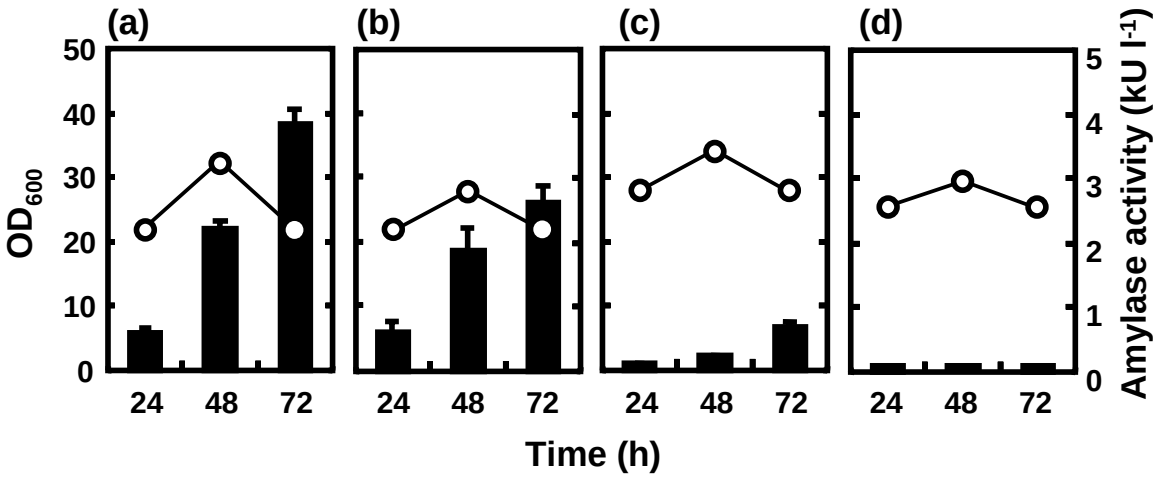

Figure 15. AmyK38 production by multiple-deletion strains. The growth (open circles) and AmyK38 production levels (black bars) of *B. subtilis* strains 168 (a), MGB625 (b), MGB723 (c), and MGB874 (d) harboring pHYK38 were evaluated. The results presented are the means of three individual experiments. Error bars represent standard deviations (n=3).

2. Investigation of the bottleneck in AmyK38 production in genome-reduced strains.

We examined whether the observed decrease in AmyK38 production was due to impaired transcription of *amyK38* by quantitative real-time PCR (qRT-PCR). However, we found that the transcriptional levels of *amyK38* were higher for the multiple-deletion mutant cells than those of wild-type strain 168 cells (Figure 16A). This finding of increased target gene transcription in these genome-reduced strains is consistent with the result in Chapter 1 of this thesis and does not appear to be related to the nature of the gene product.

We next examined the concentration of AmyK38 in culture supernatants and cell fractions by Western blotting. As shown in Figure 16B, the levels of AmyK38 in the supernatants decreased in the order of strains 168, MGB625, MGB723, and MGB874, which closely correlated with the α-amylase activities measured at 48 h (Figure 15). Additionally, the levels of AmyK38 detected in the cellular fraction in the genome-reduced strains were also lower than that of strain 168 (Figure 16B). As the size of AmyK38 observed in the cellular fraction was equivalent to that of purified (mature) AmyK38, these cell-associated AmyK38 would be

translocated mature protein that has not yet been released into the growth medium. The isoelectric point (pI) of AmyK38 is 4.2 (Hagihara et al., 2001b), and AmyK38 we detected in cellular fraction could not be removed by washing with 5M LiCl (data not shown), suggesting that it is not bound to cell wall, but bound to cell membrane.

To investigate the possible degradation of secreted AmyK38 in the genome-reduced strains, we evaluated the stability of mature AmyK38 in culture medium following the growth of strains 168 and MGB874 harboring pHYK38 to the stationary phase (at 48 h). As shown in Figure 16C, AmyK38 was stable in the spent culture medium of both strains over an incubation period of 24 h at 30 °C. This finding indicates that following the folding of AmyK38 into its native conformation and release from the cells into the growth medium, the enzyme is highly stable.

Finally, we measured the transcriptional levels of *htrA* and *htrB,* which encode membrane-bound proteases that respond to secretion stress in *B. subtilis* (Darmon et al., 2002). The data shown in Figure 16D indicates that the secretion stress levels resulting from the overproduction of AmyK38 were higher in strains MGB723 and MGB874 than those in strains 168 and MGB625. Westers et al. (Westers et al., 2004) have demonstrated that the intensity of the secretion stress response in *B. subtilis* correlates with the cellular level of AmyQ. However, in the present study, the concentration of AmyK38 in the cellular fraction of strains MGB723 and MGB874 was inversely related to the levels of secretion stress, although the amount of cell-associated AmyK38 was also reduced in MGB625 without induction of HtrA and HtrB.

These findings raise the possibility that unfolded forms of AmyK38 accumulated after translocation and they were degraded rapidly at the membrane-cell wall interface in strains MGB723 and MGB874. It was reported that the predominant proteases responsible for protein degradation at the membrane-cell wall interface are the WprA-derived cell wall-bound

protein CWBP52 (Stephenson and Harwood, 1998) and CssRS-dependent membrane bound proteases HtrA and HtrB (Hyyrylainen et al., 2001). However, the gene encoding WprA was deleted during the multiple deletion process used to construct strains MGB723 and MGB874 (Ara et al., 2007; Morimoto et al., 2008). Thus, the main proteases responsible for the degradation of AmyK38 before its release into the growth medium appear to be HtrA and HtrB. In an attempt to confirm this speculation, we evaluated AmyK38 production in *cssRS* mutants, but no transformants harboring pHYK38 for AmyK38 production could be obtained. This result is consistent with previous reports that found inactivation of *cssRS* causes growth defects under secretion stress conditions and does not improve the yield of heterologous proteins (Vitikainen et al., 2005).

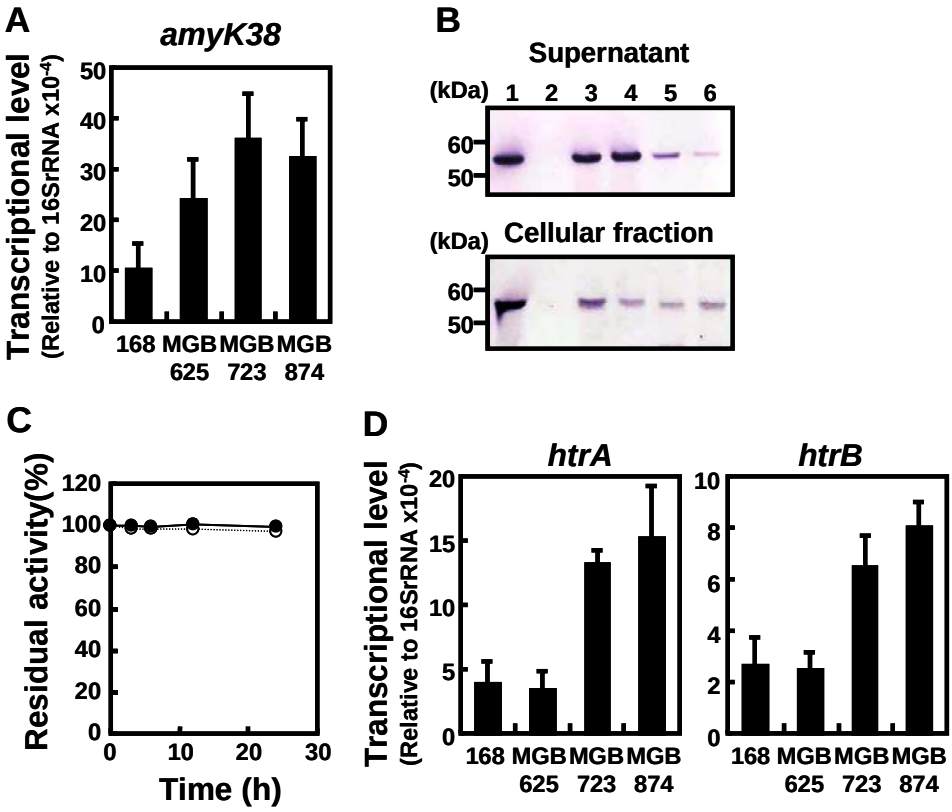

Figure 16. Investigation of bottleneck causing a decrease in AmyK38 production. (A) Transcriptional levels of *amyK38* were determined by qRT-PCR after 48 h of cultivation and are reported relative to those of 16S rRNA. (B) Secretion and cellular amounts of AmyK38 in the genome-reduced strains. The concentrations of AmyK38 in supernatants and cellular fractions after 48 h cultivation were analyzed by Western blotting. Cellular fractions were 16-fold enriched compared to supernatants. The positions of the protein standards are indicated in kDa to the left of the gel. Lanes: 1, purified AmyK38 (10 ng); 2, strain 168/pHY300PLK (empty vector); 3, strain 168/pHYK38; 4, strain MGB625/pHYK38; 5, strain MGB723 /pHYK38; and 6, strain MGB874/pHYK38. (C) Stability of AmyK38 in spent culture medium. The spent culture media of strains 168 (open circles) and MGB874 harboring pHYK38 (closed circles) were collected after 48 h cultivation. Time intervals of α-amylase activities of the spent media were measured at 30 °C. (D) Transcriptional levels of *htrA* and *htrB* after 48-h cultivation were determined by qRT-PCR and are reported relative to those of 16S rRNA. The results presented in (A) and (D) are the means of three individual experiments. Error bars represent standard deviations (n=3).

3. Genetic cause for decreased AmyK38 production

To determine the underlying genetic cause for the significant decrease in AmyK38 production in the genome-reduced strains, we examined the regions deleted during the generation of strain MGB723 from strain MGB625, which involved deletion of the genomic region from *pdp* to *rocR* (nucleotides 4,049,059 to 4,147,133 in sequence NC_000964.3; NCBI GenBank Database (Barbe et al., 2009)). Deletion of this genomic region significantly increased the production of cellulase Egl-237 and M-protease (Ara et al., 2007; Morimoto et al., 2008), with subsequent analyses revealing that deletion of the *rocDEF-rocR* region was responsible for the enhanced enzyme production (Manabe et al., 2011) (Please refer to the Chapter 1 in this thesis). However, here, we found that deletion of the *rocDEF-rocR* region caused a significant decrease in the production level of AmyK38 (Figure 17). Thus, deletion of the *rocDEF-rocR* region has a negative effect on the production of the α-amylase AmyK38, but leads to increased production of Egl-237 and M-protease (Manabe et al., 2011).

RocR is a transcriptional activator of the arginine degradation pathway, which is encoded by the *rocABC* and *rocDEF* operons, and *rocG* gene (Sonenshein et al., 2002). To determine the specific gene(s) responsible for the decreased production of AmyK38, we evaluated single-deletion mutants of the RocR regulon (Figure 18). From this analysis, we found that inactivation of the *rocG* gene significantly reduces the production of AmyK38 in *B. subtilis* (Figure 18).

To investigate the relationship between *rocG* expression and AmyK38 production and secretion stress responses, an isopropyl-β-D-thiogalactopyranoside (IPTG)-inducible P_{spac}-*rocG* gene and transcriptional *htrB-lacZ* gene fusion were introduced into strain MGB874, generating strain R-1926 (MGB874 P_{spac}-*rocG* and P_{htrB}-*lacZ*). The *htrB-lacZ* fusion is commonly used as a reporter of secretion stress in *B. subtilis* (Darmon et al., 2002; Hyyrylainen et al., 2001). Detailed time course analyses of strain R-1926 are shown in Figure

19. Notably, the induction of *rocG* expression by 1 mM IPTG increased the production level of AmyK38, although the culture OD_{600} in the stationary phase were decreased (Figure 19A). Furthermore, the secretion stress response was also decreased by the induction of *rocG* expression (Figure 19B).

RocG is a catabolic glutamate dehydrogenase that catalyzes the conversion of glutamate to 2-oxoglutarate and ammonia (Belitsky and Sonenshein, 1998). As the deamination of glutamate by RocG is a major ammonia-releasing reaction (Kada et al., 2008), which would lead to increased external pH, we focused on ammonia generation and changes in external pH of the culture medium (Figure 19C). We found that the ammonia concentrations in the growth media and external pH were higher under *rocG*-induced conditions compared to those measured under non-inducing conditions. In the non-inducing conditions, the production of AmyK38 was arrested in the stationary phase (Figure 19A, white bars, 24 to 48 h). During this growth phase, the external pH was lower (Figure 19C) and the secretion stress levels were higher (Figure 19B) compared to those detected under inducing conditions. Together, these data suggest the possibility that a lower pH leads to decreased extracellular production of AmyK38, which is accompanied by increased levels of secretion stress in *B. subtilis*. At 72 h of cultivation, the external pH for strain MGB874 was drastically increased, likely due to sugar starvation (Figure 19D) (Spira and Silverman, 1979). In accordance with this increase in external pH, the production of AmyK38 increased from 48 to 72 h of cultivation under non-inducing conditions of *rocG* (Figure 19A).

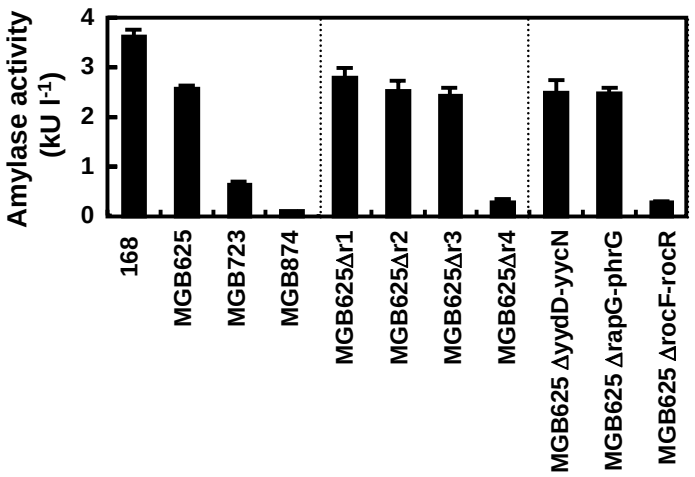

Figure 17. Determination of the gene deletions responsible for decreased AmyK38 production. Amylase activities in the growth media of *B. subtilis* strains 168, MGB625, MGB723, MGB874, and MGB625 derivative strains harboring pHYK38 after 72 h of cultivation. Please refer to Chapter I concerning the construction of the MGB625 derivative strains.

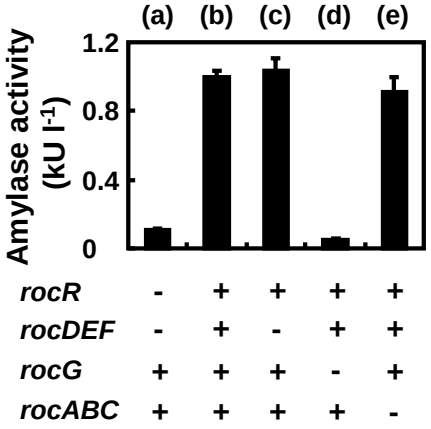

Figure 18. Contribution of the RocR regulon to amylase production. (A) Regulation of the RocR regulon in *B. subtilis*. The RocR regulon consists of two gene clusters, the *rocDEF-rocR* and *rocG-rocABC* regions. The *rocDEF-rocR* region was deleted during the construction of strain MGB723 from strain MGB625 (B) Contribution of the RocR regulon to amylase production in *B. subtilis*. *B. subtilis* MGB874 derivative strains in the presence or absence of the indicated genes were transformed with pHYK38. Amylase activities were measured after 72-h cultivation. The following strains were evaluated: (a), MGB874; (b), 874DEFR; (c), 874RocR; (d), 874DEFRrocG; and (e), 874DEFRΔrocABC.

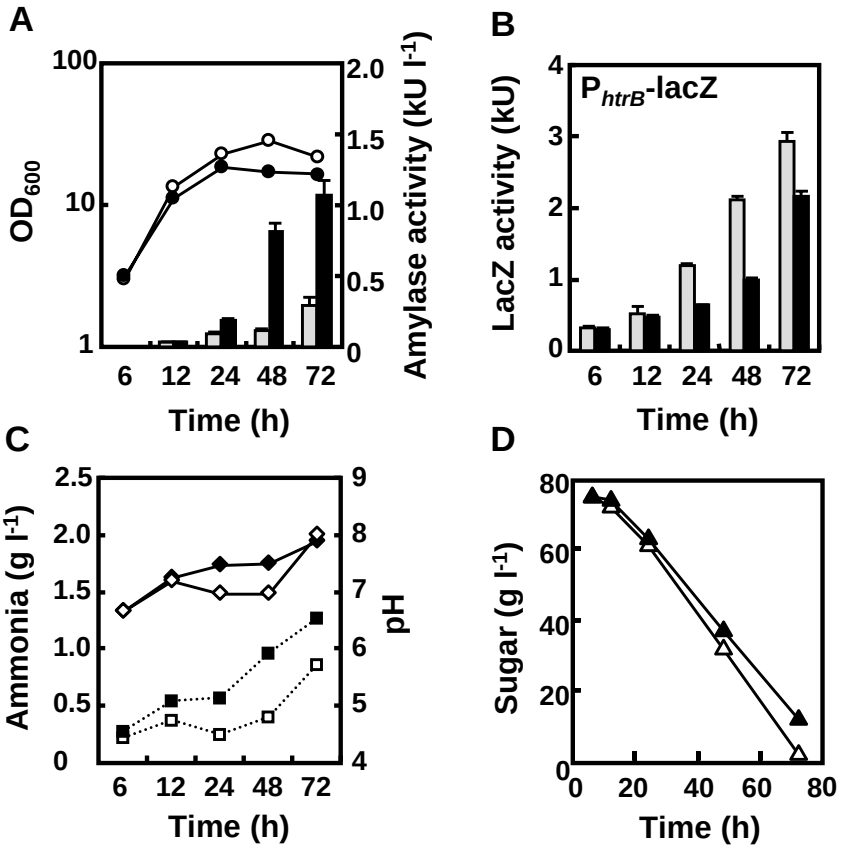

Figure 19. Effect of *rocG* expression on AmyK38 production, secretion stress responses, and external pH. (A) Strain R-1926 (MGB874 P_{spac}-*rocG* and P_{htrB}-*lacZ*) harboring pHYK38 was cultured in the absence (white) or presence (black) of 1 mM IPTG. (A-a) Growth profiles (circles) and amylase activities in the growth medium (bars). (A-b) Secretion stress levels were determined by measuring β-galactosidase activities of cells expressing a transcriptional *htrB-lacZ* fusion. (A-c) Ammonia concentrations (squares) and pH of culture broth (diamonds). All results presented are the averages of three individual experiments. Error bars represent standard deviations (n=3). (B) The enzyme reaction catalyzed by the glutamate dehydrogenase RocG. RocG is a catabolic enzyme that catalyzes the conversion of glutamate to 2-oxoglutarate and ammonia.

4. Up-shift in external pH enhances AmyK38 production levels and decreases secretion stress

To investigate the effects of external pH on AmyK38 production, we added different concentrations of sodium carbonate (Na_2CO_3) as an alkaline solution to the growth medium during the transition phase (12 h of cultivation) (Figure 20A). Surprisingly, the addition of up

to 0.9% Na_2CO_3 significantly improved α-amylase production not only by strain MGB874, but also by strain 168, and this effect far exceeded the increase resulting from the induction of *rocG* (Figure 19A). Additionally, the enhancement of enzyme production was observed in the culture supernatants and cellular fractions by western blotting analysis (Figure 20B). As Hagihara et al. (Hagihara et al., 2001a) previously reported that AmyK38 contains three Na^+ ions in the protein structure, an NaCl solution was added to the growth medium to give the same amount of Na^+ ions as resulting from the addition of 0.9% (w/v) Na_2CO_3. Additionally, we added an NH_3 solution as a second alkaline solution. As a result, the production levels of AmyK38 significantly increased after addition of the NH_3 solution, but no significant improvement of AmyK38 production was observed by addition of the NaCl solution (Figure 21). These results strongly suggest that the optimal external pH for the production of AmyK38 is higher than the pH of standard growth medium used for culturing *B. subtilis*.

Under controlled pH conditions, the highest production level of AmyK38 (1.08 g l^{-1}) was obtained using strain MGB874 (Figure 20A, 0.9% Na_2CO_3). To examine the influence of pH up-shift on the secretion stress response, we constructed strains R-1645 and R-1646 by introducing the *htrB-lacZ* gene fusion into strains 168 and MGB874, respectively. As shown in Table 4, the accumulations of β-galactosidase in strain 168 and MGB874 cells harboring pHYK38 were clearly reduced in the presence of Na_2CO_3, which resulted in an increase of the medium pH, in comparison with untreated cells (Table 4). Thus, the up-shift of external pH could alleviate the AmyK38-induced secretion stress response in *B. subtilis*, although a degree of the response remained.

To further improve AmyK38 production, we attempted to reduce the remaining secretion stress response by further increasing the external pH (Figure 20A, 1.2% Na_2CO_3 [w/v]). Increasing the external pH from pH 8.4 to 9.1 resulted in a decrease in the culture OD_{600} at 24 h of cultivation. Under this cultivation condition, the culture OD_{600} of strain MGB874

remained low until the end of the 72 h cultivation period, whereas increases in the culture OD_{600} of strain 168 were observed after only 24 h of cultivation. Thus, the severe growth inhibition of strain MGB874 cells would result in drastically decreased AmyK38 production (Figure 20A, 1.2% Na_2CO_3 [w/v]). Therefore, further enhancement of AmyK38 production is expected by the generation of a high alkaline-tolerant mutant of strain MGB874.

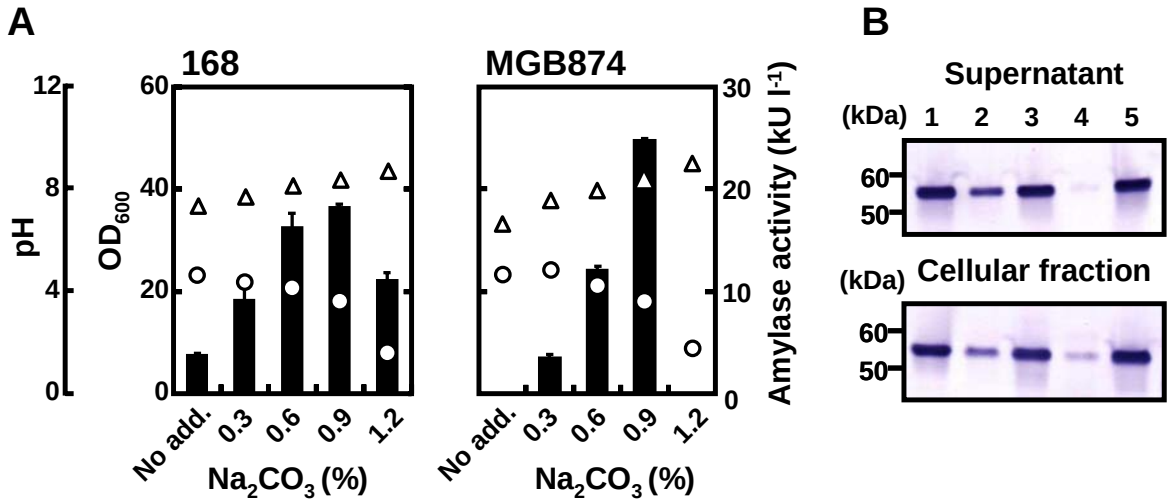

Figure 20 Effect of pH up-shift on AmyK38 production. (A) At the transition phase (12 h), a sodium carbonate solution (Na_2CO_3) was added to the growth medium of strains 168 and MGB874 harboring pHYK38 at the indicated final concentrations (w/v). Cell growth (open circles) and external pH (open triangles) were measured after 24 h of cultivation, and amylase activities (black bars) were measured after 72 h cultivation. All results presented are the averages of three individual experiments. Error bars represent standard deviations (n=3). (B) Secretion and cellular amounts of AmyK38 in strains 168 and MGB874 harboring pHYK38. Cells were grown in 2xL-Mal medium at 30 °C until the transition phase (12 h), at which point Na_2CO_3 was added to the growth medium at a final concentration of 0.9% (w/v). The amounts of AmyK38 in supernatants and cellular fractions after 48 h of cultivation were analyzed by Western blotting. Cellular fractions were 96-fold enriched compared to supernatants. The positions of the protein standards are indicated in kDa to the left of the gels. Lanes: 1, purified AmyK38 (10 ng); 2, strain 168 harboring pHYK38 without Na_2CO_3 addition; 3, strain 168 harboring pHYK38 with Na_2CO_3 addition; 4, strain MGB874 harboring pHYK38 without Na_2CO_3 addition; and 5, strain MGB874 harboring pHYK38 with Na_2CO_3 addition.

Table 4 Effect of pH up-shift on the secretion stress response in *B. subtilis*

Strain	Genotype	Plasmid	Na_2CO_3[a]	LacZ activity[b]
R-1645	168 Δ*amyE*::P_{htrB}-*lacZ*	pHY300PLK	–	6.7±0.28
R-1645	168 Δ*amyE*::P_{htrB}-*lacZ*	pHY300PLK	+	6.5±0.53
R-1646	MGB874 Δ*amyE*::P_{htrB}-*lacZ*	pHY300PLK	–	9.5±0.12
R-1646	MGB874 Δ*amyE*::P_{htrB}-*lacZ*	pHY300PLK	+	9.1±0.32
R-1645	168 Δ*amyE*::P_{htrB}-*lacZ*	pHYK38	–	700±86
R-1645	168 Δ*amyE*::P_{htrB}-*lacZ*	pHYK38	+	200±48
R-1646	MGB874 Δ*amyE*::P_{htrB}-*lacZ*	pHYK38	–	1700±36
R-1646	MGB874 Δ*amyE*::P_{htrB}-*lacZ*	pHYK38	+	590±85

[a]*B. subtilis* derivative strains were grown in 2xL-Mal medium at 30 °C. At the transition phase (12 h), a Na_2CO_3 solution was added to the growth medium at a final concentration of 0.9% (w/v). -, No addition; +, Addition.
[b]LacZ activity was determined after 48 h of cultivation. β-galactosidase-specific activities are reported in units (U) calculated using the following formula: 1000 x A420/reaction time (min) x OD_{600} of culture.

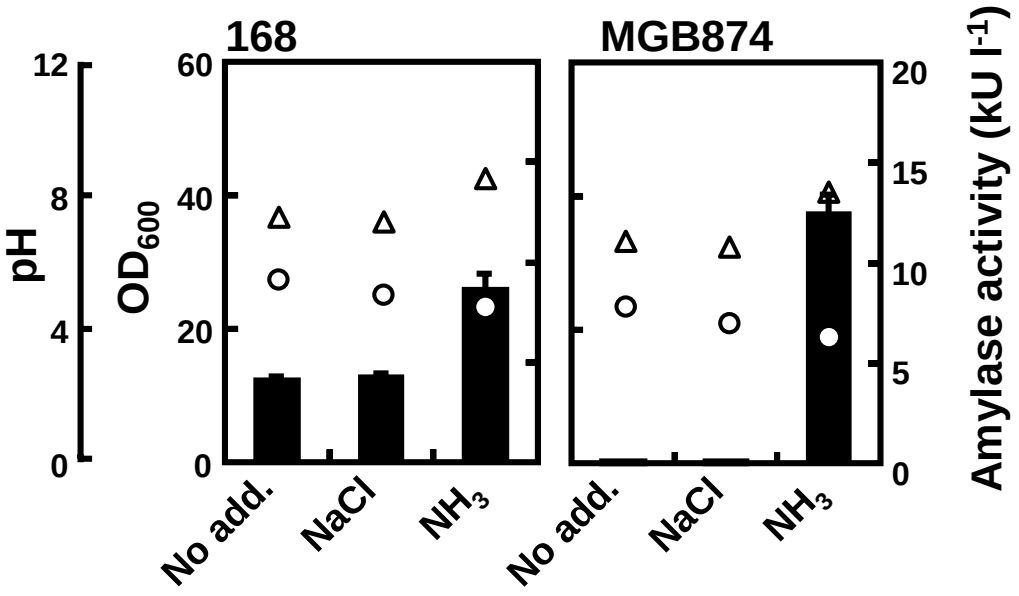

Figure 21. Effect of NaCl and NH_3 addition on AmyK38 production. At the transition phase (12 h), an NaCl or NH_3 solution was added to the growth medium at final concentrations of 1.0% (w/v) or 0.23% (v/v), respectively. Culture OD_{600} (open circles) and external pH (open triangles) were measured after 24 h of cultivation, and α-amylase activities (black bars) were measured after 72 h cultivation. All results presented are the averages of three individual experiments. Error bars represent standard deviations (n=3).

5. Reduced D-alanylation enhances production of AmyK38 in response to external pH up-shift

Under normal growth conditions (pH 6.5), cell wall teichoic acids of *B. subtilis* contain ester-linked D-alanine residues, which reduce the density of negative charge in the cell wall (Perego et al., 1995). Hyyrylainen et al. (Hyyrylainen et al., 2000) reported that a D-alanylation-deficient strain (Δ*dltB*) displays increased α-amylase production compared to the wild-type strain (Hyyrylainen et al., 2000). Importantly, under alkaline conditions (pH 8.1), cell wall teichoic acids are non-alanylated due to the lability of D-alanine ester linkages at alkaline pH (Hyyrylainen et al., 2000). These observations suggest that the enhanced production of AmyK38 in response to an external pH up-shift might be due to the loss of D-alanine esters under alkaline conditions. Thus, we constructed D-alanylation-deficient mutants (Δ*dltB*) of strains 168 and MGB874, and then evaluated the production levels of AmyK38 in the presence and absence of added alkali.

As shown in Table 5, in the absence of Na_2CO_3, deletion of *dltB* enhanced AmyK38 production by strains 168 and MGB874. These data indicate that the absence of D-alanylation enhances the production levels of AmyK38 in both strains 168 and MGB874. Although AmyK38 does not require Ca^{2+} for activity, the absence of D-alanylation would increase the concentration of metal ions at the cell wall and membrane interface and metal ions could still influence its rate of folding. However, an external pH up-shift enhanced the production levels of AmyK38 even in the *dltB* mutants, and no significant differences in AmyK38 production were observed between the *dltB* mutants and their respective parental strains when the external pH was up-shifted (Table 5). Thus, the data presented here suggest that a deficit of D-alanylation is one of the factors enhancing production of AmyK38 under conditions of external pH up-shift.

In summary, the observed improvement of AmyK38 production by *B. subtilis* in response to

an up-shift of external pH is considered to be a result of the following: (i) direct improvement of the folding efficiency and/or stability of AmyK38 prior to its release into the growth medium; (ii) indirect stabilization of AmyK38 through an increase in the net negative charge of the cell wall by not only the loss of protons, but also from the loss of D-alanine in the cell wall. (iii) reduced activities of the membrane-bound serine proteases HtrA and HtrB; and (iv) possible secondary effects of gene clusters activated or inactivated by increased external pH. These four possibilities cannot be discriminated by our present data, although the experiments using *dltB* mutants suggest that the loss of D-alanine esters due to an up-shift of external pH contributes to increased AmyK38 production. It should be mentioned that the alkaline α-amylase AmyK38 might fold effectively at alkaline external pH, which might increase the folding rate of AmyK38 as it emerges from the translocon, although experimental examination of this possibility is necessary.

Table 5 AmyK38 production in *dltB* mutants with or without an up-shift of external pH

Strain	Plasmid	Na_2CO_3[a]	α-amylase activity (kU l^{-1})[b]
168	pHYK38	–	2.9±0.3
168ΔdltB	pHYK38	–	7.0±0.3
MGB874	pHYK38	–	0.10±0.01
874ΔdltB	pHYK38	–	0.27±0.02
168	pHYK38	+	14.3±0.2
168ΔdltB	pHYK38	+	14.8±0.4
MGB874	pHYK38	+	20.8±0.8
874ΔdltB	pHYK38	+	20.1±0.2

[a]*B. subtilis* derivative strains were grown in 2xL-Mal medium at 30 °C. At the transition phase (12 h), an Na_2CO_3 solution was added to the growth medium at a final concentration of 0.9% (w/v). -, No addition; +, Addition.
[b]α-amylase activity was determined after 72 h of cultivation.

Conclusions

An up-shift of external pH leads to a reduced secretion stress response in *B. subtilis* and is associated with increased production of the α-amylase AmyK38. Our results suggest that the optimization of external pH is an important prerequisite for the efficient production of AmyK38 in *B. subtilis*. Under controlled pH conditions, genome-reduced strain MGB874 was found to be a beneficial host for the production of AmyK38 and yielded the highest levels of AmyK38 reported to date. For further improvement of AmyK38 production, we are attempting to generate a high alkaline-tolerant mutant to reduce the remaining secretion stress response. Our present results are expected to find application for the overproduction of other α-amylases, such as AmyL and AmyQ, as induction of the secretion stress responses is a common problem for the overproduction of these enzymes in *B. subtilis*.

Chapter 3: Improved enzyme production in strain MGB874 via modification of glutamate metabolism and growth conditions.

Background

In Chapter 1 , we revealed that deletion of the *rocR* gene is an important contributor to the high level of enzyme production we observe in genome-reduced strain MGB874 (Manabe et al., 2011). The RocR protein is a positive regulator of genes related to the arginine degradation pathway, including RocG, a major catabolic glutamate dehydrogenase (Ali et al., 2003; Belitsky and Sonenshein, 1998, 1999; Calogero et al., 1994). RocG has another role as a regulatory protein that inhibits GltC, a regulator of the *gltAB* operon, which encodes glutamate synthase (Commichau et al., 2007a). Thus, in strain MGB874, deletion of *rocR* not only suppresses glutamate degradation pathway but also activates the glutamate synthesis pathway (Figure 22). We proposed that this change of glutamate metabolism in strain MGB874 increases the flux from 2-oxoglutarate to glutamate, which might lead to increased syntheses of the other amino acids via transamination, finally resulting in enhanced enzyme production (Manabe et al., 2011) (Please refer to the Chapter 1 in this thesis).

Additionally, in Chapter 2, we found that RocG also serves as an important factor influencing enzyme production by helping to prevent acidification of the growth medium. Decreased expression of *rocG* reduces the level of deamination of glutamate, a major cellular ammonia-releasing reaction (Kada et al., 2008), and leads to a decrease in the external pH during strain MGB874 cultivation. We found that the decreased external pH impaired production of the alkaline α-amylase AmyK38, accompanied by the induction of expression of *htrA* and *htrB*, which encode serine-type surface proteases and is known to be CssRS dependent (Manabe et al., 2012). In *B. subtilis*, the CssRS two-component system responds to

the accumulation of misfolded proteins at the membrane-cell wall interface (Darmon et al., 2002). Alkaline α-amylase AmyK38 is thought to fold ineffectively at acidic external pH, leading to secretion stress. Therefore, at least in terms of the production of the alkaline α-amylase AmyK38, RocG appears to have a positive role in preventing acidification of the growth medium.

The aim of the present study was to enhance enzyme production in genome-reduced strain MGB874 through further optimization of glutamate metabolism. Belitsky et al. reported that *rocG* is still expressed at a low level in this strain due to read-through transcription of the upstream gene *yweA*, even in the absence of the RocR activator sequence (Belitsky et al., 2004). Thus, deletion of *rocG* might release repression of *gltAB* in strain MGB874 completely, further enhancing enzyme production. However, we previously observed that deletion of *rocG* in strain MGB874 (strain 874ΔrocG) led to a dramatic decrease in production of the cellulase Egl-237, even in spite of an observed increase in cell yield (Figure 12, Chapter 1). At that time, it remained unclear if this phenomenon is caused by acidification of the growth medium, as in the case of alkaline α-amylase production.

Here, we investigated the mechanisms underlying decreased enzyme production in strain 874ΔrocG and attempted to boost production of Egl-237 by overcoming the rate-limiting factors we identified.

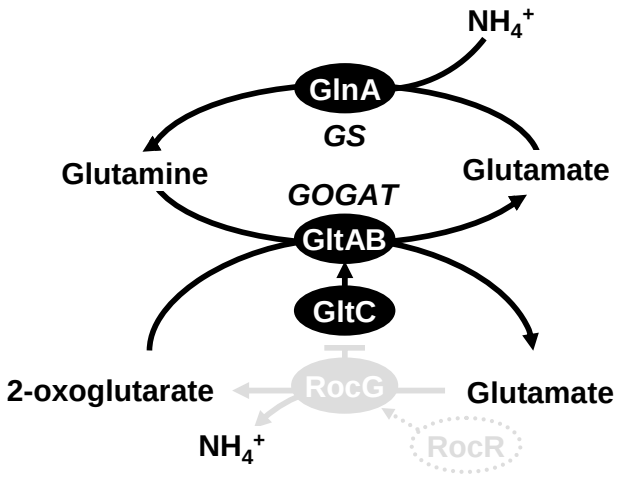

Figure 22. Major reactions and regulation involved in glutamate metabolism in *B. subtilis*. Proteins are shown as ovals. RocG, glutamate dehydrogenase; GltAB, glutamate synthase (GOGAT); GlnA, glutamine synthetase (GS). In *B. subtilis*, glutamate can be degraded by RocG. *B. subtilis* has a glutamine synthetase-glutamate synthase (GS-GOGAT) pathway for assimilation of ammonia. The RocR and GltC transcription factors positively regulate *rocG* and *gltAB*, respectively, and GltC can be inhibited via interaction with RocG. Open and closed gray ovals indicate proteins corresponding to genes that have been deleted or inactivated, respectively, in strain MGB874. Deletion of *rocR* in strain MGB874 decreases expression of *rocG*, which leads to an increase in expression of *gltAB* due to activation of GltC via disinhibition by RocG.

Results and Discussion

1. Growth characteristics of strains MGB874 and 874ΔrocG producing Egl-237 cellulase.

Previously, we found that deletion of the *rocG* in the genome-reduced strain MGB874 dramatically decreased the level of production of the cellulase Egl-237, despite an increase in cell yield (Manabe et al., 2011) (Figure 12, Chapter 1). The *B. subtilis* genome encodes a second, cryptic glutamate dehydrogenase gene, *gudB,* which harbors an insertion of three amino acids with respect to the common ancestral GluDH sequence (Belitsky and Sonenshein, 1998). Previous studies showed that mutations in *rocG* result in the rapid accumulation of suppressor mutations in *gudB* (Belitsky and Sonenshein, 1998; Commichau et al., 2008; Commichau et al., 2007b). However, sequence analysis of *gudB* alleles in strains MGB874

and 874ΔrocG revealed that in these strains, the insertion mutation of the three amino acids has been retained.

To obtain insight into the mechanism responsible for decreased enzyme production in strain 874ΔrocG, we conducted time course analyses of Egl-237 production in strains MGB874 and 874ΔrocG under batch fermentation conditions achieved using a 30-liter jar fermentor. As shown in Figures 23A and 23B, after the transition phase Egl-237 production in strain 874ΔrocG dramatically decreased as compared with strain MGB874, although the cell yield in strain 874ΔrocG was higher. Additionally, in the culture medium at the transition phase, we observed a decrease in pH and ammonium depletion for strain 874ΔrocG as compared to strain MGB874 during cultivation (Figures 23C and 23D).

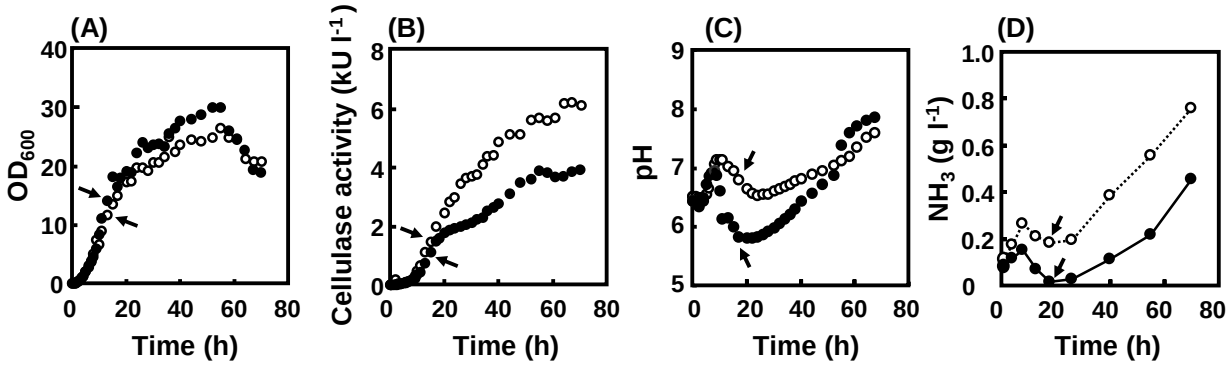

Figure 23. Growth characteristics of strains MGB874 and 874ΔrocG producing the Egl-237-encoded cellulase. Strains MGB874 (open circles) or MGB874ΔrocG (closed circles) harboring pHYS237 were cultured. Cell yield (A), extracellular cellulase activity (B), external pH of the growth media (C) and ammonia concentration in the growth media (D) were measured at the indicated times. Arrows indicate the point at which transcriptome analyses were conducted.

2. Comparison of transcriptome profiles of strains MGB874 and 874ΔrocG

We then compared transcriptome profiles of MGB874 and 874ΔrocG cells at transition phase (at 18 h, indicated by arrow in Figure 23) using a custom Affymetrix tilling chip. The top-ranked 20 up-regulated genes and bottom-ranked 20 down-regulated genes in 874ΔrocG

cells were listed in Tables 6 and 7, respectively. Firstly, we found that expression of *htrA* was markedly induced in 874ΔrocG cells (Table 6. Our previous study revealed that the decrease in external pH impaired secretion of alkaline α-amylase AmyK38 in strain MGB874, and induced *htrA* and *htrB* expression (Manabe et al., 2012). Indeed, expression of *htrB* was also induced in 874ΔrocG cells (4.62 hold) as compared to strain MGB874 cells in our transcriptome analysis. Additionally, time course analysis using qRT-PCR confirm that *htrB* expression is up-regulated in 874ΔrocG cells during early stationary phase (from 18 to 24 h, Figure 24). These results suggest that acidification of the growth medium might impair secretion of Egl-237 in 874ΔrocG cells.

Importantly, we found that many of the genes that are activated or repressed in 874ΔrocG cells are controlled by the transcriptional factor TnrA. Indeed, 10 of the bottom-ranked 20 genes and 8 of the top-ranked 20 genes were members of the TnrA regulon (Tables 6 and 7). TnrA is a major transcription factor in *B. subtilis* that controls gene expression under nitrogen-limited growth (Fisher, 1999; Wray et al., 1996; Yoshida et al., 2003). Time course analysis revealed that *nrgA,* which encodes an ammonia transporter regulated by TnrA, is transiently up-regulated in 874ΔrocG cells just before cells enter the stationary phase (at 18 h, Figure 24), which corresponds to the point that ammonium depletion occurs in the culture medium during culture of strain 874ΔrocG (Figure 23D). These results clearly indicate that nitrogen starvation is induced in 874ΔrocG cells likely due to ammonium depletion in the culture medium.

Expression of glutamate synthase (GltAB) is also known to be negatively regulated by TnrA (Belitsky et al., 2000), in addition to its regulation by GltC. Indeed, expression of *gltA* in 874ΔrocG cells significantly decreased after depletion of ammonium to levels lower than that in MGB874 cells, although *gltA* levels in 874ΔrocG cells were much higher than levels in MGB874 cells before entering stationary phase (at 18 h, Figure 24). These results indicate

that although activation of the glutamate synthetic pathway is induced via deletion of *rocG* during the early growth phase as expected, it is subsequently suppressed by depletion of ammonium in the culture medium.

Table 6 Genes up-regulated in 874ΔrocG cells (top-ranked 20 genes)

Gene	Description	Average signal[a]		Ratio[b]	Transcriptional factor[c]
		MGB874	874ΔrocG		
nrgA	ammonium transporter	208	3926	18.91	**TnrA(+)**
yvrI	function unknown and unique	92	1266	13.78	YvrH(+)
ykzB	function unknown and unique, regulated by TnrA and PhoP-phoR	92	1078	11.72	**TnrA(+)**
nasC	assimilatory nitrate reductase catalytic subunit	128	1463	11.46	GlnR(-), **TnrA(+)**
yccC	L-asparaginase, activated during nitrogen-limited growth by the TnrA transcription factor	202	1976	9.78	**TnrA(+)**
tnrA	transcriptional pleiotropic regulator involved in global nitrogen regulation (MerR family)	103	981	9.56	**TnrA(+)**
nasA	nitrate transporter	227	1975	8.70	**GlnR(-), TnrA(+)**
yvmB	possible transcriptional regulator (MarR family)	119	977	8.23	
yjgD	conserved protein	158	1185	7.51	
nasB	assimilatory nitrate reductase electron transfer subunit	180	1346	7.49	**GlnR(-), TnrA(+)**
htrA	serine protease (heat-shock protein)	719	4742	6.60	**CssR(+)**, HtrA(-)
ygxB	stage V sporulation protein R (spore cortex synthesis)	184	1156	6.29	
yqzH	function unknown and unique	248	1463	5.90	LexA(-)
spoVFB	dipicolinate synthase, B chain	82	475	5.80	
nrgB	nitrogen regulatory pII-like protein	821	4727	5.76	**TnrA(+)**
yhjL	aminosugar antibiotic 3, 3 -neotrehalosadiamine (NTD) production	133	707	5.33	YhjM(+)
bmrU	multidrug resistance protein cotranscribed with bmr	180	949	5.28	
yrbD	similar to sodium/proton-dependent alanine carrier protein	327	1721	5.27	
yitT	conserved protein	247	1301	5.26	
yuzA	conserved protein	146	758	5.20	

[a]The average signal intensities of probes in each coding sequence.
[b]The ratio of each of the genes was obtained by dividing the average signal intensity in each coding sequence of 874ΔrocG cells by that for MGB874 cells.
[c]The Database of Transcriptional Regulation in *Bacillus subtilis* (DBTBS) was used as a reference (De Hoon et al., 2004). Transcriptional activators or repressors are described with (+) or (-), respectively. TnrA, GlnR and CssR are shown in bold type.

Table 7 Genes down-regulated in 874ΔrocG cells (bottom-ranked 20 genes)

Gene	Description	Average signal[a]		Ratio[b]	Transcriptional factor[c]
		MGB874	874ΔrocG		
yuiA	conserved protein	4307	533	0.12	
yycC	function unknown and unique	1915	273	0.14	**TnrA(-)**
yycB	probable transporter	1883	287	0.15	**TnrA(-)**
dhbC	isochorismate synthase, dihydroxybenzoylglycine biosynthesis	2560	529	0.21	Fur(-)
pel	pectate lyase	3736	808	0.22	ComA(+), **TnrA(-)**
ilvB	acetolactate synthase large subunit	2106	459	0.22	CcpA(+), CodY(-), **TnrA(-)**, TrnS-Leu2(+)
leuB	3-isopropylmalate dehydrogenase	2072	467	0.23	CcpA(+), CodY(-), **TnrA(-)**, TrnS-Leu2(+)
dhbF	non-ribosomal peptide synthetase, dihydroxybenzoylglycine biosynthesis	2081	474	0.23	Fur(-)
serA	phosphoglycerate dehydrogenase	2575	603	0.23	
leuA	2-isopropylmalate synthase	1680	396	0.24	CcpA(+), CodY(-), **TnrA(-)**, TrnS-Leu2(+)
dhbB	isochorismatase (2,3 dihydro-2,3 dihydroxybenzoate synthase), dihydroxybenzoylglycine biosynthesis	1897	447	0.24	Fur(-)
leuC	3-isopropylmalate dehydratase large subunit	2166	516	0.24	CcpA(+), CodY(-), **TnrA(-)**, TrnS-Leu2(+)
ilvC	ketol-acid reductoisomerase (acetohydroxy-acid isomeroreductase)	2981	713	0.24	CcpA(+), CodY(-), **TnrA(-)**, TrnS-Leu2(+)
yocS	similar to sodium-dependent transporter	1028	248	0.24	
yodF	similar to proline permease	737	182	0.25	**TnrA(-)**
ydzA	conserved membrane protein	1035	266	0.26	
yxxG	function unknown and unique	435	119	0.27	DegU(-), YvrH(+)
dhbE	2,3-dihydroxybenzoate-AMP ligase (enterobactin synthetase component E), dihydroxybenzoylglycine biosynthesis	1539	439	0.29	Fur(-)
leuD	3-isopropylmalate dehydratase small subunit	1137	327	0.29	CcpA(+), CodY(-), **TnrA(-)**, TrnS-Leu2(+)
yuiB	conserved membrane protein	3785	1150	0.30	

[a]The average signal intensities of probes in each coding sequence.
[b]The ratio of each of the genes was obtained by dividing the average signal intensity in each coding sequence of 874□rocG cells by that for MGB874 cells.
[c]The Database of Transcriptional Regulation in *Bacillus subtilis* (DBTBS) was used as a reference (De Hoon et al., 2004). Transcriptional activators or repressors are indicated by a (+) or (-), respectively. TnrA is shown in bold type.

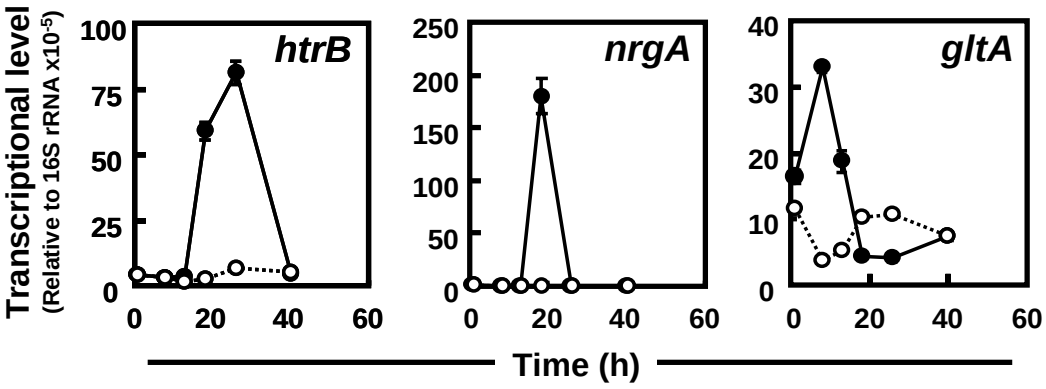

Figure 24 Time course of transcription during growth of *B. subtilis* strains MGB874 and 874ΔrocG. The strains MGB874 (open circles) and 874ΔrocG (closed circles) harboring pHY-S237 were cultured using shake-flask fermentation. Transcript levels for *htrB, nrgA* and *gltA* were determined by qRT-PCR (primers shown in Table 3). Transcript levels were normalized to 16S rRNA levels. Error bars represent standard deviations (*n*=3).

3. Cultivation using the NH_3-pH auxostat approach improves enzyme production in strain 874ΔrocG

To exclude the influence of decreased pH and depletion of ammonia in the growth medium associated with culture of strain 874ΔrocG, we next performed pH-stat fermentation using NaOH or aqueous NH_3 and a 2-L jar fermentor (Figure 25). The pH of the growth media was adjusted to 7.2, which corresponds to the highest pH observed in the growth medium of strain MGB874 in the absence of pH control (Figure 25A). Additionally, to prevent the carbon source from becoming a limiting factor, the initial concentration of maltose in the growth media was increased from 7.5% to 12.5%, which is sufficient in these fermentation conditions.

When fermentation was performed without pH control, the growth characteristics were similar to results shown in Figure 23. On the other hand, when pH-stat fermentation using NaOH was performed, the production of Egl-237 in strain 874ΔrocG was improved to nearly

the same level as that observed for strain MGB874 (Figure 25B). In both these cases, the concentrations of ammonia were significantly decreased as compared to that reached during cultivation without pH control. To examine if the decrease in ammonia affects Egl-237 production, we performed pH-stat fermentation using aqueous NH_3, using a so-called NH_3-pH auxostat (Swift et al., 1998) (Figure 25C). The enzyme production period in strain 874ΔrocG was prolonged with use of the NH_3-pH auxostat, whereas the Egl-237 production profile in MGB874 cells was similar in both cultivation conditions. With the NH_3-pH auxostat, the Egl-237 production in strain 874ΔrocG was 1.67-fold higher than that in strain MGB874 at the end of the cultivation period (Figure 25C). Production of Egl-237 in strain 874ΔrocG corresponded to about 5.5 g l^{-1}, the highest level reported so far.

Notably, the level of residual ammonia in the growth medium from strain 874ΔrocG was lower than that from strain MGB874, although the total amount of ammonia introduced into the growth medium for strain 874ΔrocG was considerably larger than that for strain MGB874 (Figure 25C). These data suggest that the ratio of assimilated ammonia in 874ΔrocG cells was higher than that in MGB874 cells and furthermore, that assimilation activity is maintained through late stages of cultivation.

It should be noted that the *rocG* deletion in wild-type strain 168 also enhanced Egl-237 production with the NH_3-pH auxostat (Figure 26). However, the production level from strain 168ΔrocG (2.8 g l^{-1}) was about half of that of strain 874ΔrocG, indicating the importance of the genetic background of the genome-reduced strain for higher levels of Egl-237 production.

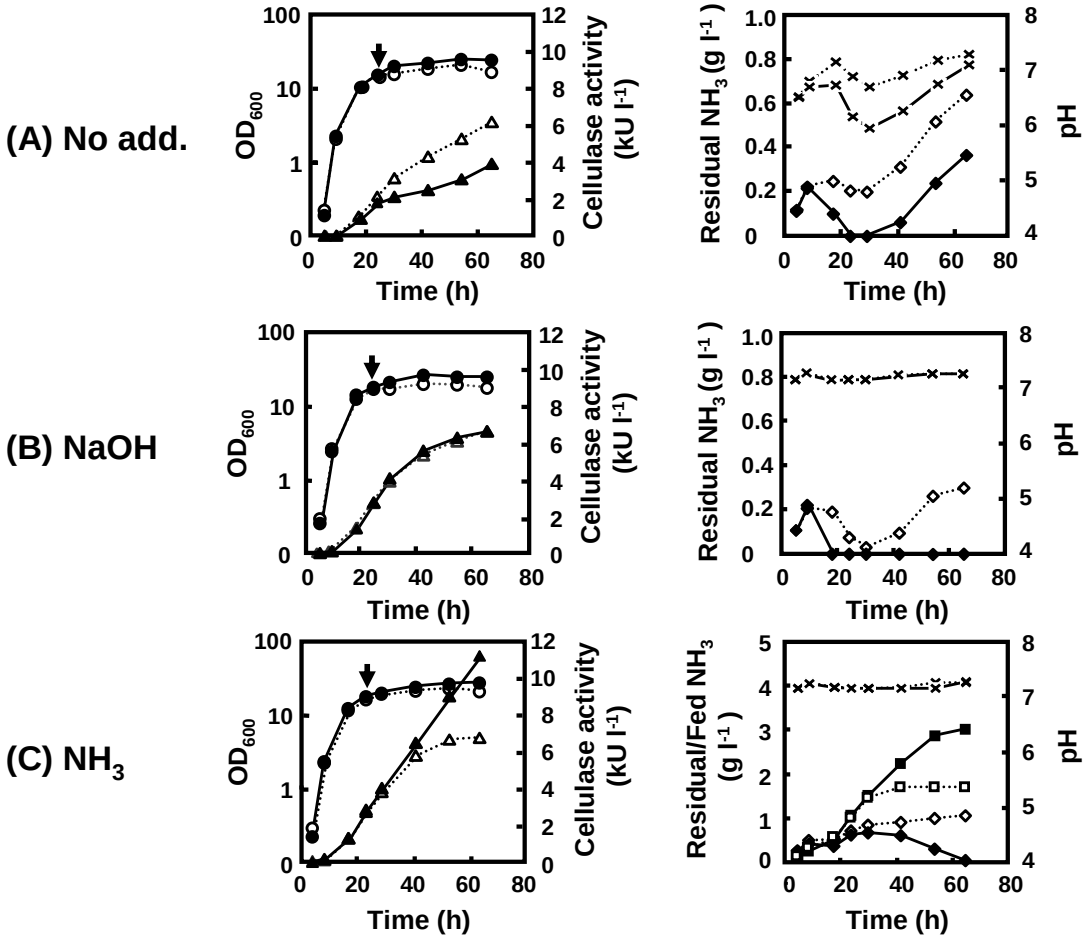

Figure 25. Growth characteristics of strains MGB874 and 874ΔrocG producing Egl-237-encoded cellulase. The strains MGB874 (open symbols and dotted lines) and 874ΔrocG (closed symbols and solid lines) harboring pHYS237 were cultured in 2xL medium containing 12.5% (w/v) maltose monohydrate by the pH-Stat fermentation using 2-L jar fermentor. Fermentation without pH control was done as a reference (A). The pH was adjusted to 7.2 by the automatic addition of 1M NaOH (B) or 10% (w/v) aqueous NH_3 (C). Cell yields (circles) and extracellular cellulase activities (triangles) were shown on the left side of the figure. Residual ammonia concentrations (diamonds) and external pHs (crosses) in the growth media were shown on the right side of the figure. Additionally, total amounts of ammonia fed (squares) were also displayed under the NH_3-pH auxostat. Arrows indicate the point at which transcriptional analysis was conducted.

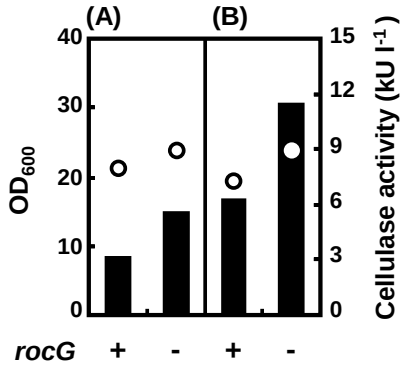

Figure 26. Cell yield and Egl-237 production under the NH_3-pH auxostat. The strains in the presence (+) or absence (-) of *rocG* harboring pHYS237 were cultured by the pH-Stat fermentation. The pH was adjusted to 7.2 by addition aqueous NH_3. The cell yields (at 42 h; open circles) and the cellulase activities in growth media (72h; black bars) were measured. (A) The wild-type strain 168 and strain 168ΔrocG. (B) The genome-reduced strain MGB874 and strain 874ΔrocG.

4. Changes in gene expression underlying improvement in enzyme production with pH-stat fermentation

To investigate the changes in gene expression underlying the improvement of enzyme production in 874ΔrocG cells under pH-stat fermentation, RNA was extracted from cells at 24 h of cultivation (Figure 25; arrows), and expression levels of selected genes were measured by qRT-PCR (Figure 27). Although transcriptional levels for selected genes were not significantly changed in MGB874 cells under any fermentation conditions, remarkable changes in expression of these genes were observed in 874ΔrocG.

Firstly, expression of *htrB* was reduced to the same level in strain MGB874 under fermentation conditions with pH-control not only with aqueous NH_3 but also with NaOH, clearly indicating that the CssRS-dependent secretion stress response is induced by overproduction of Egl-237 in 874ΔrocG cells under the low external pH condition (Figure 27). Notably, production of Egl-237 did not induce the secretion stress response in MGB874 cells (Figures 24 and 27) but overproduction of alkaline α-amylase AmyK38 induced this response

to a high degree in MGB874 cells (Manabe et al., 2012). Because the decrease of external pH was more severe in 874ΔrocG cultivation (without pH control) compared to that in MGB874 cultivation (Figure 25A), the threshold value of external pH leading to secretion stress responses for overproduction of Egl-237 would be lower than for the overproduction of AmyK38.

We also found that expression of *nrgA,* known to be activated under nitrogen-limited growth, was down-regulated in 874ΔrocG cells using the NH_3-pH auxostat, suggesting avoidance of nitrogen starvation (Figure 27). Furthermore, the expression level of *gltA*, encoding a subunit of glutamate synthase, was 9-fold higher in 874ΔrocG cells than in MGB874 when using the NH_3-pH auxostat (Figure 27). As ammonia can be assimilated via the glutamine synthetase-glutamate synthase (GS-GOGAT) pathway in *B. subtilis* (Figure 22), activation of the glutamate synthetic pathway might indirectly contribute to the enhancement of ammonia assimilation ability in 874ΔrocG cells (Figures 25C and 27). With the NH_3-pH auxostat, the continuous conversion of ammonia to glutamate in 874ΔrocG cells might lead to increased flux in the synthesis of other amino acids via transamination, resulting in enhancement of Egl-237 production.

As mentioned, enzyme productivity lasted through the end of the cultivation period in strain 874ΔrocG with use of the NH_3-pH auxostat but this was not observed for strain MGB874 under the same conditions (Figure 25C). Activation of the glutamate synthetic pathway in 874ΔrocG cells could account for this difference. Furthermore, we found that expression of the gene encoding aconitase (*citB*) was up-regulated in 874ΔrocG cells but not MGB874 cells under NH_3-pH auxostat (Figure 27). Expression of *citB* has been reported to be indirectly repressed by 2-oxoglutarate, which competitively represses the reaction of citrate synthase (CitZ), leading to repression of *citB* by the transcriptional regulator CcpC in the absence of the effector citrate (Jourlin-Castelli et al., 2000; Sonenshein, 2007). Therefore,

improvement of metabolic flux from 2-oxoglutarate to glutamate in strain 874ΔrocG might lead to activation of *citB* via de-repression of CcpC. Activation of *citB* might contribute to prolonged high enzyme productivity through the generation of reducing power via the tricarboxylic acid (TCA) cycle.

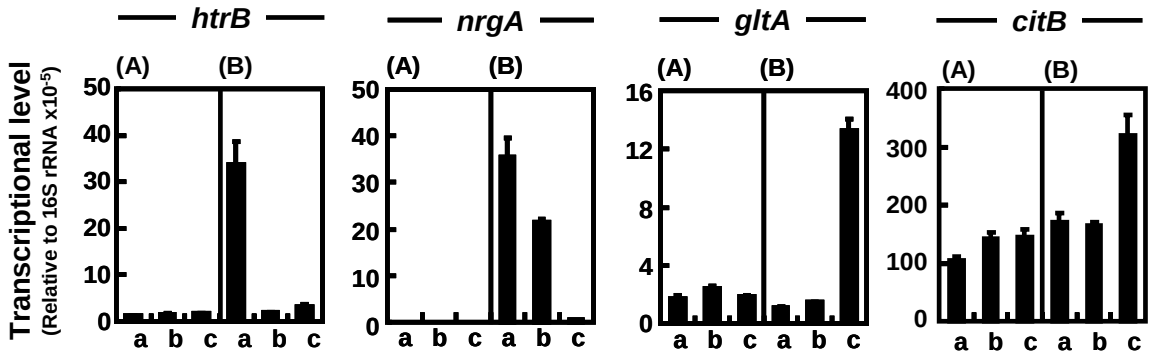

Figure 27. Transcriptional levels of selected genes in strains MGB874 and 874ΔrocG. The strains MGB874 (A) and 874ΔrocG (B) harboring pHYS237 were cultured by the pH-Stat fermentation. Fermentation without pH control was done as a reference (a). The pH was adjusted to 7.2 by addition of NaOH (b) or aqueous NH_3 (c). RNA was isolated from the cells at the 24h of the cultivation time (indicated by arrows in Fig. 4), and expression level of *htrB, nrgA*, *gltA* and *citB* were determined by qRT-PCR. The transcriptional levels are expressed relative to those of 16S rRNA. Error bars represent standard deviations (*n*=3).

Conclusion

Here, we describe conditions resulting in the highest levels of production of the recombinant enzyme Egl-237 in *B. subtilis* cells reported to date. We found that deletion of the glutamate dehydrogenase gene *rocG* in the genome-reduced strain MGB874 (874ΔrocG) and cultivation of 874ΔrocG using NH_3-pH auxostat conditions leads to enhanced enzyme production through prolonged high enzyme productivity until the end of cultivation. This beneficial effect would be due to enhancement of metabolic flux from 2-oxoglutarate to

glutamate and generation of metabolic energy through activation of the TCA cycle.

Additionally, we found that the overproduction of Egl-237 causes the induction of CssRS-dependent secretion stress responses in the acidified growth medium below the threshold pH value, which is lower than that for the overproduction of alkaline α-amylase AmyK38.

With the NH_3-pH auxostat, levels of Egl-237 produced by strain 874ΔrocG far exceeded those produced by the wild-type genetic-background strain 168ΔrocG, and reached the highest level reported so far, corresponding to 5.5 g/L. However, it is not clear at the moment if these improvements are attributable to a global synergistic effect of large-scale genome reduction or the deletion of one or more specific genes. To further improve enzyme production, we are presently attempting to elucidate the mechanisms underlying the improvement in productivity we have observed.

Summary

In this study, we revealed that two factors contribute to the high enzyme production levels in genome-reduced strain MGB874: increased specific productivity and improved cell yield. The improved cell yield is attributable to the deletion of *rocDEF-rocR* region. On the other hand, the mechanism of the increased specific productivity remains unclear. Thus, investigation of this mechanism would be important to achieve further enhancement of enzyme production. Additionally, although the deletion of *rocDEF-rocR* actually compensates for the decrease of cell yield in the genome-reduced strains, it would be useful to identify the nature of this defect in the future work.

We revealed that deletion of *rocR* not only suppresses glutamate degradation pathway but also activates the glutamate synthesis pathway in strain MGB874. We proposed that this change of glutamate metabolism in strain MGB874 increases the flux from 2-oxoglutarate to glutamate, which might lead to increased syntheses of the other amino acids via transamination, finally resulting in enhanced enzyme production. Additionally, we found that RocG also serves as an important factor influencing enzyme production by helping to prevent acidification of the growth medium. Decreased external pH impaired production of the alkaline α-amylase AmyK38 and alkaline cellulase Egl-237 accompanied with secretion stress response, although the threshold value of external pH leading to secretion stress responses for overproduction of Egl-237 would be lower than for the overproduction of AmyK38. Although it is common knowledge that strict pH control in fermentations is critical for optimal enzyme yields, we recognized the importance of control of the fermentation condition.

Furthermore, we found that the deletion of *rocG* in strain MGB874 dramatically decreased the production level of Egl-237 under batch fermentation. This phenomenon was attributable to the ammonium starvation in addition to the impairment in secretion of Egl-237, which caused by decreased external pH. Under NH_3-pH auxostat fermentation system, the

production level of Egl-237 in strain MGB874 was corresponded to about 5.5 g l^{-1}, which was the highest level reported so far. This result also reminds us of the importance of controlling cultivation condition.

To date, we have attempted to reduce the genome size of *B. subtilis* by deleting unnecessary genome regions for the cell growth and recombinant enzyme production. In this process, we have used batch fermentation method to evaluate the production of recombinant enzymes alkaline cellulase Egl-237 (Ara et al., 2007; Morimoto et al., 2008). Therefore, some strains possessed high Egl-237 production capacity in potential might be regarded as inappropriate strains because of the decreased productivity due to the deterioration of the medium environment, such as nutrient depletion or decrease in external pH, likewise demonstrated in the present study. Therefore, the fermentation system with higher homeostatic condition, such as pH-stat fermentation and continuous fermentation, must enable us to construct more simplified microbial cell factory for recombinant protein production in the future.

Acknowledgements

I would like to express my sincere gratitude and appreciation to my supervisor, Nara Institute of Science and Technology Prof. Naotake Ogasawara and Prof. Hisaji Maki, for valuable advice, supervisions, and crucial contributions throughout this study, and for my good opportunities that they provided. I am deeply grateful to Yoshinori Takema (Kao Corp.) who gave me this opportunity, constructive comments and warm support. I would like to give heartful thanks to Tadayuki Imanaka who is my professor of the Kyoto University era and gave me valuable advice. Special thanks also go to Haruyuki Atomi (Kyoto University) who gave me invaluable comments and warm encouragements.

I am greatly indebted to Katsuya Ozaki (Kao Corp.) and Katsutoshi Ara (Kao Corp.), who have been responsible for helping me in this research. This work could not have been completed without their helps. My special thanks go to my senior associate Yasushi Kageyama (Kao Corp.), who is a best collaborator for this work. I also thank Junichi Sekiguchi (Shinshu University), Kouji Nakamura (University of Tsukuba), Fujio Kawamura (University of Rikkyo), and Yasutaro Fujita (Fukuyama University) for valuable advice and discussions. I also would like to give heartful thanks Tadashi Hase and Katsuhisa Saeki, who are my current supervisors in Kao Corp.

I owe a very important debate to my advisory committee, Prof. Hirotada Mori, Prof Kazuhiro Shiozaki and Associate Prof. Yukio Kimata.

My great appreciation is also extended to my coworkers in Kao corporation; Takuya Morimoto, Hiroshi Kakeshita, Takeko Kodama, Keiji Endo, Masatoshi Tohata, Kazuhisa Sawada, Shengao Liu, Tadahiro Ozawa, Akihito Kawahara, Nozomu Shibata, Hiroshi Kodama, Kazuhiro Saito and Reiko Shimooka who worked with me under the same project related to this research.

I would like to give special thanks to my workmate in Kao corporation; Haruko Toyoshima,

Yasushi Takimura, Akira Hachiya, Fumikazu Takahashi, Kenta Masuda and Mami Sakai for their warm encouragements. I also would like to express my gratitude to my friends Shoutarou Ito, Atsuko Hayase, Takashi Sakamoto and Nanae Mugita for their moral support. Special thanks to my families Satoko Iwai, Hiroko Manabe, Ayako Iwai, Takako Iwai and Masashi Iwai who all have been supportive and caring.

This research was conducted as part of the Project for the Development of a Technological Infrastructure for Industrial Bioprocesses through R&D on New Industrial Science and Technology Frontiers of the Ministry of Economy, Trade, and Industry (METI), Japan, and was supported by the New Energy and Industrial Technology Development Organization (NEDO), Japan.

References

Ali, N.O., Jeusset, J., Larquet, E., Le Cam, E., Belitsky, B., Sonenshein, A.L., Msadek, T., and Debarbouille, M. (2003). Specificity of the interaction of RocR with the rocG-rocA intergenic region in *Bacillus subtilis*. Microbiology *149*, 739-750.

Anagnostopoulos, C., and Spizizen, J. (1961). Requirements for Transformation in *Bacillus subtilis*. J Bacteriol *81*, 741-746.

Ara, K., Ozaki, K., Nakamura, K., Yamane, K., Sekiguchi, J., and Ogasawara, N. (2007). *Bacillus* minimum genome factory: effective utilization of microbial genome information. Biotechnol Appl Biochem *46*, 169-178.

Asai, K., Baik, S.H., Kasahara, Y., Moriya, S., and Ogasawara, N. (2000). Regulation of the transport system for C4-dicarboxylic acids in *Bacillus subtilis*. Microbiology *146 (Pt 2)*, 263-271.

Barbe, V., Cruveiller, S., Kunst, F., Lenoble, P., Meurice, G., Sekowska, A., Vallenet, D., Wang, T., Moszer, I., Medigue, C., *et al.* (2009). From a consortium sequence to a unified sequence: the *Bacillus subtilis* 168 reference genome a decade later. Microbiology *155*, 1758-1775.

Belitsky, B.R. (2002). Biosynthesis of amino acids of the glutamate and aspartate families, alanine, and polyamines, p. 203-231. In A. L. Sonenshein, J. A. Hoch, and R. Losick (ed.). *Bacillus subtilis* and its closest relatives: from genes to cells. . ASM Press, Washington, DC5

Belitsky, B.R., Kim, H.J., and Sonenshein, A.L. (2004). CcpA-dependent regulation of *Bacillus subtilis* glutamate dehydrogenase gene expression. J Bacteriol *186*, 3392-3398.

Belitsky, B.R., and Sonenshein, A.L. (1998). Role and regulation of *Bacillus subtilis* glutamate dehydrogenase genes. J Bacteriol *180*, 6298-6305.

Belitsky, B.R., and Sonenshein, A.L. (1999). An enhancer element located downstream of the major glutamate dehydrogenase gene of *Bacillus subtilis*. Proc Natl Acad Sci U S A *96*, 10290-10295.

Belitsky, B.R., Wray, L.V., Jr., Fisher, S.H., Bohannon, D.E., and Sonenshein, A.L. (2000). Role of TnrA in

nitrogen source-dependent repression of *Bacillus subtilis* glutamate synthase gene expression. J Bacteriol *182*, 5939-5947.

Blencke, H.M., Reif, I., Commichau, F.M., Detsch, C., Wacker, I., Ludwig, H., and Stulke, J. (2006). Regulation of citB expression in *Bacillus subtilis*: integration of multiple metabolic signals in the citrate pool and by the general nitrogen regulatory system. Arch Microbiol *185*, 136-146.

Bohannon, D.E., and Sonenshein, A.L. (1989). Positive regulation of glutamate biosynthesis in *Bacillus subtilis*. J Bacteriol *171*, 4718-4727.

Bolten, C.J., Kiefer, P., Letisse, F., Portais, J.C., and Wittmann, C. (2007). Sampling for metabolome analysis of microorganisms. Anal Chem *79*, 3843-3849.

Calogero, S., Gardan, R., Glaser, P., Schweizer, J., Rapoport, G., and Debarbouille, M. (1994). RocR, a novel regulatory protein controlling arginine utilization in *Bacillus subtilis*, belongs to the NtrC/NifA family of transcriptional activators. J Bacteriol *176*, 1234-1241.

Chan, A.Y., and Lim, B.L. (2003). Interaction of a putative transcriptional regulatory protein and the thermo-inducible cts-52 mutant repressor in the *Bacillus subtilis* phage phi105 genome. J Mol Biol *333*, 21-31.

Chang, S., and Cohen, S.N. (1979). High frequency transformation of *Bacillus subtilis* protoplasts by plasmid DNA. Mol Gen Genet *168*, 111-115.

Commichau, F.M., Gunka, K., Landmann, J.J., and Stulke, J. (2008). Glutamate metabolism in *Bacillus subtilis*: gene expression and enzyme activities evolved to avoid futile cycles and to allow rapid responses to perturbations of the system. J Bacteriol *190*, 3557-3564.

Commichau, F.M., Herzberg, C., Tripal, P., Valerius, O., and Stulke, J. (2007a). A regulatory protein-protein interaction governs glutamate biosynthesis in *Bacillus subtilis*: the glutamate dehydrogenase RocG moonlights in controlling the transcription factor GltC. Mol Microbiol *65*, 642-654.

Commichau, F.M., Wacker, I., Schleider, J., Blencke, H.M., Reif, I., Tripal, P., and Stulke, J. (2007b). Characterization of *Bacillus subtilis* mutants with carbon source-independent glutamate biosynthesis. J Mol Microbiol Biotechnol *12*, 106-113.

Cruz Ramos, H., Hoffmann, T., Marino, M., Nedjari, H., Presecan-Siedel, E., Dreesen, O., Glaser, P., and Jahn, D. (2000). Fermentative metabolism of *Bacillus subtilis*: physiology and regulation of gene expression. J Bacteriol *182*, 3072-3080.

Csonka, L.N., and Hanson, A.D. (1991). Prokaryotic osmoregulation: genetics and physiology. Annu Rev Microbiol *45*, 569-606.

Darmon, E., Noone, D., Masson, A., Bron, S., Kuipers, O.P., Devine, K.M., and van Dijl, J.M. (2002). A novel class of heat and secretion stress-responsive genes is controlled by the autoregulated CssRS two-component system of *Bacillus subtilis*. J Bacteriol *184*, 5661-5671.

De Hoon, M.J., Imoto, S., Kobayashi, K., Ogasawara, N., and Miyano, S. (2004). Predicting the operon structure of *Bacillus subtilis* using operon length, intergene distance, and gene expression information. Pac Symp Biocomput, 276-287.

Eymann, C., Homuth, G., Scharf, C., and Hecker, M. (2002). *Bacillus subtilis* functional genomics: global characterization of the stringent response by proteome and transcriptome analysis. J Bacteriol *184*, 2500-2520.

Feher, T., Papp, B., Pal, C., and Posfai, G. (2007). Systematic genome reductions: theoretical and experimental approaches. Chem Rev *107*, 3498-3513.

Fisher, S.H. (1999). Regulation of nitrogen metabolism in *Bacillus subtilis*: vive la difference! Mol Microbiol *32*, 223-232.

Fisher, S.H., and Wray, L.V., Jr. (2006). Feedback-resistant mutations in *Bacillus subtilis* glutamine synthetase are clustered in the active site. J Bacteriol *188*, 5966-5974.

Gardan, R., Rapoport, G., and Debarbouille, M. (1995). Expression of the *rocDEF* operon involved in arginine catabolism in *Bacillus subtilis*. J Mol Biol *249*, 843-856.

Gardan, R., Rapoport, G., and Debarbouille, M. (1997). Role of the transcriptional activator RocR in the arginine-degradation pathway of *Bacillus subtilis*. Mol Microbiol *24*, 825-837.

Guerout-Fleury, A.M., Shazand, K., Frandsen, N., and Stragier, P. (1995). Antibiotic-resistance cassettes for *Bacillus subtilis*. Gene *167*, 335-336.

Hagihara, H., Hayashi, Y., Endo, K., Igarashi, K., Ozawa, T., Kawai, S., Ozaki, K., and Ito, S. (2001a). Deduced amino-acid sequence of a calcium-free alpha-amylase from a strain of *Bacillus*: implications from molecular modeling of high oxidation stability and chelator resistance of the enzyme. Eur J Biochem *268*, 3974-3982.

Hagihara, H., Igarashi, K., Hayashi, Y., Endo, K., Ikawa-Kitayama, K., Ozaki, K., Kawai, S., and Ito, S. (2001b). Novel α-amylase that is highly resistant to chelating reagents and chemical oxidants from the alkaliphilic *Bacillus* isolate KSM-K38. Appl Environ Microbiol *67*, 1744-1750.

Hakamada, Y., Hatada, Y., Koike, K., Yoshimatsu, T., Kawai, S., Kobayashi, T., and Ito, S. (2000). Deduced amino acid sequence and possible catalytic residues of a thermostable, alkaline cellulase from an Alkaliphilic *Bacillus* strain. Biosci Biotechnol Biochem *64*, 2281-2289.

Hashimoto, M., Ichimura, T., Mizoguchi, H., Tanaka, K., Fujimitsu, K., Keyamura, K., Ote, T., Yamakawa, T., Yamazaki, Y., Mori, H., *et al.* (2005). Cell size and nucleoid organization of engineered *Escherichia coli* cells with a reduced genome. Mol Microbiol *55*, 137-149.

Hirai, M.Y., Klein, M., Fujikawa, Y., Yano, M., Goodenowe, D.B., Yamazaki, Y., Kanaya, S., Nakamura, Y., Kitayama, M., Suzuki, H., *et al.* (2005). Elucidation of gene-to-gene and metabolite-to-gene networks in arabidopsis by integration of metabolomics and transcriptomics. J Biol Chem *280*, 25590-25595.

Horinouchi, S., and Weisblum, B. (1982). Nucleotide sequence and functional map of pC194, a plasmid that specifies inducible chloramphenicol resistance. J Bacteriol *150*, 815-825.

Horton, R.M., Hunt, H.D., Ho, S.N., Pullen, J.K., and Pease, L.R. (1989). Engineering hybrid genes without the use of restriction enzymes: gene splicing by overlap extension. Gene *77*, 61-68.

Hyyrylainen, H.L., Bolhuis, A., Darmon, E., Muukkonen, L., Koski, P., Vitikainen, M., Sarvas, M., Pragai, Z., Bron, S., van Dijl, J.M., *et al.* (2001). A novel two-component regulatory system in *Bacillus subtilis* for the survival of severe secretion stress. Mol Microbiol *41*, 1159-1172.

Hyyrylainen, H.L., Pietiainen, M., Lunden, T., Ekman, A., Gardemeister, M., Murtomaki-Repo, S., Antelmann, H., Hecker, M., Valmu, L., Sarvas, M., *et al.* (2007). The density of negative charge in the cell wall influences two-component signal transduction in *Bacillus subtilis*. Microbiology *153*, 2126-2136.

Hyyrylainen, H.L., Vitikainen, M., Thwaite, J., Wu, H., Sarvas, M., Harwood, C.R., Kontinen, V.P., and Stephenson, K. (2000). D-Alanine substitution of teichoic acids as a modulator of protein folding and stability at the cytoplasmic membrane/cell wall interface of *Bacillus subtilis*. J Biol Chem *275*, 26696-26703.

Igo, M.M., and Losick, R. (1986). Regulation of a promoter that is utilized by minor forms of RNA polymerase holoenzyme in *Bacillus subtilis*. J Mol Biol *191*, 615-624.

Jourlin-Castelli, C., Mani, N., Nakano, M.M., and Sonenshein, A.L. (2000). CcpC, a novel regulator of the LysR family required for glucose repression of the *citB* gene in *Bacillus subtilis*. J Mol Biol *295*, 865-878.

Jung, H.M., Park, K.H., Kim, S.Y., and Lee, J.K. (2004). L-glutamate enhances the expression of Thermus

maltogenic amylase in *Escherichia coli*. Biotechnol Prog *20*, 26-31.

Kada, S., Yabusaki, M., Kaga, T., Ashida, H., and Yoshida, K. (2008). Identification of two major ammonia-releasing reactions involved in secondary natto fermentation. Biosci Biotechnol Biochem *72*, 1869-1876.

Kageyama, Y., Takaki, Y., Shimamura, S., Nishi, S., Nogi, Y., Uchimura, K., Kobayashi, T., Hitomi, J., Ozaki, K., Kawai, S., *et al.* (2007). Intragenomic diversity of the V1 regions of 16S rRNA genes in high-alkaline protease-producing *Bacillus* clausii spp. Extremophiles *11*, 597-603.

Kim, L., Mogk, A., and Schumann, W. (1996). A xylose-inducible *Bacillus subtilis* integration vector and its application. Gene *181*, 71-76.

Kobayashi, K., Ehrlich, S.D., Albertini, A., Amati, G., Andersen, K.K., Arnaud, M., Asai, K., Ashikaga, S., Aymerich, S., Bessieres, P., *et al.* (2003). Essential *Bacillus subtilis* genes. Proc Natl Acad Sci U S A *100*, 4678-4683.

Kobayashi, T., Hakamada, Y., Adachi, S., Hitomi, J., Yoshimatsu, T., Koike, K., Kawai, S., and Ito, S. (1995). Purification and properties of an alkaline protease from alkalophilic *Bacillus* sp. KSM-K16. Appl Microbiol Biotechnol *43*, 473-481.

Kunst, F., Ogasawara, N., Moszer, I., Albertini, A.M., Alloni, G., Azevedo, V., Bertero, M.G., Bessieres, P., Bolotin, A., Borchert, S., *et al.* (1997). The complete genome sequence of the gram-positive bacterium *Bacillus subtilis*. Nature *390*, 249-256.

Liu, S., Endo, K., Ara, K., Ozaki, K., and Ogasawara, N. (2008). Introduction of marker-free deletions in *Bacillus subtilis* using the AraR repressor and the *ara* promoter. Microbiology *154*, 2562-2570.

Lorentz, K. (1998). Approved recommendation on IFCC methods for the measurement of catalytic concentration of enzymes. Part 9. IFCC method for alpha-amylase (1,4-alpha-D-glucan 4-glucanohydrolase, EC 3.2.1.1). International Federation of Clinical Chemistry and Laboratory Medicine (IFCC). Committee on Enzymes. Clin Chem Lab Med *36*, 185-203.

Lowry, O.H., Rosebrough, N.J., Farr, A.L., and Randall, R.J. (1951). Protein measurement with the Folin phenol reagent. J Biol Chem *193*, 265-275.

Makarova, K.S., Mironov, A.A., and Gelfand, M.S. (2001). Conservation of the binding site for the arginine repressor in all bacterial lineages. Genome Biol *2*, RESEARCH0013.

Manabe, K., Kageyama, Y., Morimoto, T., Ozawa, T., Sawada, K., Endo, K., Tohata, M., Ara, K., Ozaki, K., and Ogasawara, N. (2011). Combined Effect of Improved Cell Yield and Increased Specific Productivity Enhances Recombinant Enzyme Production in Genome-Reduced *Bacillus subtilis* Strain MGB874. Appl Environ Microbiol *77*, 8370-8381.

Manabe, K., Kageyama, Y., Tohata, M., Ara, K., Ozaki, K., and Ogasawara, N. (2012). High external pH enables more efficient secretion of alkaline alpha-amylase AmyK38 by *Bacillus subtilis*. Microb Cell Fact *11*, 74.

McKenzie, T., Hoshino, T., Tanaka, T., and Sueoka, N. (1986). The nucleotide sequence of pUB110: some salient features in relation to replication and its regulation. Plasmid *15*, 93-103.

Morimoto, T., Kadoya, R., Endo, K., Tohata, M., Sawada, K., Liu, S., Ozawa, T., Kodama, T., Kakeshita, H., Kageyama, Y., *et al.* (2008). Enhanced recombinant protein productivity by genome reduction in *Bacillus subtilis*. DNA Res *15*, 73-81.

Morimoto, T., Loh, P.C., Hirai, T., Asai, K., Kobayashi, K., Moriya, S., and Ogasawara, N. (2002). Six GTP-binding proteins of the Era/Obg family are essential for cell growth in *Bacillus subtilis*. Microbiology *148*, 3539-3552.

Noone, D., Howell, A., Collery, R., and Devine, K.M. (2001). YkdA and YvtA, HtrA-like serine proteases in *Bacillus subtilis*, engage in negative autoregulation and reciprocal cross-regulation of *ykdA* and *yvtA* gene expression. J Bacteriol *183*, 654-663.

Nyberg, K., Palva, A., and Palva, I. (1985). Exceptionally high copy numbers of a staphylococcal plasmid in *Bacillus subtilis* revealed by a sandwich hybridization technique. FEMS Microbiology Letters *29*, 305-310.

Ogura, M., Shimane, K., Asai, K., Ogasawara, N., and Tanaka, T. (2003). Binding of response regulator DegU to the *aprE* promoter is inhibited by RapG, which is counteracted by extracellular PhrG in *Bacillus subtilis*. Mol Microbiol *49*, 1685-1697.

Perego, M., Glaser, P., Minutello, A., Strauch, M.A., Leopold, K., and Fischer, W. (1995). Incorporation of D-alanine into lipoteichoic acid and wall teichoic acid in *Bacillus subtilis*. Identification of genes and regulation. J Biol Chem *270*, 15598-15606.

Picossi, S., Belitsky, B.R., and Sonenshein, A.L. (2007). Molecular mechanism of the regulation of *Bacillus subtilis gltAB* expression by GltC. J Mol Biol *365*, 1298-1313.

Pietiainen, M., Gardemeister, M., Mecklin, M., Leskela, S., Sarvas, M., and Kontinen, V.P. (2005). Cationic antimicrobial peptides elicit a complex stress response in *Bacillus subtilis* that involves ECF-type sigma factors and two-component signal transduction systems. Microbiology *151*, 1577-1592.

Posfai, G., Plunkett, G., 3rd, Feher, T., Frisch, D., Keil, G.M., Umenhoffer, K., Kolisnychenko, V., Stahl, B., Sharma, S.S., de Arruda, M., *et al.* (2006). Emergent properties of reduced-genome *Escherichia coli*. Science *312*, 1044-1046.

Quackenbush, J. (2002). Microarray data normalization and transformation. Nat Genet *32 Suppl*, 496-501.

Rozen, S., and Skaletsky, H. (2000). Primer3 on the WWW for general users and for biologist programmers. Methods Mol Biol *132*, 365-386.

Schallmey, M., Singh, A., and Ward, O.P. (2004). Developments in the use of *Bacillus* species for industrial production. Can J Microbiol *50*, 1-17.

Shibahara, H.I.a.H. (1985). New shuttle vectors for Escherichia coli and *Bacillus subtilis* III. Nucleotide sequence analysis of tetracycline resistance gene of pAMα1 and ori-177 The Japanese journal of genetics *60*, 485-498.

Simonen, M., and Palva, I. (1993). Protein secretion in *Bacillus* species. Microbiol Rev *57*, 109-137.

Skulj, M., Okrslar, V., Jalen, S., Jevsevar, S., Slanc, P., Strukelj, B., and Menart, V. (2008). Improved determination of plasmid copy number using quantitative real-time PCR for monitoring fermentation processes. Microb Cell Fact *7*, 6.

Soga, T., Ohashi, Y., Ueno, Y., Naraoka, H., Tomita, M., and Nishioka, T. (2003). Quantitative metabolome analysis using capillary electrophoresis mass spectrometry. J Proteome Res *2*, 488-494.

Sonenshein, A.L. (2007). Control of key metabolic intersections in *Bacillus subtilis*. Nat Rev Microbiol *5*, 917-927.

Spira, W.M., and Silverman, G.J. (1979). Effects of glucose, pH, and dissolved-oxygen tension on *Bacillus* cereus growth and permeability factor production in batch culture. Appl Environ Microbiol *37*, 109-116.

Stephenson, K., and Harwood, C.R. (1998). Influence of a cell-wall-associated protease on production of alpha-amylase by *Bacillus subtilis*. Appl Environ Microbiol *64*, 2875-2881.

Swift, R.J., Wiebe, M.G., Robson, G.D., and Trinci, A.P. (1998). Recombinant glucoamylase production by Aspergillus niger B1 in chemostat and pH auxostat cultures. Fungal Genet Biol *25*, 100-109.

Vagner, V., Dervyn, E., and Ehrlich, S.D. (1998). A vector for systematic gene inactivation in *Bacillus subtilis*. Microbiology *144 (Pt 11)*, 3097-3104.

Vallee, B.L., Stein, E.A., Sumerwell, W.N., and Fischer, E.H. (1959). Metal content of alpha-amylases of various origins. J Biol Chem *234*, 2901-2905.

Vitikainen, M., Hyyrylainen, H.L., Kivimaki, A., Kontinen, V.P., and Sarvas, M. (2005). Secretion of heterologous proteins in *Bacillus subtilis* can be improved by engineering cell components affecting post-translocational protein folding and degradation. J Appl Microbiol *99*, 363-375.

Westers, H., Darmon, E., Zanen, G., Veening, J.W., Kuipers, O.P., Bron, S., Quax, W.J., and van Dijl, J.M. (2004). The *Bacillus* secretion stress response is an indicator for alpha-amylase production levels. Lett Appl Microbiol *39*, 65-73.

Westers, H., Dorenbos, R., van Dijl, J.M., Kabel, J., Flanagan, T., Devine, K.M., Jude, F., Seror, S.J., Beekman, A.C., Darmon, E.*, et al.* (2003). Genome engineering reveals large dispensable regions in *Bacillus subtilis*. Mol Biol Evol *20*, 2076-2090.

Wray, L.V., Jr., Ferson, A.E., Rohrer, K., and Fisher, S.H. (1996). TnrA, a transcription factor required for global nitrogen regulation in *Bacillus subtilis*. Proc Natl Acad Sci U S A *93*, 8841-8845.

Yan, D., Ikeda, T.P., Shauger, A.E., and Kustu, S. (1996). Glutamate is required to maintain the steady-state potassium pool in *Salmonella typhimurium*. Proc Natl Acad Sci U S A *93*, 6527-6531.

Yoshida, K., Yamaguchi, H., Kinehara, M., Ohki, Y.H., Nakaura, Y., and Fujita, Y. (2003). Identification of additional TnrA-regulated genes of *Bacillus subtilis* associated with a TnrA box. Mol Microbiol *49*, 157-165.